

RD-A168 888

ENVIRONMENTAL AND WATER QUALITY OPERATIONAL STUDIES
INITIAL EVALUATION OF. (U) ARMY ENGINEER WATERWAYS
EXPERIMENT STATION VICKSBURG MS ENVIR. M J ZIMMERNAN

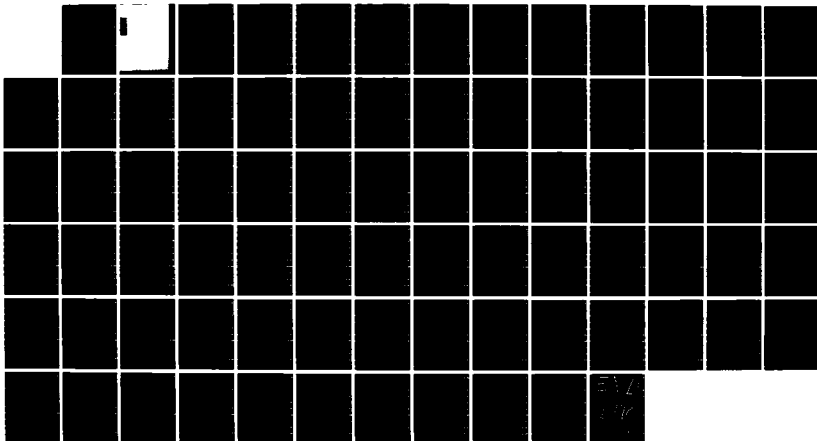
1/1

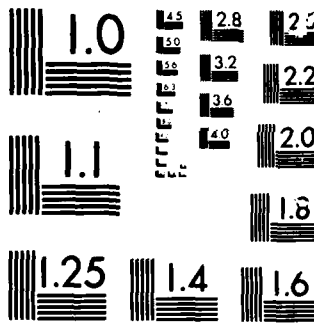
UNCLASSIFIED

FEB 86 MES/MP/E-86-1

F/G 8/8

NL





MICROCOMTM

CHART

AD-A168 000

Unclassified

SECURITY CLASSIFICATION OF THIS PAGE (When Data Entered)

Unclassified

SECURITY CLASSIFICATION OF THIS PAGE(When Data Entered)

20. ABSTRACT (Continued).

quality. This evaluation documents procedures used early in the development and testing of the algorithms and has since led to modifications which have already improved CE-QUAL-R1 simulations in other applications. Field data derived from studies of DeGray Lake, Ark., provide the basis for calibrating and evaluating the algorithms.

New model features specifically related to the simulation of anaerobic water quality conditions include a simplified approach to relevant aquatic chemistry, a dissolved oxygen threshold concentration to initiate anaerobic processes, and simultaneous release from sediments of reduced materials and dissolved phosphorus. Oxidation and reduction processes in the water column are subject to the same constraints as those affecting sediment release.

Two years of data from field studies, 1979 and 1980, were used to calibrate and evaluate simulations. In calibrating the model for assessing the new algorithms, sediment release rates were found to affect predictions most significantly. Although there were some discrepancies between observed and predicted conditions, trends and peak concentrations generally matched well. Further studies and applications of the model should help to assess its value as a tool in reservoir water quality management.

Unclassified

SECURITY CLASSIFICATION OF THIS PAGE(When Data Entered)

PREFACE

This study was sponsored by the Office, Chief of Engineers (OCE), US Army, as part of the Environmental and Water Quality Operational Studies (EWQOS), Work Unit IB.2 entitled "Develop and Verify Description for Aerobic/Anaerobic Chemical Processes." The OCE Technical Monitors for EWQOS were Mr. Earl Eiker, Dr. John Bushman, and Mr. James L. Gottesman.

The work was conducted during the period March 1980 to September 1982 by the Environmental Laboratory, US Army Engineer Waterways Experiment Station (WES), Vicksburg, Miss., under the direction of Dr. John Harrison, Chief of the Environmental Laboratory (EL), and under the general supervision of Mr. D. L. Robey, Chief of the Ecosystem Research and Simulation Division (ERSD). Program Manager of EWQOS was Dr. J. L. Mahloch, EL.

This study was conducted and the text was prepared by Dr. Marc J. Zimmerman. Dr. Allan S. Lessem wrote the computer subroutines constituting the basis for the study. Drs. Joseph Wlosinski and James Martin reviewed the report. The report was edited by Ms. Jessica S. Ruff of the WES Publications and Graphic Arts Division.

Director of WES was COL Allen F. Grum, USA. Technical Director was Dr. Robert W. Whalin.

This report should be cited as follows:

Zimmerman, M. J. 1986. "Initial Evaluation of a Computer Algorithm for Simulating Anaerobic Conditions in Reservoirs and Lakes," Miscellaneous Paper E-86-1, US Army Engineer Waterways Experiment Station, Vicksburg, Miss.

Accession For	
NTIS CRA&I	<input checked="" type="checkbox"/>
DTIC TAB	<input type="checkbox"/>
Unannounced	<input type="checkbox"/>
Justification	
By _____	
Distribution /	
Availability Codes	
Dist	Avail and/or Special
A-1	

CONTENTS

	<u>Page</u>
PREFACE	1
PART I: INTRODUCTION	3
Study Objective	3
Model Background	3
Innovations for Simulating Anaerobic Conditions	5
Anaerobic Subroutines	7
PART II: CALIBRATION OF ANAEROBIC SUBROUTINES	13
Site Characteristics	13
Sampling Procedures	15
Calibration Overview	16
Oxygen Calibration	17
Calibration of Anaerobic Materials	28
Discussion	61
PART III: 1980 CONFIRMATION SIMULATION	63
PART IV: IMPACT OF ANAEROBIC SUBROUTINES ON CE-QUAL-R1	70
PART V: SUMMARY	72
REFERENCES	74

INITIAL EVALUATION OF A COMPUTER ALGORITHM FOR SIMULATING
ANAEROBIC CONDITIONS IN RESERVOIRS AND LAKES

PART I: INTRODUCTION

Study Objective

1. The potential for development of low dissolved oxygen (DO) or anoxic conditions is a major concern for reservoir managers. Low DO concentrations in impoundments can lead to the generation of undesirable chemical products of anaerobic biogeochemical processes. These products, which include dissolved manganese (Mn^{+2}), iron (Fe^{+2}), and sulfur (S^{-2}), along with the low DO condition, can degrade recreational aesthetics and fisheries and can cause taste, odor, and staining problems that increase water treatment costs. Hydrogen sulfide (H_2S) releases are known to cause illness in reservoir project operators, and also accelerate corrosion of outlet works (Keeley et al. 1978). In addition, increased regeneration of phosphorus ($PO_4^{+3}-P$) and ammonia (NH_4^+-N) may stimulate nuisance algal blooms.

2. In order to simulate effects of low oxygen conditions on water quality in planned and operational reservoirs, the Corps of Engineers (CE) has incorporated new algorithms, in the form of 13 subroutines, into its one-dimensional numerical model of water quality, CE-QUAL-R1 (Environmental Laboratory 1982). The objective of this report is to document the development and testing of the new subroutines in simulating anaerobic processes as they pertain to reservoirs. This work was performed during early stages of model development and does not reflect recent improvements, some of which came in response to results of this study.

Model Background

3. CE-QUAL-R1 describes the vertical distribution of thermal

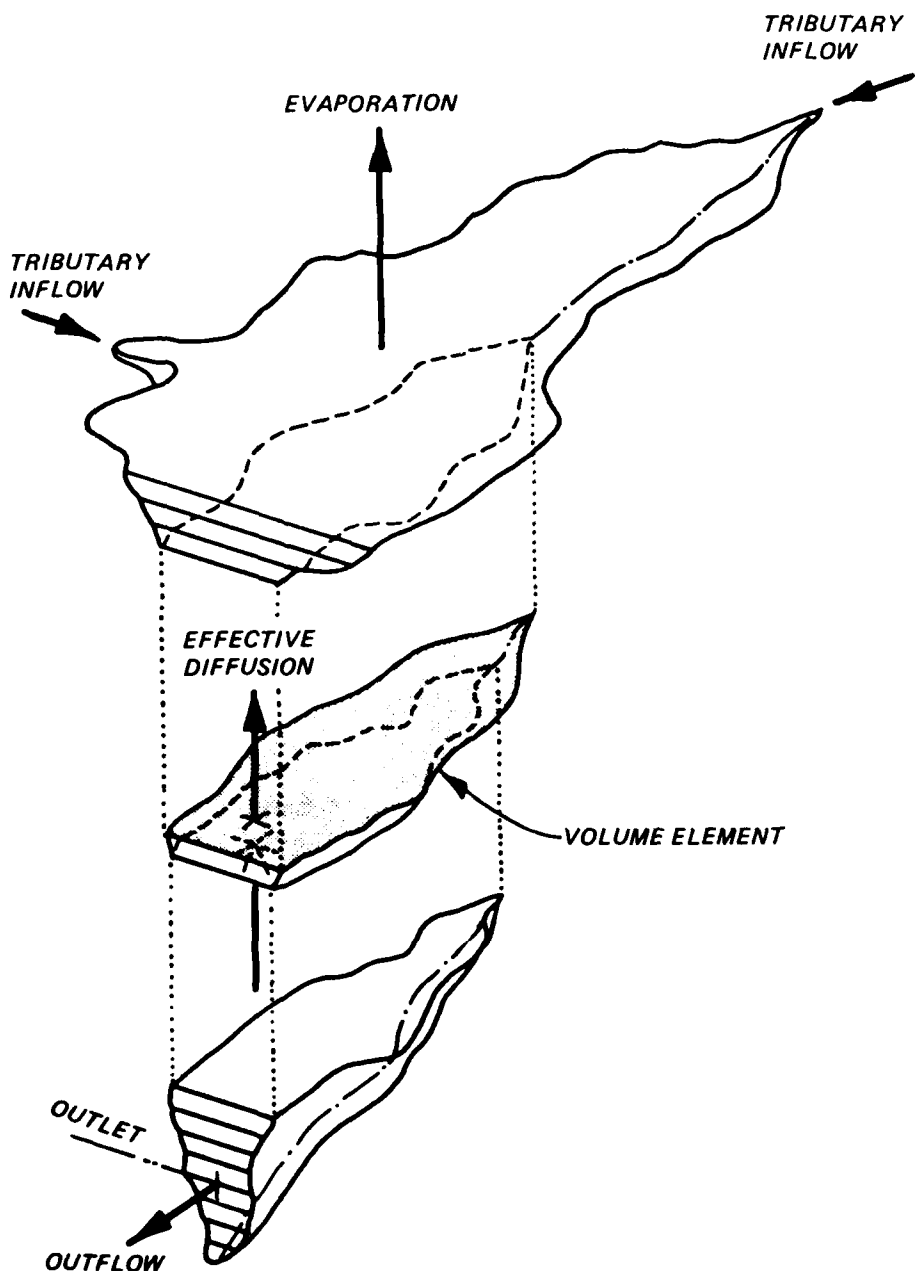


Figure 1. Geometric representation of a stratified reservoir and mass transport mechanisms

energy and biological and chemical material for preimpoundment and post-impoundment studies of water quality. Conceptually, CE-QUAL-R1 depicts a reservoir as a series of horizontal layers (Figure 1) within each of which thermal energy and mass are uniformly distributed. Mathematically, the model's structure is based on variable horizontal layer thickness, which depends on inflowing and outflowing water volume; inflowing water is distributed among the layers by density. Vertical transport of energy and mass is achieved through entrainment and turbulent diffusion.

4. The model can simulate the dynamics of many water quality variables including temperature, DO, phytoplankton, zooplankton, dissolved solids, pH, alkalinity, dissolved inorganic carbon, suspended solids, dissolved organic matter, phosphorus, nitrogen, iron, manganese, and sulfur. Water quality simulations are performed for each layer of the model. A complete description is given in the CE-QUAL-R1 User's Manual (Environmental Laboratory 1982).

Innovations for Simulating Anaerobic Conditions

5. An overriding consideration in developing the new, anaerobic algorithms is to keep the model as simple as possible while adequately representing the system. To this end, the chemistry has been simplified, although the number of additional variables may seem to indicate otherwise.

6. The original concepts for subroutines to deal with anaerobic processes within the framework of CE-QUAL-R1 appear in previous technical reports (Brannon et al. 1978, Gunnison and Brannon 1981). Those reports also contain valuable background information and data. Additional important concepts for the new algorithms are based on data from Environmental and Water Quality Operational Studies (FWQOS) field studies and on the model's one-dimensional assumption.

7. Two simplifying conceptual innovations mark the operation of the anaerobic algorithms. The first is the use of a DO concentration in the water column as a cue to initiate anaerobic processes. Intensive

scrutiny of field data from several locations suggested that a reasonable correlation existed between oxygen decline in the water column and the release and reduction of anaerobic materials. Lum, Armstrong, and Fruh (1981) and Fillos and Molof (1972) have reached similar conclusions. Based on field data from DeGray Lake in the 1979 model calibration year, threshold DO concentration selected was $0.5 \text{ mg} \cdot \text{l}^{-1}$. That is, examination of field data indicates that when declining DO concentrations fall to $0.5 \text{ mg} \cdot \text{l}^{-1}$, dissolved anaerobic materials appear in the water samples. This threshold value subsumes many organic decay or oxygen-depleting processes which may vary among different systems.

8. It may seem that redox chemistry axioms are being violated deliberately by invoking the DO cue. However, the primary redox processes of concern in these subroutines are those resulting in sediment release of dissolved materials. Since we have no data on redox state or dynamic chemical conditions in the sediments, DO in the water column is used as a correlate of sediment redox condition. The assumption that this cue is valid in the water column, as well, may be questioned.

9. Subsequent to the threshold DO concentration being reached, releases of so-called "anaerobic materials" (PO_4^{3-} -P, NH_4^+ -N, Mn^{+2} , Fe^{+2} , and S^{-2}) from sediments and reduction processes in the water column do not occur sequentially as they might if redox potentials were used as cues. Thus, the second major innovation consists of starting the anaerobic processes of sediment release and chemical reduction simultaneously. Each process, however, has its own rate which is fixed initially but may be affected by temperature.

10. The model predicts water quality as though a specific point in a given layer represents the whole layer. A real system would likely be more diverse in composition; that is, spatially separated points at the same elevation are unlikely to be chemically identical. Allowing simultaneous release from the sediments of the various anaerobic materials at different rates is intended to account for the true heterogeneity of the reservoir system within the context of a one-dimensional model. Initiating anaerobic processes simultaneously and calibrating rates to simulate field conditions may resolve electrochemical paradoxes

such as the contemporaneous appearance of dissolved oxygen and dissolved reduced metals.

Anaerobic Subroutines

11. Thirteen new mathematical subroutines in CE-QUAL-R1 calculate water quality variables specifically pertinent to anoxic or low DO conditions. Each subroutine deals with an individual chemical component of water quality and its physical, chemical, and biological interactions with other water quality constituents in the same or adjacent layers.

12. In a conceptualized horizontal layer, anaerobic constituents (or compartments) occur either in the water column or in the sediments (Figure 2). In the water column, anaerobic water quality constituents are generally present either in the oxidized (particulate) or reduced (dissolved) state, depending on DO concentration and duration of anoxia; oxidized, dissolved sulfur (SO_4^{-2}) and reduced, particulate iron sulfide are exceptions.

13. Anaerobic materials in the sediments comprise 6 of the 13 compartments. These sediment compartments have two primary functions. First, they serve as a source for most of the anaerobic materials. Second, they provide a method of accounting for net fluxes of anaerobic materials between the sediments and overlying waters. Within the sediments, actual oxidation states are immaterial for simulation purposes since sediment electrochemistry is not explicitly considered. Again, the important idea is that anaerobic materials are released simultaneously when DO concentrations fall below the threshold value.

14. The following brief summary describes the events depicted in Figure 2 as DO falls below the threshold concentration.

- a. Ammonia (NH_4^+-N), dissolved (reduced) manganese (Mn^{+2}), dissolved (reduced) iron (Fe^{+2}), sulfide (S^{-2}), and dissolved phosphate ($PO_4^{-3}-P$) are released from the sediments at specific rates.

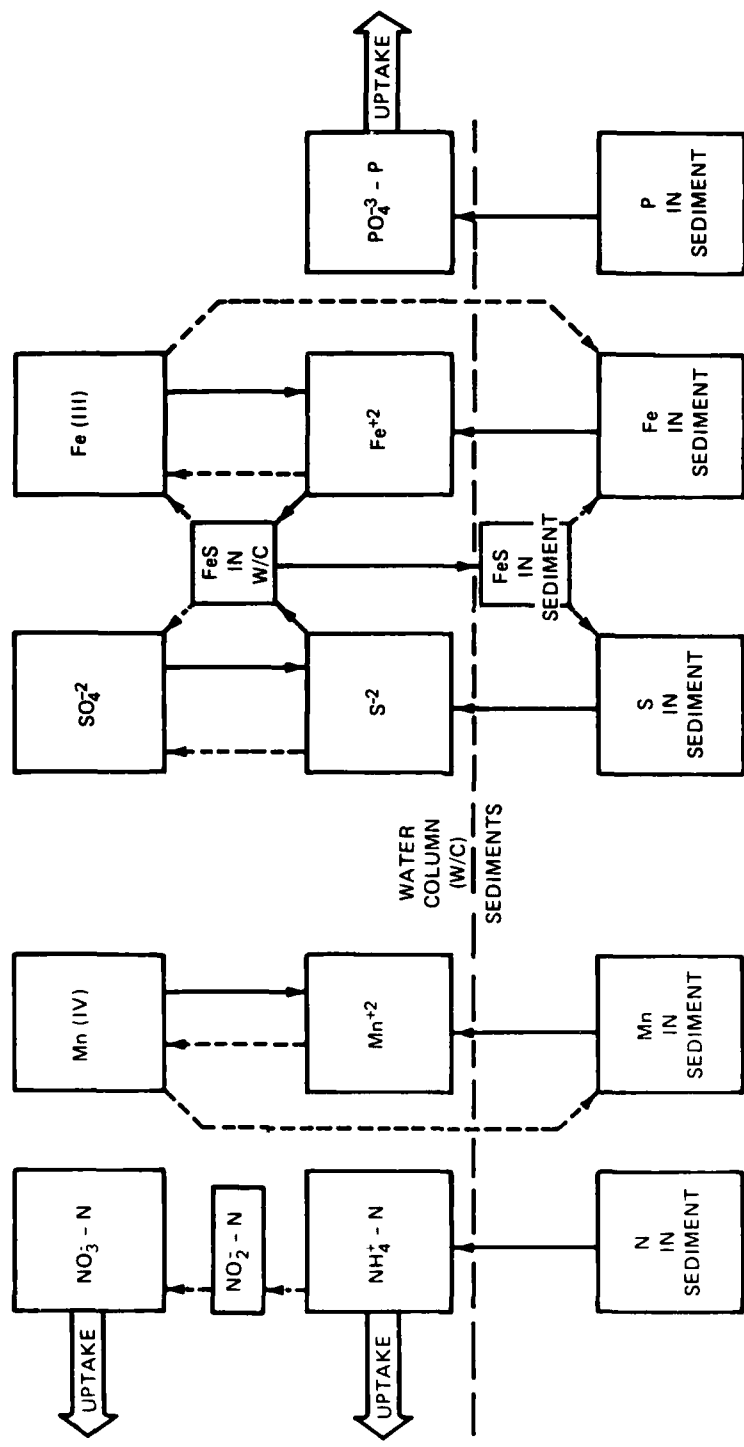


Figure 2. Simplified chemistry associated with anaerobic variables. Dashed lines indicate aerobic pathways; solid lines indicate anaerobic pathways

- b. Particulate manganese (Mn(IV)), particulate iron (Fe(III)), and sulfate (SO_4^{-2}) may be reduced in the water column.
- c. Dissolved iron and sulfide may form insoluble iron sulfide, which may precipitate through the water column to the sediments.

15. To ensure that the supply of anaerobic materials from the sediment is not depleted prematurely, a coefficient defining an active sediment depth is included. When this value is multiplied by concentration in the sediment and the sediment surface area, the product is the available mass of a given sediment component in a particular layer.

This allowed a check on mass balance.

16. When DO is replenished and exceeds the threshold value, oxidation processes predominate: ammonia oxidizes to nitrite and then to nitrate; particulate manganese and iron are generated from dissolved sulfide; sulfide is oxidized to sulfate; and iron sulfide is oxidized to sulfate and particulate iron.

17. The subroutines representing anaerobic processes contain both stoichiometric and kinetic coefficients. The stoichiometric coefficients determine oxygen depletion resulting from oxidation processes. These reactions and their stoichiometric oxygen requirements (grams O_2 consumed:gram material oxidized) are listed in Table 1 by the name assigned each coefficient in the computer program.

18. In calculating the dynamics of a given compartment describing an anaerobic material, additional rate coefficients are required for oxidation-reduction processes, sediment release of reduced substances, and settling velocities of particulates. Reaction rate coefficients express the fraction of the oxidation or reduction reaction completed per day. Release rates refer to the amount of anaerobic material released across a square meter of sediment surface per day. A settling velocity, in meters/day, describes the downward movement of a precipitated chemical compound (oxidized iron or manganese, or iron sulfide) in the water column. Other simplifications involve the use of zero-order

Table 1
Stoichiometric Coefficients Affecting Dissolved
Oxygen Concentration

Coefficient	Reaction	O_2 Requirement*
02NH3	$2NH_4^+ + 3O_2 + 2HCO_3^- = 2CO_2 + 2NO_2^- + 2H^+$	3.43
02NO2	$2NO_2^- + O_2 = 2NO_3^-$	1.14
02DET	$C_5H_7NO_2 + 5O_2 = 5CO_2 + 2H_2O + NH_3$	1.4
02RESP	$C_6H_{12}O_6 + 6O_2 = 6CO_2 + 6H_2O$	1.1
02FAC	same as 02DET	1.4†
02DOM	same as 02DET	1.4
02MN2	$2Mn^{+2} + 1/2 O_2 + 3H_2O = 2MnOOH + 4H^+ \dagger\dagger$	0.15
02FE2	$O_2 + 4Fe^{+2} + 4H^+ = 4Fe^{+3} + 2H_2O \ddagger$	0.14
02S2	$S^{+2} + 2O_2 = SO_4^{-2}$	

* Grams O_2 consumed/gram material oxidized.

** Mean algal and bacterial composition (Golterman 1975, Wang et al. 1978).

† Grams O_2 consumed/gram material produced.

†† Hem (1981).

‡ Stumm and Morgan (1981).

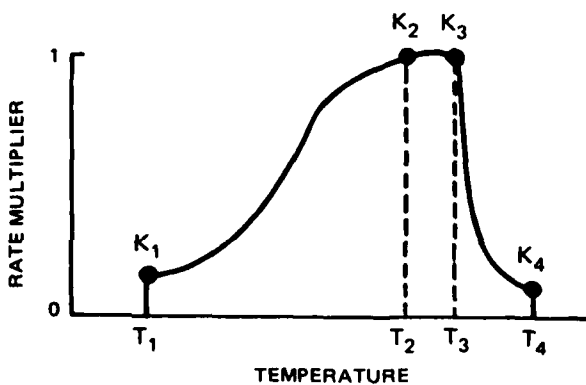


Figure 3. The temperature rate multiplier

kinetics to describe rates of release of anaerobic materials from sediments and first-order reaction kinetics for oxidation-reduction transformations.

19. Reaction rates are supplied initially by the CE-QUAL-R1 user, but may be affected by temperature. Because most chemical and biological reaction rates are temperature dependent, a mathematical function is incorporated in the model to determine the effect of this relationship (Thornton and Lessem 1978). Figure 3 shows the variations of the rate multiplier factors from user-supplied temperatures (T_1 to T_4) and multiplier coefficients (K_1 to K_4), as discussed in the RMULT section of the CE-QUAL-R1 User's Manual (Environmental Laboratory 1982).

20. As an example of the calculations involved, the following equation describes the various processes affecting the concentration of Fe^{+2} in a given layer in the model's formulation:

$$\frac{d}{dt} (VC) = \frac{d}{dz} \left(DA \frac{dc}{dz} \Delta z \right) + \sum Q_{in} C_{in} - Q_{out} C + \gamma_1 \gamma_2 K_{red} V C^* \\ - \gamma_1 \gamma_2 K_{ox} V C - \gamma_3 \gamma_4 K_D V C + \gamma_5 \gamma_6 K_{rel} A_s$$

where

V = layer volume in m^3

C = Fe^{+2} concentration in $g \cdot m^{-3}$

D = Fe^{+2} diffusion coefficient in $m^2 \cdot hr^{-1}$

A = layer area

Δz = layer thickness in m

Q_{in} = layer inflow in $m^3 \cdot hr^{-1}$

Q_{out} = layer outflow in $m^3 \cdot hr^{-1}$

$\gamma_1 \gamma_6$ = temperature rate multipliers (dimensionless)

K_{red} = reduction rate of Fe (III), hr^{-1}

C^* = Fe (III) concentration in $g \cdot m^{-3}$

K_{ox} = oxidation rate of Fe^{+2} , hr^{-1}

K_D = Fe^{+2} reaction rate with S^{+2} to form FeS

K_{rel} = sediment release rate of Fe^{+2} in $g \cdot m^{-2} \cdot hr^{-1}$

A_s = area of sediment releasing Fe^{+2} , m^2

Thus, the first right-hand term in the equation describes changes in Fe^{+2} due to diffusion between layers; the second term accounts for additions from inflowing waters summed over all tributaries; the next term subtracts losses through layer outflow; the fourth term adds Fe^{+2} derived from $\text{Fe}(\text{III})$ reduction; the next term determines losses of Fe^{+2} via oxidation to $\text{Fe}(\text{III})$; the sixth term calculates the amount of dissolved Fe^{+2} lost through reaction with S^{-2} to form FeS ; and the final term increments Fe^{+2} from sediment release. The CE-QUAL-R1 User's Manual contains complete descriptions of the chemical equations and the details of their programming.

PART II: CALIBRATION OF ANAEROBIC SUBROUTINES

Site Characteristics

21. In 1972, DeGray Lake was selected as a field study site for research on water quality modeling under the CE Environmental Impact Research Program (EIRP). The lake was chosen because of the availability of preimpoundment and postimpoundment baseline data, its multiple outlet structure, and pumped storage hydropower capability. In 1977, the EWQOS program selected DeGray Lake as one of four reservoir study sites to provide, among other objectives, information needed in developing and verifying water quality predictive techniques. In this study, data from 1979 were used to calibrate the model, and data from 1980 were used to confirm the model.

Description

22. DeGray Lake, created in 1970 by the impoundment of the Caddo River, is located near Arkadelphia in south-central Arkansas. Its watershed is approximately 30 percent agricultural, with the rest forested. DeGray Lake is a multipurpose reservoir with flood control, power generation, recreation, water supply, and low-flow augmentation of the Ouachita River as project purposes. The lake is a highly dendritic system, approximately 32 km long, with a mean depth of 15 m and a maximum depth of 60 m. The project has pumped storage capability and can withdraw water at three levels in the lake (Ford and Stein 1982). Average hydraulic residence time is 0.8 year (Thornton et al. 1982).

Climatology

23. DeGray Lake experiences a modified continental climate. Summers tend to be long, warm, and humid with air temperatures occasionally exceeding 40° C. Short, mild winters are occasionally affected by cold polar fronts capable of dropping temperatures to -20° C. Mean annual temperature is around 17° C.

24. Precipitation is relatively evenly distributed throughout the year, with the March-May period accounting for about one-third of the total. Summer rains generally consist of scattered showers and

thunderstorms that may be locally intense. In summer and fall, there may be extended periods of drought or near-drought conditions. Late fall is usually marked by increasing rainfall. Average annual precipitation at Arkadelphia is 134 cm.

25. Late winter and early spring are marked by the highest average daily wind speed, while lowest wind speeds are experienced in mid-to late-summer.

26. The meteorological background information given above was based on the report of Ford and Stein (1984). The following material comes from examination of dry bulb temperatures, fractional cloud cover, and wind speed data taken at Little Rock, Ark., approximately 80 km northeast. From these data, some general comparisons can be made between the calibration (1979) and verification (1980) years.

27. Winter 1979 was considerably colder than 1980. In late winter 1979, warming occurred with an abrupt jump of about 5-6° C, before continuing a steady, gradual rise, barely reaching 30° C in summer. In 1980, the gradual warming trend was not marked by an initial fast rise but reached peaks in excess of 30° C several times during the summer. Autumn temperatures declined somewhat faster in 1980 than 1979.

28. Cloud cover may reflect the temperature regimes for 1979 and 1980. Cloud cover seems to have been slightly less in early 1980 than 1979. Summer 1980 had significantly less cloud cover resulting in greater insolation and higher temperatures. The latter part of 1980 was perhaps slightly cloudier than 1979.

29. Average daily wind speed, a significant factor in reservoir mixing, averaged about $12-14 \text{ km}\cdot\text{hr}^{-1}$ during the first half of 1979, dropped to about $8-10 \text{ km}\cdot\text{hr}^{-1}$ during the summer, and picked up again to about $12-13 \text{ km}\cdot\text{hr}^{-1}$ for the rest of the year; highest winds rarely exceeded $20 \text{ km}\cdot\text{hr}^{-1}$. In 1980, wind speeds were about $15 \text{ km}\cdot\text{hr}^{-1}$ during the first third of the year, dropped to about $12 \text{ km}\cdot\text{hr}^{-1}$ in the middle of the year, and rose to around $13-14 \text{ km}\cdot\text{hr}^{-1}$ during the final third. Highest wind speeds in 1980 reached or surpassed $25 \text{ km}\cdot\text{hr}^{-1}$ at the beginning and end of the year. Overall, wind speeds were probably a bit higher in 1980 than 1979.

30. These trends or differences are relatively crude comparisons, but they do serve to point out that year-to-year weather variations may be significant. The ultimate effect of these differences on ecological simulations is at times difficult to assess.

Stratification-destratification cycle

31. DeGray Lake is a warm, monomictic system that typically stratifies by late March. Following thermal stratification, metalimnetic oxygen minima develop in the lake's upper reaches and eventually extend to the rest of the reservoir. Oxygen depletion occurs rapidly and may result in total hypolimnetic anoxia in the relatively shallow, up-reservoir regions. The main body of the reservoir does not exhibit such intense anoxia. This general stratification behavior typifies many CE reservoirs.

32. Historically, complete vertical mixing first occurs in the upper part of the reservoir in October and in the main body by December; however, overturn expected in late fall 1979 was delayed until February 1980. Hydrometeorological conditions left the system poised for mixing (isothermal but chemically stratified) but lacking an energy impulse (e.g., wind) to initiate mixing.

Sampling Procedures

Sampling routine

33. Fortnightly sampling at several locations in the DeGray Lake system provided data necessary for computer simulations. Other intensive, short-term studies of storm events, primary productivity, and areal variation of selected water quality constituents complemented the routine sampling program. Water samples were taken and observations made at locations representing the major inflow and outflow sites in the system as well as at several in-pool locations.

Water quality data

34. Water quality sampling in 1979 was performed on a 2-week basis, with the exception of the last quarter of the year when weekly

samples were taken (for sampling techniques, see Kennedy, Montgomery, and James 1983). In order to make the best possible use of available data, weekly updates were used for simulation input, and missing alternate weekly values for the first 9 months were determined by linear interpolation. Missing analytical data points were also determined in this manner. In order to account for several minor sources of inflowing water affecting water balance, a second tributary was included, with water quality characteristics identical to the major inflow, the Caddo River.

35. Several of the model's variables reflect theoretical considerations. Their values and those of their associated coefficients are either theoretical or based on assumptions concerning, and calculations based on, other data. Variables that are calculated from field data include detritus, dissolved organic matter (DOM), and suspended solids. Anaerobic constituents of sediments--nitrogen, iron, manganese, phosphate, and sulfur--are defined as variables and given values calculated from bulk sediment analysis; these variables are included mainly to track fluxes between water and sediments.

Calibration Overview

36. It is of the utmost importance to predict accurately the temporal and spatial occurrence of the threshold DO concentration that cues the initiation of anaerobic processes. Photosynthesis, algal respiration, and biologically mediated decay processes, as well as physical processes that affect mixing, may significantly influence simulated oxygen profiles. In particular, parameters associated with algal physiology and growth and organic decay appear critical in calibrating biological effects on oxygen concentrations in the water column, as indicated in preliminary work.

37. The influence on the anaerobic subroutines of the biological processes associated with phytoplankton are beyond the scope of this report.

Oxygen Calibration

38. Once the model has been calibrated to provide satisfactory thermal profiles, the graphics utility of CE-QUAL-R1 should be used to examine DO profiles for the time period under consideration. Experience and intuition may play important roles in deciding which coefficients and variables to examine first to achieve the best data fit. Table 2 lists initial coefficient values used in this calibration study. Values for coefficients not originating with the anaerobic algorithms were used in earlier work and may be found in the User's Manual (Environmental

Table 2
Initial Values of Coefficients Used in Calibration Study of
Anaerobic Processes in CE-QUAL-R1

Coefficient	Initial Value
Oxygen cue	$0.5 \text{ mg} \cdot \text{L}^{-1}$
Sediment thickness	5.0 cm
Mn(IV) settling rate	$0.05 \text{ m} \cdot \text{day}^{-1}$
Mn(IV) reduction rate	0.02 day^{-1}
Mn ⁺² sediment release rate	$0.10 \text{ g} \cdot \text{m}^{-2} \cdot \text{day}^{-1}$
Mn ⁺² oxidation rate	0.00 day^{-1}
Fe(III) settling rate	$0.05 \text{ m} \cdot \text{day}^{-1}$
Fe(III) reduction rate	0.03 day^{-1}
Fe ⁺² sediment release rate	$0.10 \text{ g} \cdot \text{m}^{-2} \cdot \text{day}^{-1}$
Fe ⁺² oxidation rate	0.00 day^{-1}
Fe ⁺² -FeS formation rate	0.00 day^{-1}
FeS oxidation rate in sediment	0.00 day^{-1}
FeS settling rate	0.00 day^{-1}
FeS oxidation rate in water column	0.00 day^{-1}
SO ₄ ⁻² reduction rate	0.00 day^{-1}
S ⁻² sediment release rate	$0.00001 \text{ g} \cdot \text{m}^{-2} \cdot \text{day}^{-1}$
S ⁻² oxidation rate	0.3 day^{-1}

(Continued)

Table 2 (Concluded)

Coefficient	Initial Value
S^{-2} -FeS formation rate	0.00 day $^{-1}$
P_4O_3 sediment release rate	0.30 g·m $^{-2}·day^{-1}$
NH_4^+ sediment release rate	0.01 g·m $^{-2}·day^{-1}$

Laboratory 1982). FeS reactions were not examined in this report, so associated initial values are set to 0.0.

39. Reservoirs frequently develop metalimnetic DO minima. As thermal stratification develops and intensifies, anoxic conditions may first occur in the metalimnion and then extend more or less gradually to the hypolimnion, which has been "sealed off" by the metalimnetic density gradient. Therefore, when these conditions are known to occur, the initial step in oxygen calibration should concern accurately predicting the onset of anoxia in the metalimnion. Table 3 summarizes the simulations performed in this study.

40. Figure 4 demonstrates the development of the DO minimum in DeGray Lake simulations and field observations. The simulation compares favorably with the observed data with regard to the initiation of anoxic conditions in early August. The model slightly underestimates the amount of oxygen present in the hypolimnion after stratification is well established in the summer. Changes in the decay rate of an organic component, such as DOM, detritus, or sediment, would seem to provide a remedy for this discrepancy. However, to decrease overall rates would also affect epilimnetic oxygen concentrations, which appear satisfactory. Therefore, modification of the temperature rate multiplier (see Figure 3) for DOM to decrease decay rates in the cooler hypolimnetic waters should consequently result in higher oxygen concentrations.

Table 3
Summary of Simulation Figures

Figure No.	Graph of:	Type of Simulation or Coefficient Tested	Value Used
4	O_2	Initial simulation	Values in Table 2
5	O_2	DOM rate multiplier	0.10
6	O_2	DOM rate multiplier	0.04
7	O_2	DOM decay rate	0.0040 day ⁻¹
8	O_2	Sediment decay rate	0.009 day ⁻¹
9	O_2	Detritus decay rate	0.10 day ⁻¹
10	NH_4^+-N	Initial simulation	0.01 g N·m ⁻² ·day ⁻¹
11	NH_4^+-N	NH_4^+-N release rate	0.00 g N·m ⁻² ·day ⁻¹
12	$PO_4^{3-}-P$	Initial simulation	0.001 g P·m ⁻² ·day ⁻¹
13	$PO_4^{3-}-P$	$PO_4^{3-}-P$ release rate	0.000 g P·m ⁻² ·day ⁻¹
14	Mn^{+2}	Initial simulation	0.1 g Mn·m ⁻² ·day ⁻¹
15	Total Mn	Initial simulation	0.1 g Mn·m ⁻² ·day ⁻¹
16	Mn^{+2}	Mn^{+2} release rate	0.05 g Mn·m ⁻² ·day ⁻¹
17	Mn^{+2}	Mn^{+2} release rate	0.20 g Mn·m ⁻² ·day ⁻¹
18	Total Mn	Mn^{+2} release rate	0.05 g Mn·m ⁻² ·day ⁻¹
19	Total Mn	Mn^{+2} release rate	0.20 g Mn·m ⁻² ·day ⁻¹
20	Mn^{+2}	Mn (IV) reduction rate	0.00 day ⁻¹
21	Total Mn	Mn (IV) reduction rate	0.00 day ⁻¹
22	Mn^{+2}	Mn (IV) reduction rate	0.02 day ⁻¹
23	Total Mn	Mn (IV) reduction rate	0.02 day ⁻¹
24	Fe^{+2}	Initial simulation	0.10 g Fe·m ⁻² ·day ⁻¹
25	Total Fe	Initial simulation	0.10 g Fe·m ⁻² ·day ⁻¹
26	Fe^{+2}	Fe^{+2} release rate	0.05 g Fe·m ⁻² ·day ⁻¹
27	Total Fe	Fe^{+2} release rate	0.05 g Fe·m ⁻² ·day ⁻¹
28	Fe^{+2}	Fe^{+2} release rate	0.20 g Fe·m ⁻² ·day ⁻¹
29	Total Fe	Fe^{+2} release rate	0.20 g Fe·m ⁻² ·day ⁻¹

(Continued)

Table 3 (Concluded)

Figure No.	Graph of:	Type of Simulation or Coefficient Tested	Value Used
30	Fe^{+2}	Fe(III) reduction rate	0.00 day^{-1}
31	Total Fe	Fe(III) reduction rate	0.00 day^{-1}
32	Fe^{+2}	Fe(III) reduction rate	0.06 day^{-1}
33	Total Fe	Fe(III) reduction rate	0.06 day^{-1}
34	S^{-2}	Initial simulation	$10^{-5} \text{ g S} \cdot \text{m}^{-2} \cdot \text{day}^{-1}$
35	S^{-2}	S^{-2} release rate	$10^{-4} \text{ g S} \cdot \text{m}^{-2} \cdot \text{day}^{-1}$
36	S^{-2}	SO_4^{-2} reduction rate	0.000 day^{-1}
37	S^{-2}	SO_4^{-2} reduction rate	0.002 day^{-1}
38	S^{-2}	SO_4^{-2} reduction rate	0.000 day^{-1}
		S^{-2} release rate	$0.1 \text{ g S} \cdot \text{m}^{-2} \cdot \text{day}^{-1}$
39	O_2	1980 simulation	as in Table 2
40	Mn^{+2}	1980 simulation	as in Table 2
41	Fe^{+2}	1980 simulation	as in Table 2
42	S^{-2}	1980 simulation	as in Table 2
43	O_2	Anaerobic versus nonanaerobic	as in Table 2

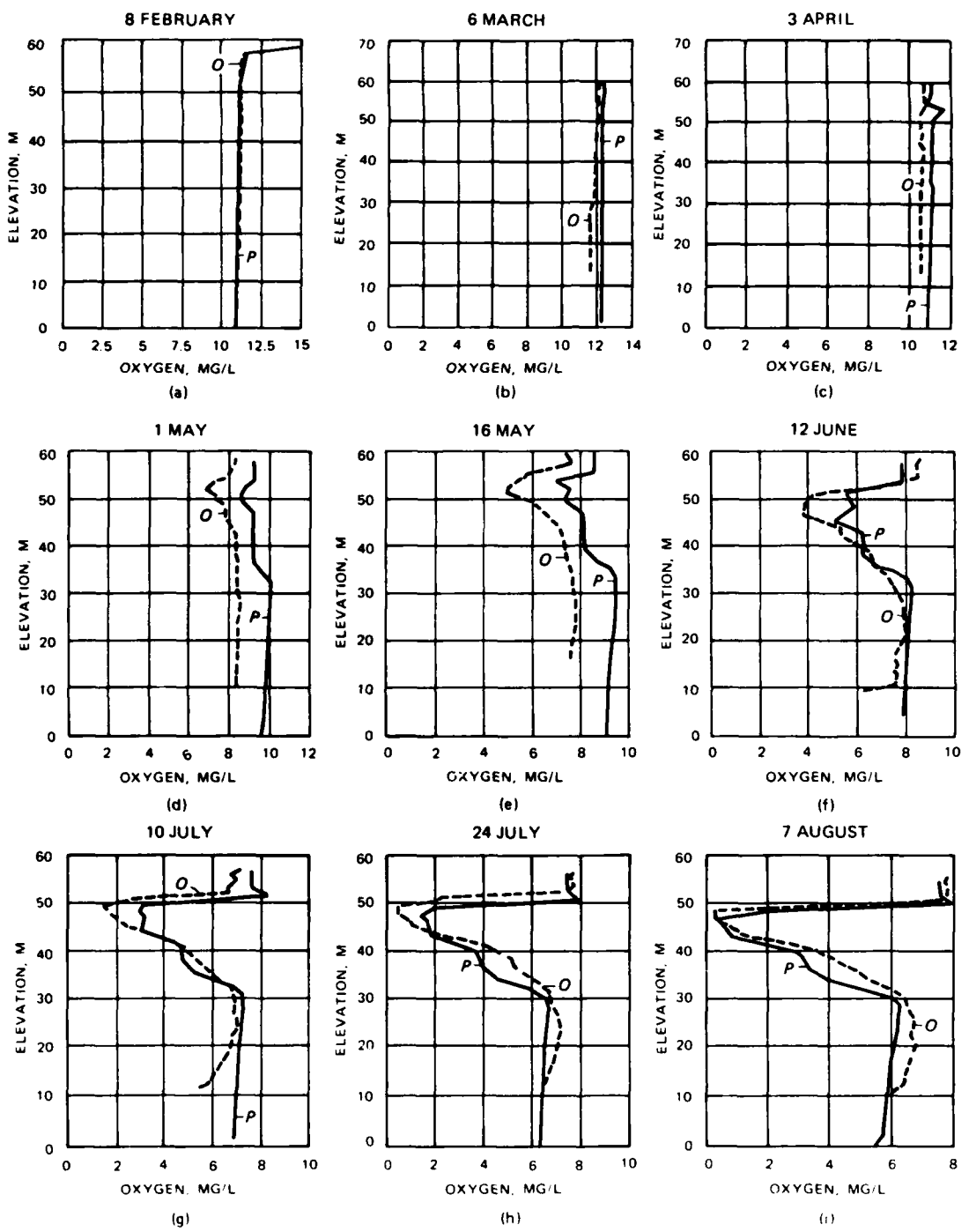


Figure 4. Predicted (P) and observed (O) oxygen profiles for DeGray Lake in 1979 (Continued)

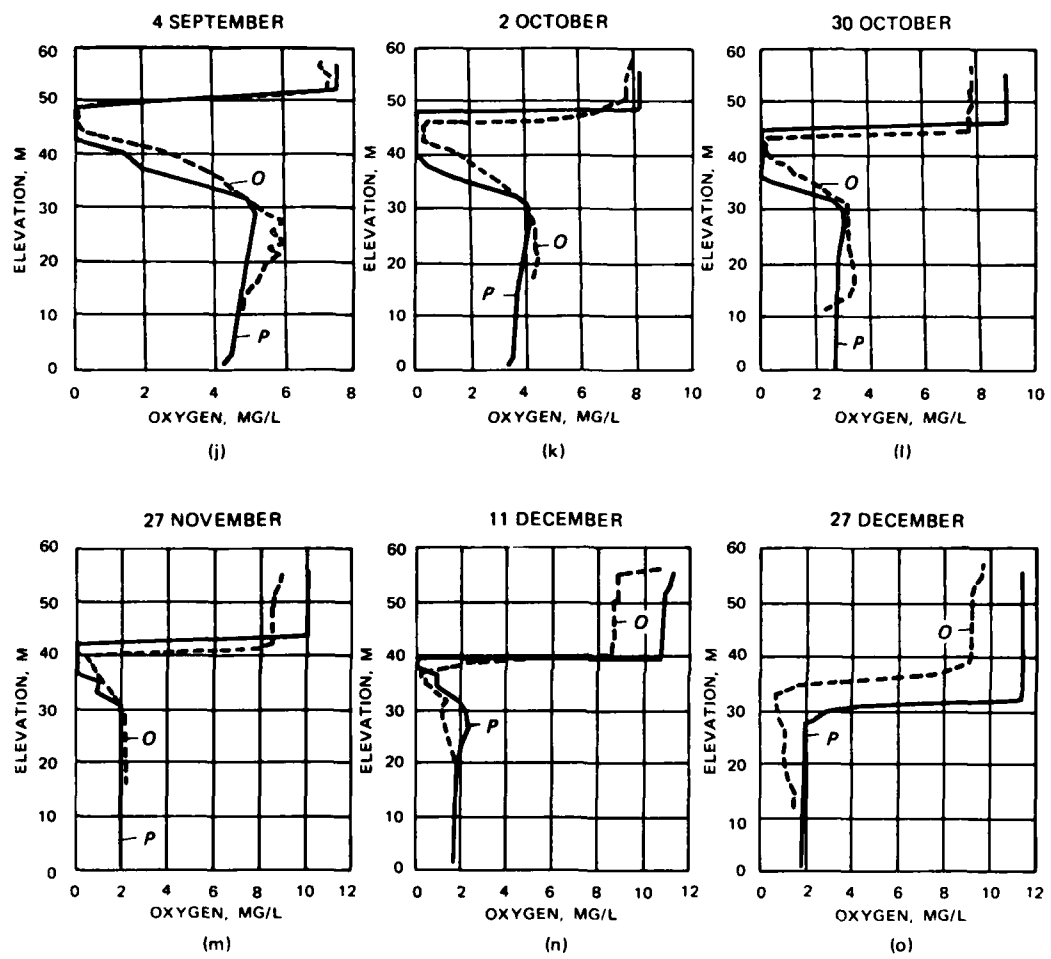


Figure 4. (Concluded)

41. For example, the lower DOM temperature rate multiplier is initially set equal to 0.12. As a first test, lowering the value to 0.10 should provide an indication of the system's sensitivity to this parameter. Figure 5 presents selected simulated and observed oxygen profiles. Differences from the original profiles (Figure 4) are marginal. More drastic changes, e.g. setting the temperature rate multiplier to 0.04, yield variable results (Figure 6). The simulation curve fits the observed profile very well just below the oxygen minimum; however, in the hypolimnion, the fit is considerably worse. In this case, then, it seems best to leave the rate at 0.12 and to attempt to improve the simulation by altering other parameters.

42. Another constant that may have an impact on the rate of oxygen depletion is the DOM decay rate, initially set at 0.0045 day^{-1} . Reducing this rate to 0.0040 day^{-1} significantly slows the dissolved oxygen loss (Figure 7). While this change does generate a good fit below the metalimnetic oxygen minimum, it also delays the onset of anoxia in the metalimnion and causes the hypolimnion to experience higher than observed oxygen levels at the end of the year. Results such as these are somewhat ambiguous; since the 0.0045 day^{-1} value gives the better approach to anoxia initiation, it will be used even though a value of 0.0040 day^{-1} may generally improve the hypolimnetic oxygen simulation. In any event, it is obvious that DO is very sensitive to manipulations of this rate.

43. Organic sediment, too, comprises a potentially large oxygen sink through its decay. Sediment is one of the model's variables for which field data are not used because of the lack of information on the depth of sediment interaction with the water column. The organic sediment value is set sufficiently large to prevent depletion. The sediment decay rate thus may exert a sizable influence on the rate of oxygen depletion. Figure 8 shows the effect of a 50-percent increase in the rate, from 0.006 to 0.009 day^{-1} . Through the onset of metalimnetic anoxia, the effect appears minimal, primarily causing a slight increase in oxygen loss in the hypolimnion which persists through the calendar year.

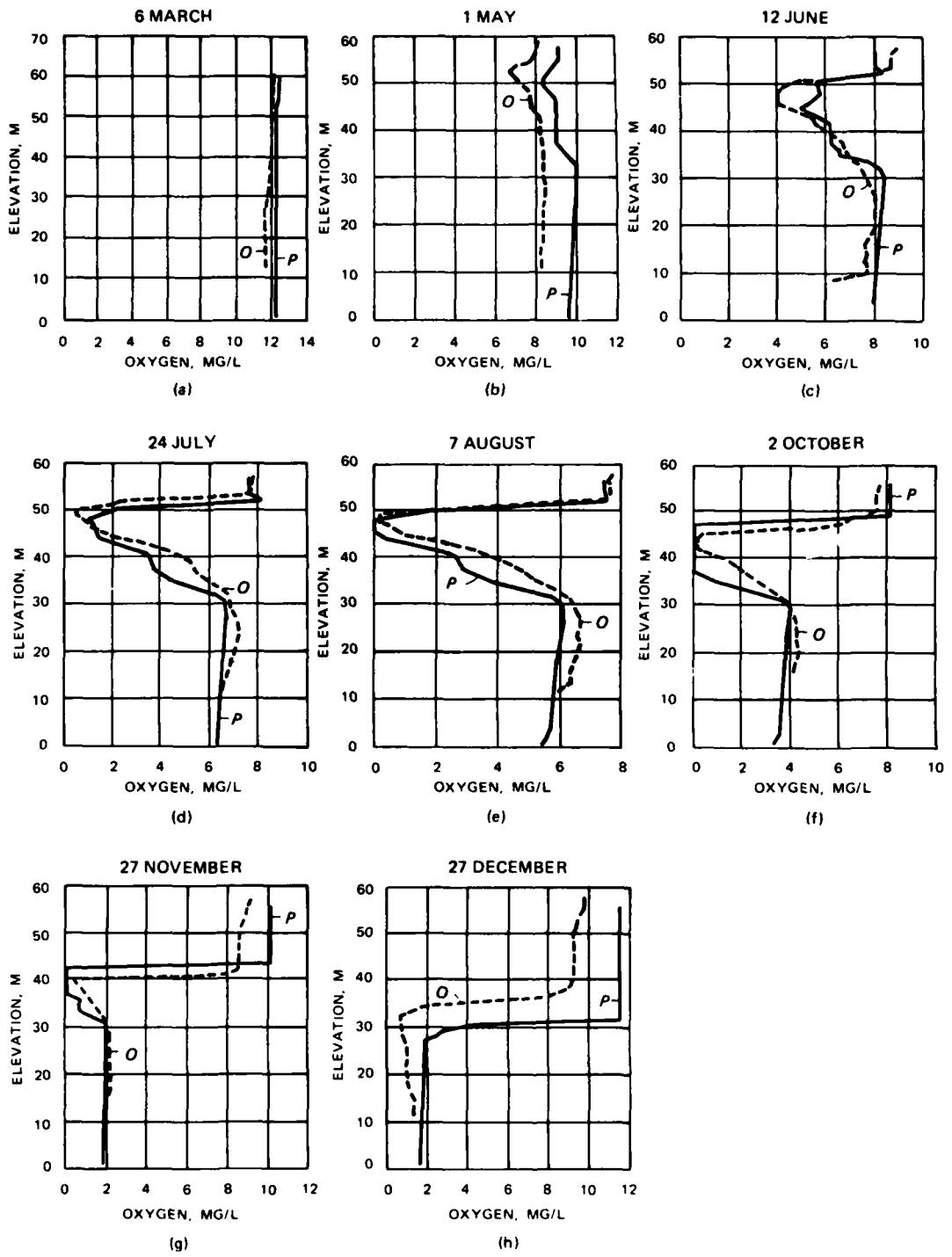


Figure 5. Selected DeGray Lake oxygen profiles in 1979 with the DOM temperature rate multiplier set at 0.10 (P = predicted value; O = observed)

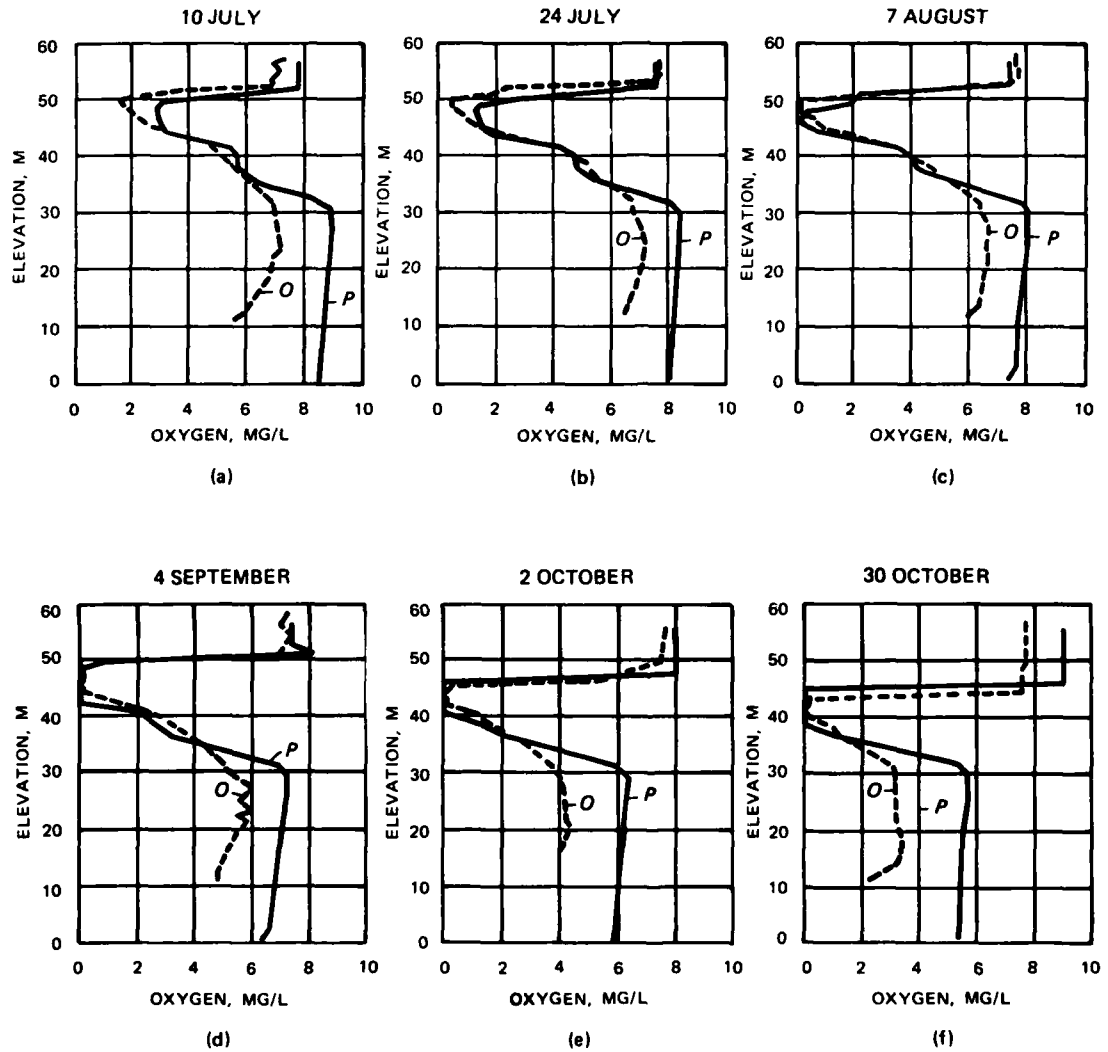


Figure 6. Selected DeGray Lake oxygen profiles in 1979 with the DOM temperature rate multiplier set at 0.04 (P = predicted value; O = observed)

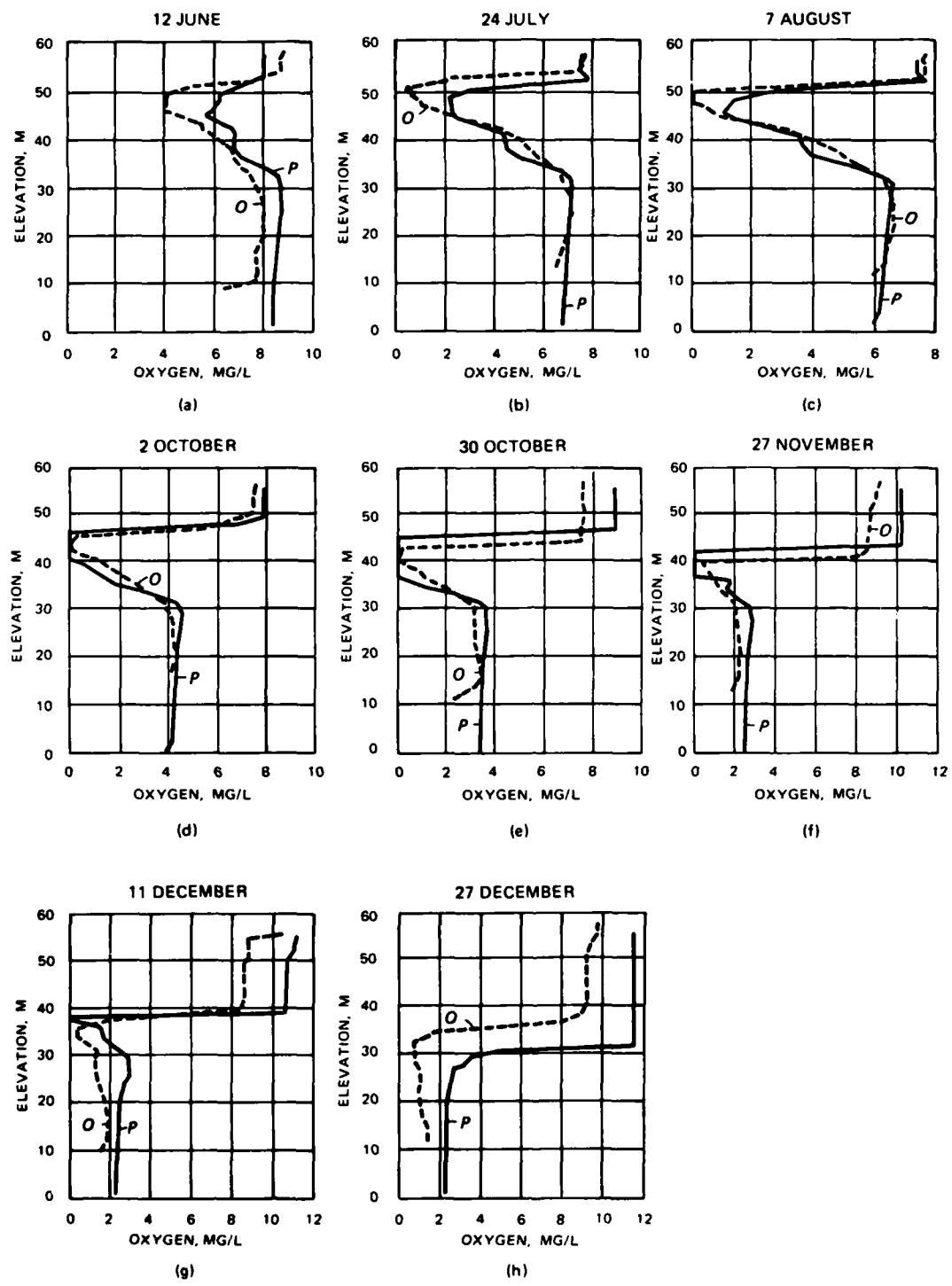


Figure 7. Selected DeGray Lake oxygen profiles in 1979 with the DOM temperature rate multiplier set at 0.004 (P = predicted value; O = observed)

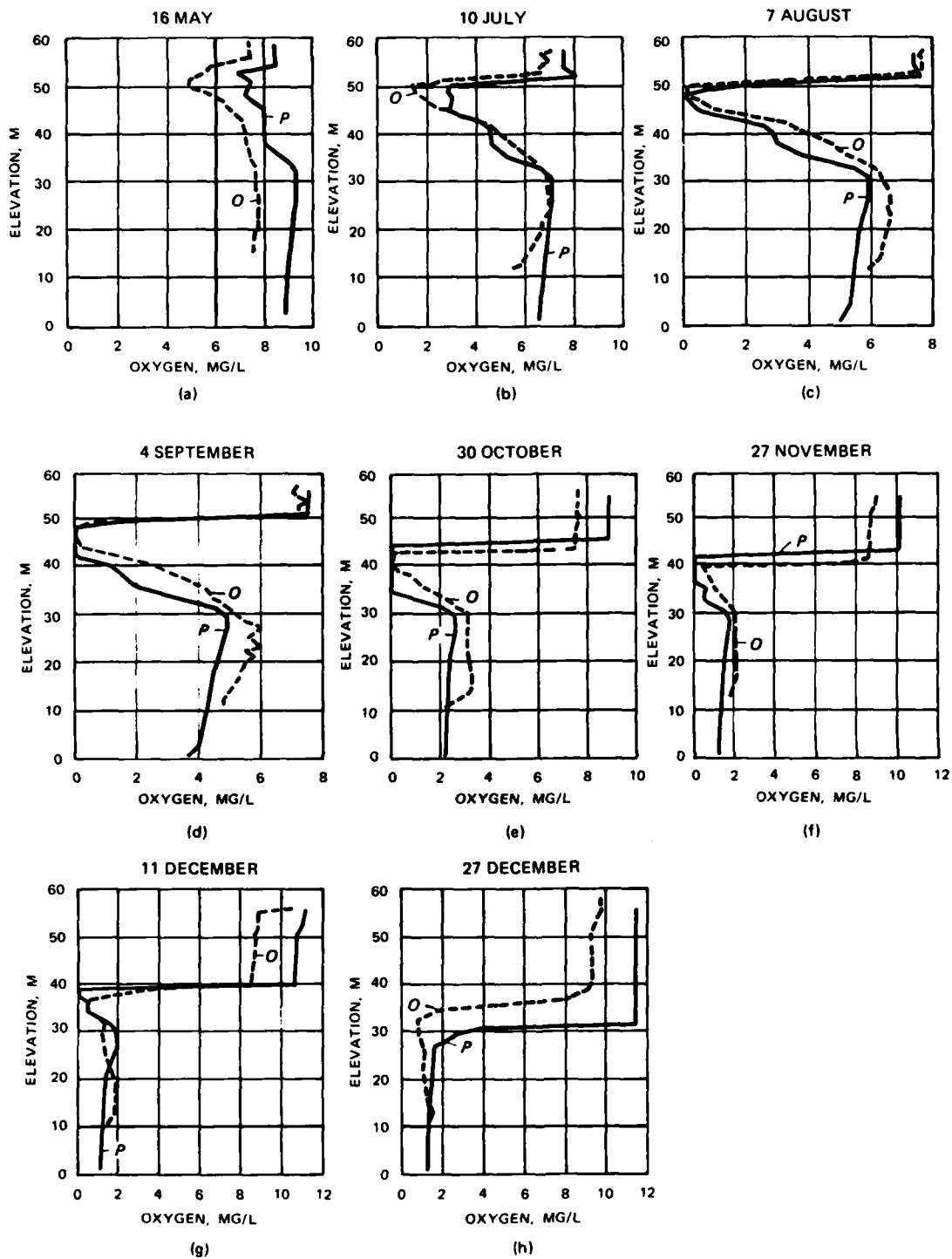


Figure 8. Selected DeGray Lake oxygen profiles in 1979 with the sediment decay rate at 0.009 day^{-1} (P = predicted value; O = observed)

44. Similarly, increases in the rate of detritus decay from 0.006 to 0.10 day^{-1} have an insignificant effect on oxygen profiles (Figure 9).

45. In short, for this particular data set, manipulations of DOM decay most strongly affect DO concentrations when compared with other organic material decay rates. While conditions may vary among data sets, this suggests, at minimum, that DOM decay should be the first rate to test when calibrating other data sets. Finer adjustments may be possible with detritus and sediment decay rates.

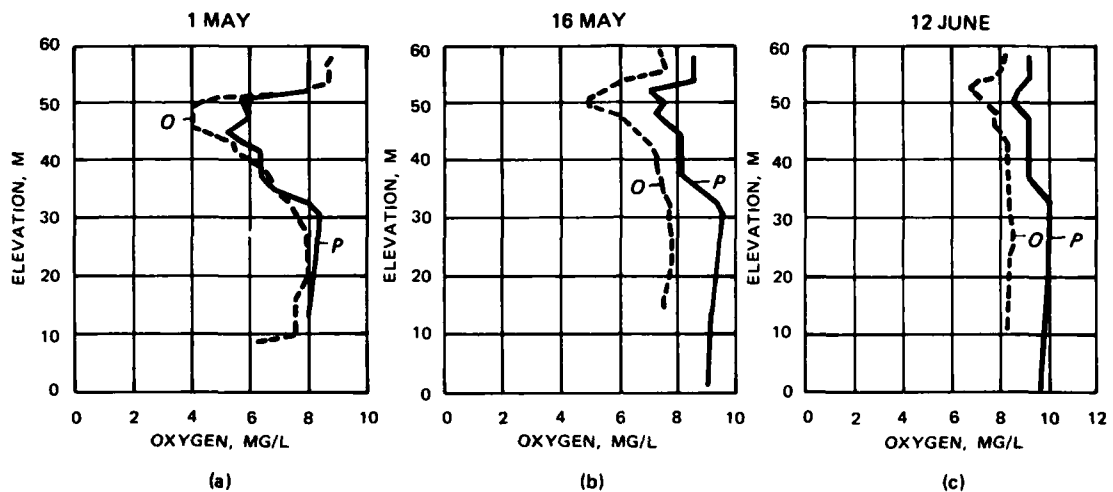


Figure 9. Selected DeGray Lake oxygen profiles in 1979 with the detritus decay rate set at 0.10 day^{-1} (P = predicted value; O = observed)

Calibration of Anaerobic Materials

Ammonium and orthophosphate

46. The anaerobic subroutines deal with the effects of anoxic conditions on five elements. Two of these elements, nitrogen (in the form of ammonia, $\text{NH}_4^+ \text{-N}$) and phosphorus (as orthophosphate, $\text{PO}_4^{3-} \text{-P}$), are also included as variables in the "aerobic" portions of CE-QUAL-R1; decay and other aerobic processes may act to mask the effects of anaerobic release.

47. Comparison between output (Figure 10) from an initial

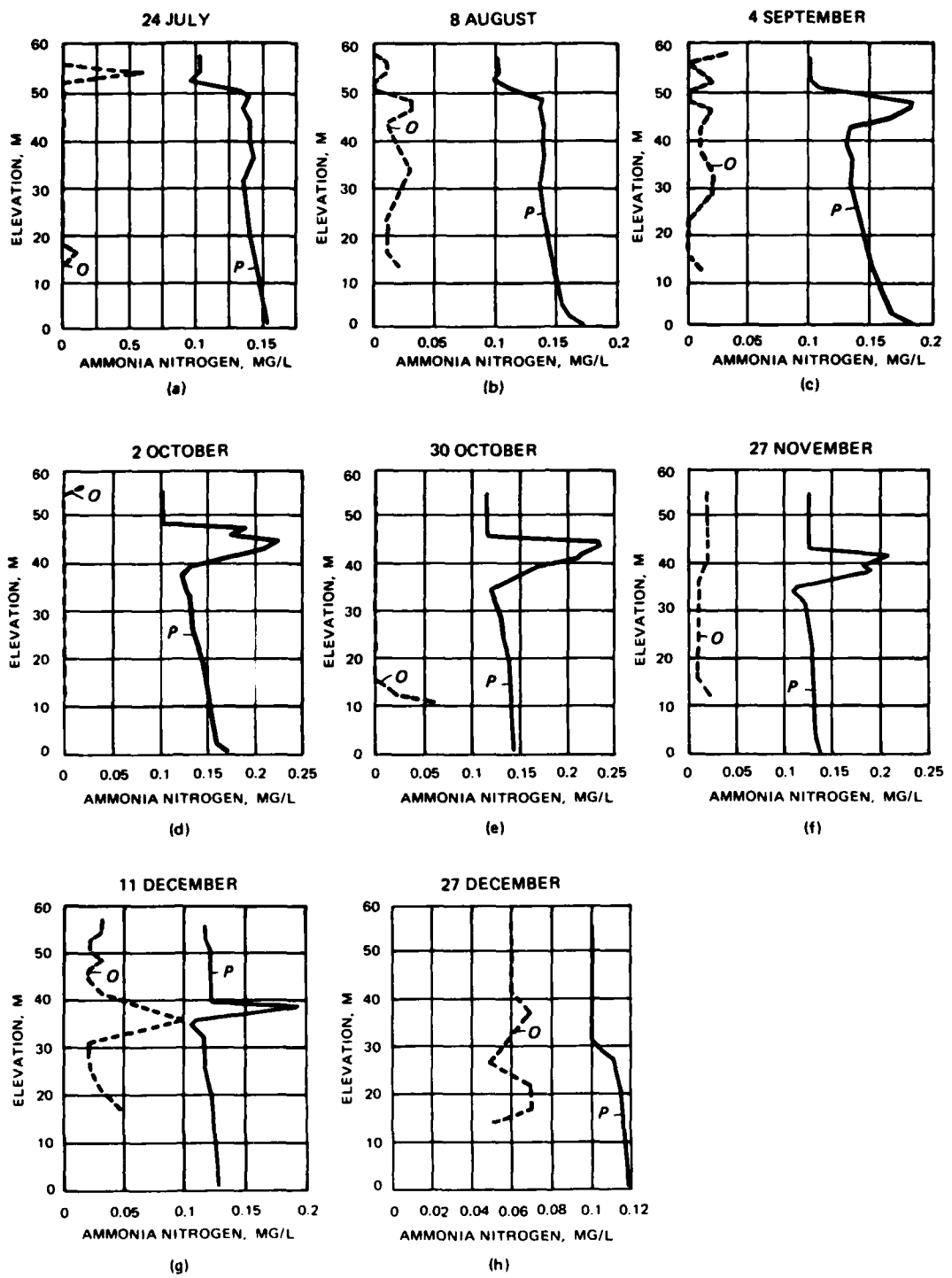


Figure 10. Selected NH_4^+ -N profiles for DeGray Lake 1979
(P = predicted value; O = observed)

simulation with an anaerobic NH_4^+ -N release rate of $0.01 \text{ g N} \cdot \text{m}^{-2} \cdot \text{day}^{-1}$ and a second run with a zero release rate (Figure 11) reveals two important results. First, the model overestimates NH_4^+ -N concentrations throughout the year irrespective of anaerobic conditions. Second, the decrease in NH_4^+ -N concentration in the $0.00 \text{ g N} \cdot \text{m}^{-2} \cdot \text{day}^{-1}$ release rate simulation demonstrates that a slight change in release rate may significantly affect concentrations in those layers experiencing anaerobic conditions; however, the potential impact of this latter observation is uncertain when one considers the overall high simulated NH_4^+ -N concentrations.

48. PO_4^{3-} -P simulations (Figure 12) also overestimate total concentrations (except at the surface, where comparison is quite good). Even when the phosphorus release rate from sediments under anaerobic conditions is set to zero, improvement is minimal (Figure 13).

49. The discrepancies between predicted and observed values for NH_4^+ -N and PO_4^{3-} -P cloud this aspect of the evaluation of the anaerobic subroutines; because these vital nutrients are available in excess, subsequent, interrelated phenomena of algal growth, photosynthesis, and respiration may be distorted. It may be that the instantaneous dispersal into the water column of inflowing nutrients, implicit in the one-dimensional assumption, is at fault. Nutrient adsorption to suspended solids may also contribute to these discrepancies. Program modifications to appropriately model the nutrients' dispersal to better reflect actual reservoir conditions by adding nutrient adsorption and settling algorithms to the model were incorporated following completion of this study (Wlosinski and Collins 1985).

Manganese

50. In the simulated reservoir system, manganese may occur as the dissolved, reduced metal (referred to as Mn^{+2}) or as total manganese (the sum of dissolved and particulate manganese, assumed to be the oxy-hydroxide, $\text{Mn}(\text{IV})\text{OOH}$). Following the onset of anoxia and during stratification, sediment release and Mn^{+2} reduction rates control manganese concentrations.

51. After metalimnetic anoxic conditions develop, computer

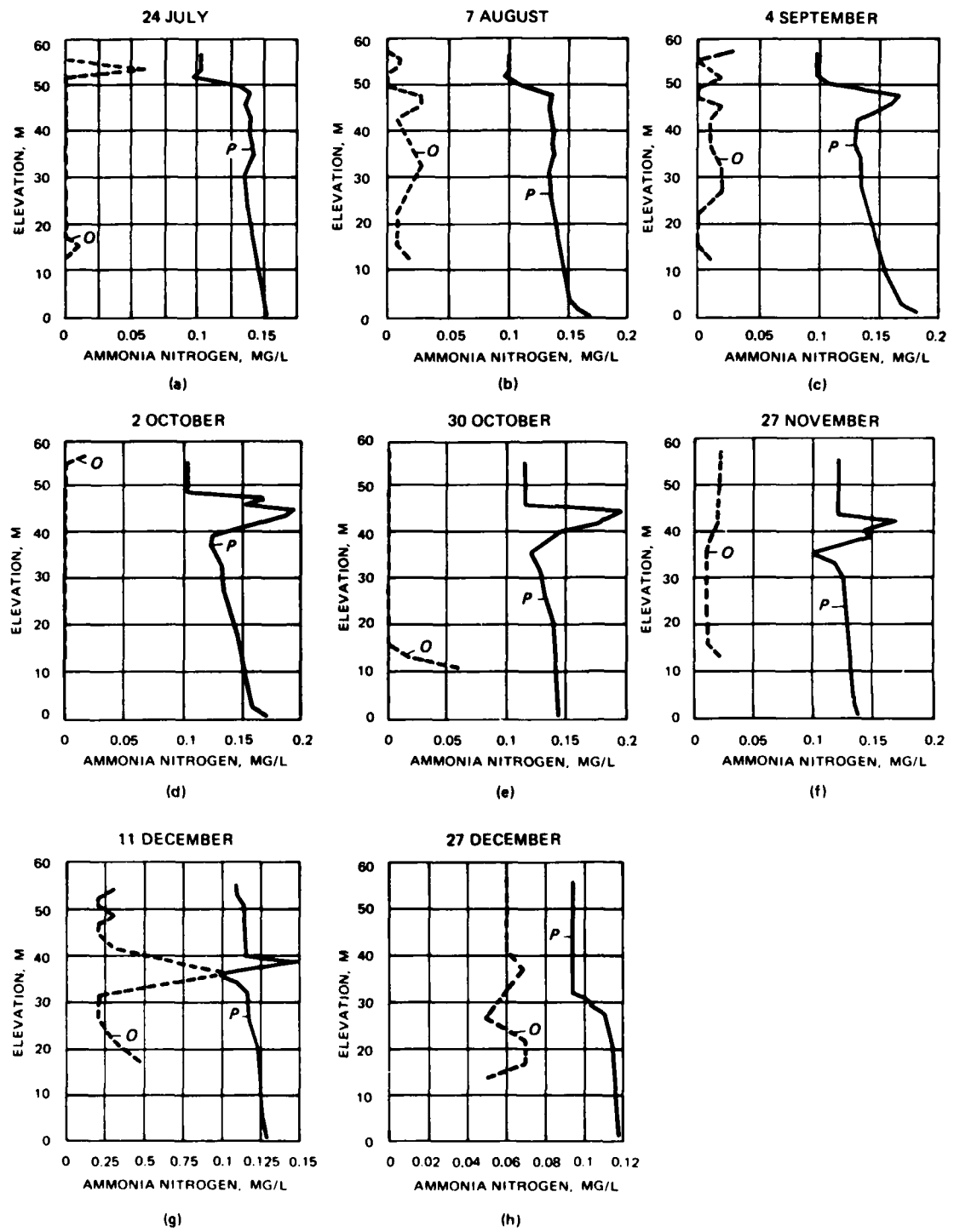


Figure 11. Selected NH_4^+ -N profiles for DeGray Lake in 1979 with sediment release rate = $0.00 \text{ g N} \cdot \text{m}^{-2} \cdot \text{day}^{-1}$ (P = predicted value; O = observed)

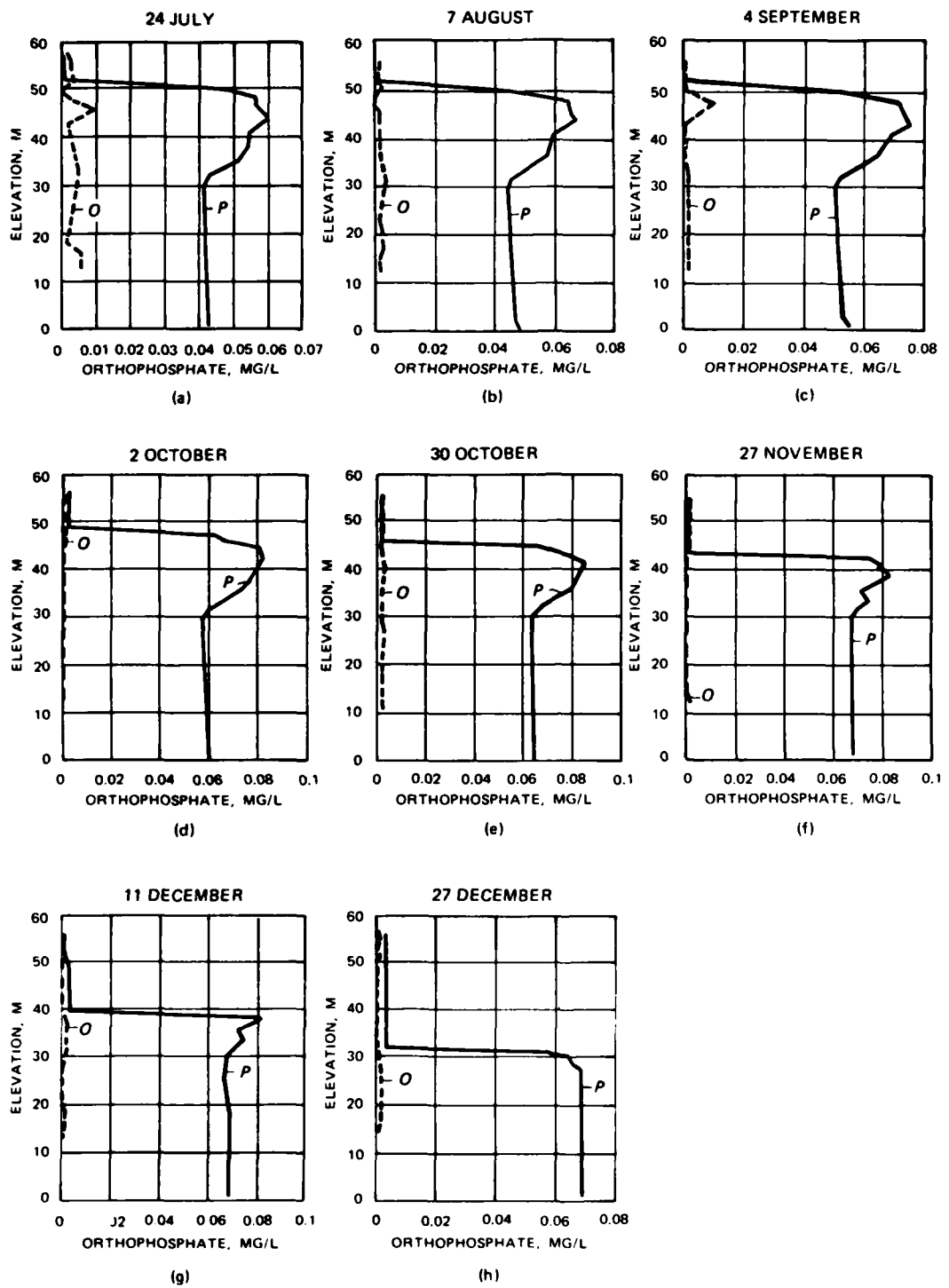


Figure 12. Selected PO_4^{3-} -P profiles for DeGray Lake in 1979
(P = predicted value; O = observed)

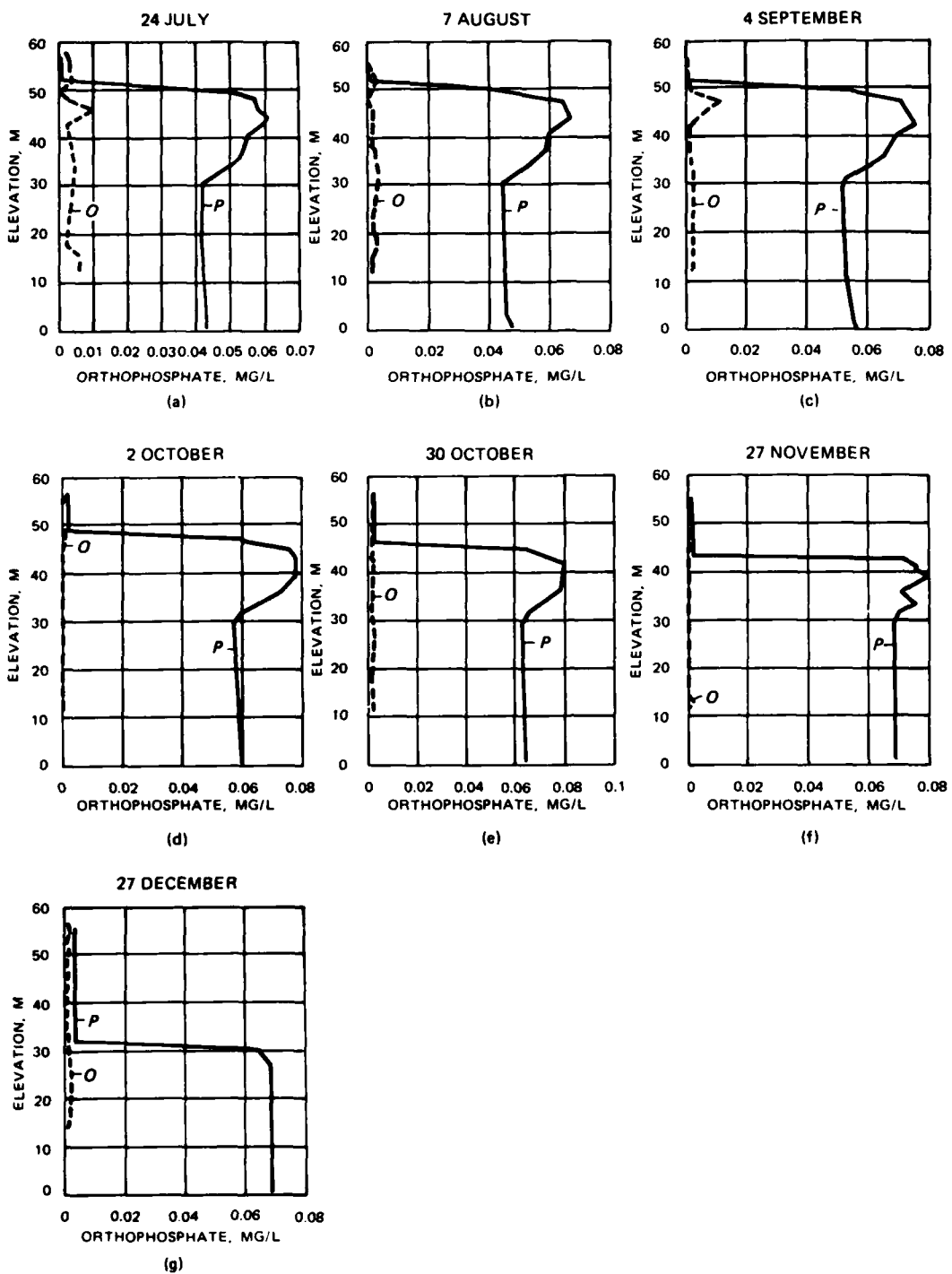


Figure 13. Selected PO_4^{3-} -P profiles for DeGray Lake in 1979 with sediment release rate = $0.00 \text{ g P} \cdot \text{m}^{-2} \cdot \text{day}^{-1}$ (P = predicted value; O = observed)

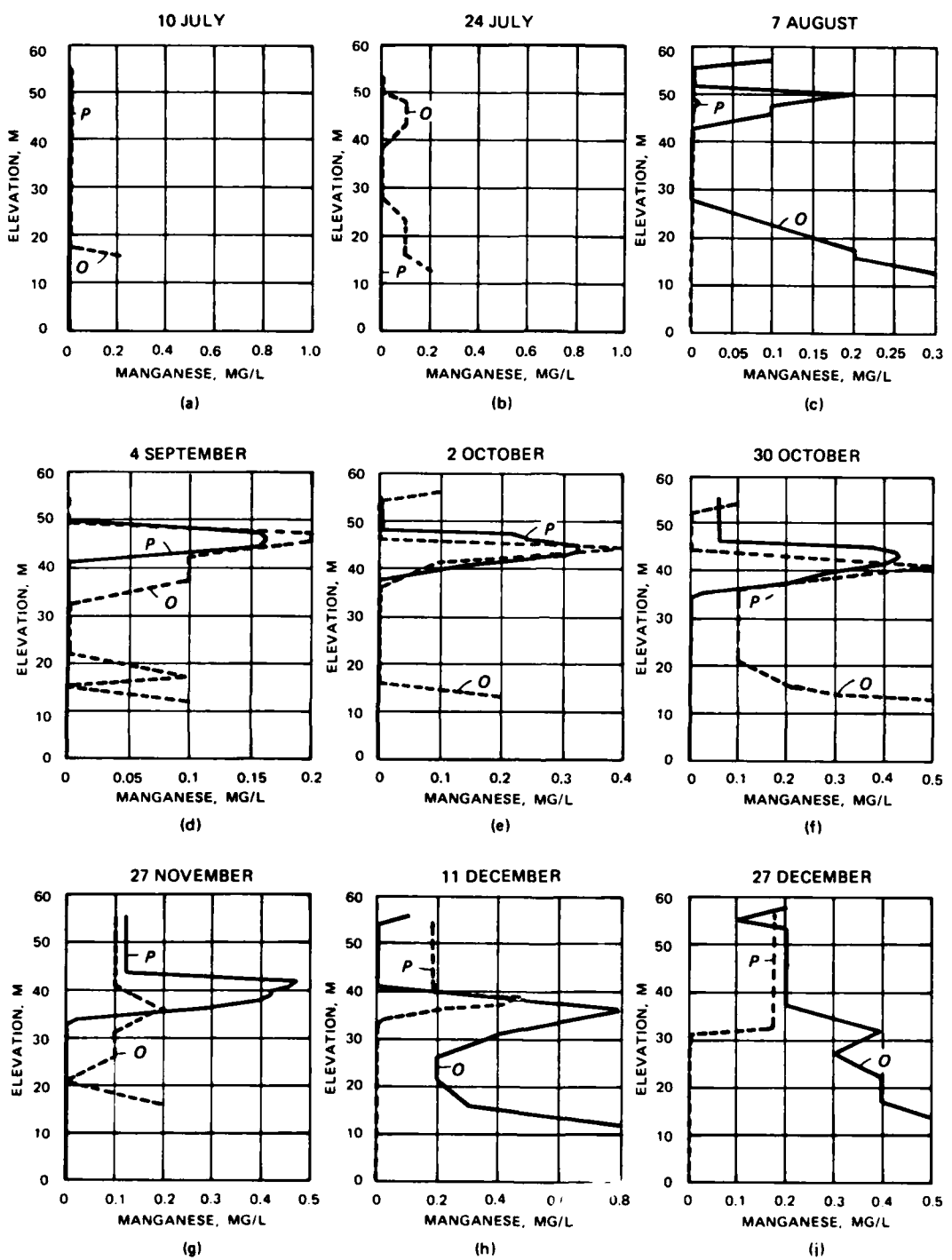


Figure 14. Selected dissolved Mn^{2+} profiles for DeGray Lake in 1979 (P = predicted value; O = observed)

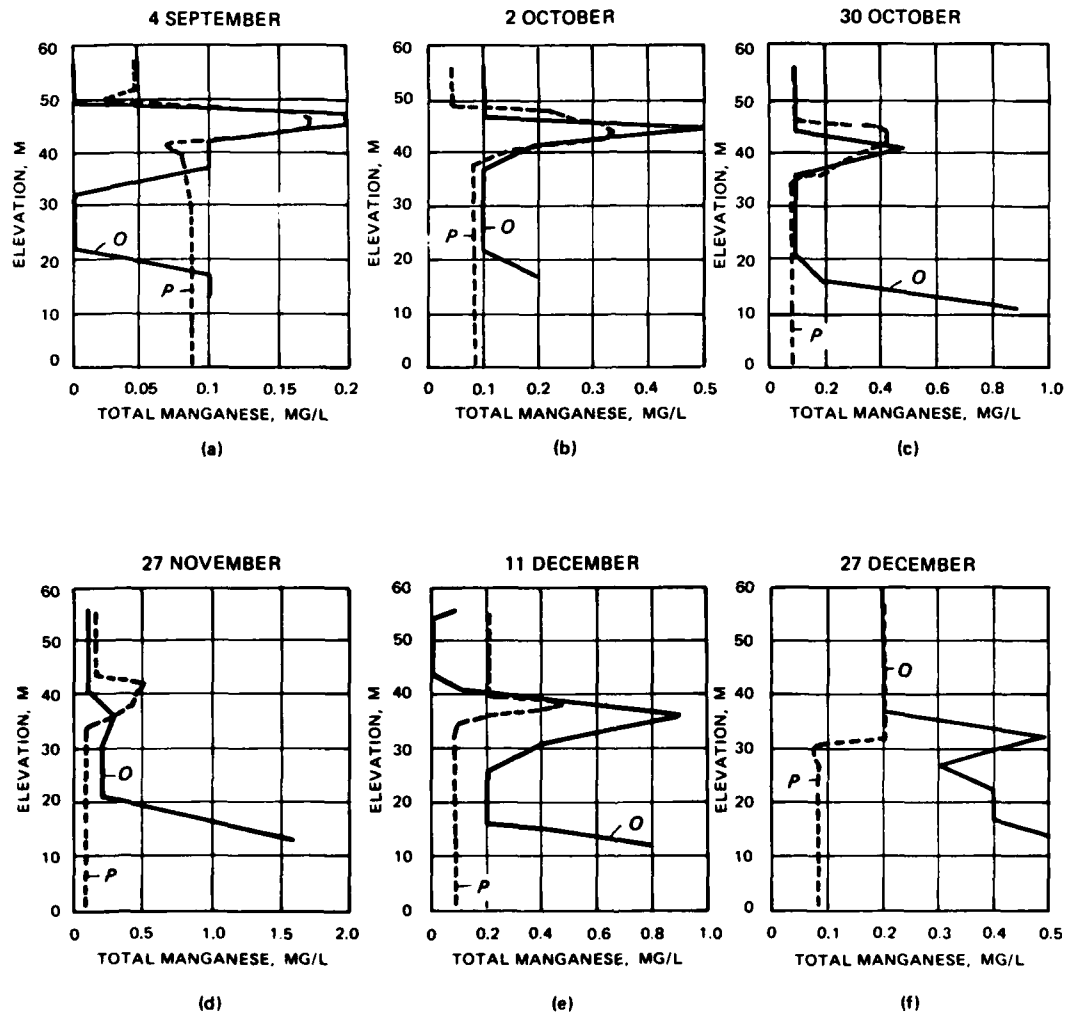


Figure 15. Selected total Mn profiles for DeGray Lake in 1979 (P = predicted value; O = observed)

predictions match measured values quite well in the anoxic zone (Figures 14 and 15). Maximum simulated Mn^{+2} concentrations occur in late November on a date when measured values are incongruously low (Figure 14g); after that dip, concentrations return to higher levels (Figure 14h). Total Mn concentrations develop similarly, peaking in mid-December when some of the dissolved Mn^{+2} begins to oxidize (Figure 15e). Observed hypolimnetic values of total and dissolved manganese are higher than in simulations. Observed DO concentrations are about $1-2 \text{ mg} \cdot \text{L}^{-1}$. Standard redox chemistry principles would deny the presence of Mn^{+2} at the observed hypolimnetic oxygen concentrations, which more than suffice to prevent sediment release of Mn^{+2} with the $0.5 \text{ mg DO} \cdot \text{L}^{-1}$ threshold.

52. The nominal value for Mn^{+2} release from sediments is $0.1 \text{ g Mn} \cdot \text{m}^{-2} \cdot \text{day}^{-1}$. For heuristic purposes, several figures are presented in which this value is halved (Figures 16 and 17) or doubled (Figures 18 and 19). Concentrations of dissolved and total manganese correspondingly decrease by one-half or double. No effect is seen in the hypolimnion.

53. Figures 20-23 depict effects of varying Mn(IV) reduction rates. Setting the rate to 0.00 day^{-1} has no apparent influence on dissolved Mn^{+2} (Figure 20) and only a minor effect on total manganese in the metalimnion (Figure 21). Doubling the initial reduction rate of 0.02 day^{-1} changes neither dissolved nor total manganese concentrations (Figures 22 and 23, respectively).

54. In short, the manganese sediment release rate appears to be the principal controlling factor affecting manganese concentration in the model.

Iron

55. Iron chemistry, with the potential for reaction between reduced iron and sulfide, presents a more complex picture than manganese. As in the case of manganese, the model adequately simulates dissolved and total iron in the anoxic metalimnion (Figures 24 and 25). Like manganese, however, the problem of high observed hypolimnetic iron concentrations recurs in spite of DO levels in excess of $0.5 \text{ mg O}_2 \cdot \text{L}^{-1}$.

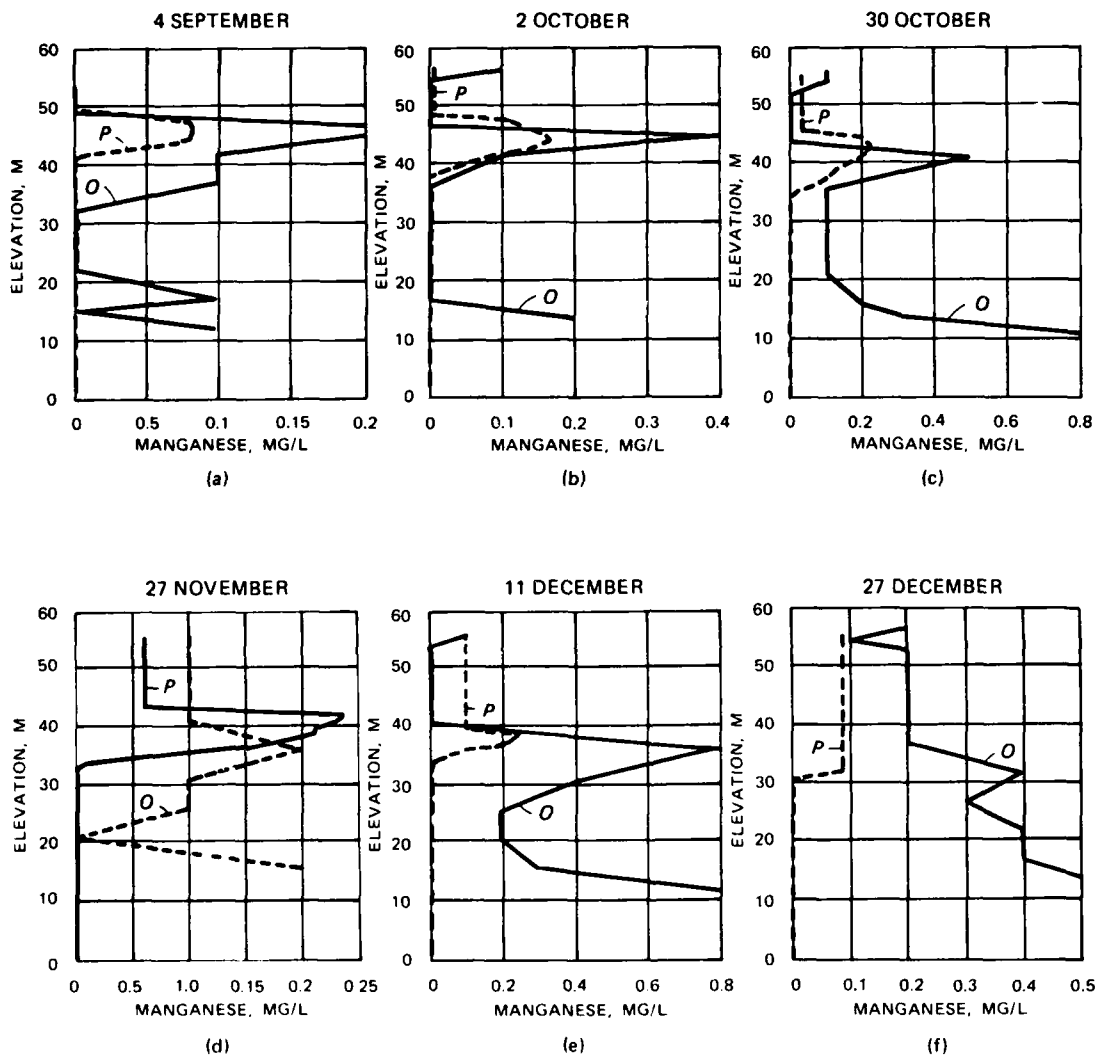


Figure 16. Selected dissolved Mn profiles with sediment release rate = $0.05 \text{ g Mn}^{+2} \cdot \text{m}^{-2} \cdot \text{day}^{-1}$ (P = predicted value; O = observed)

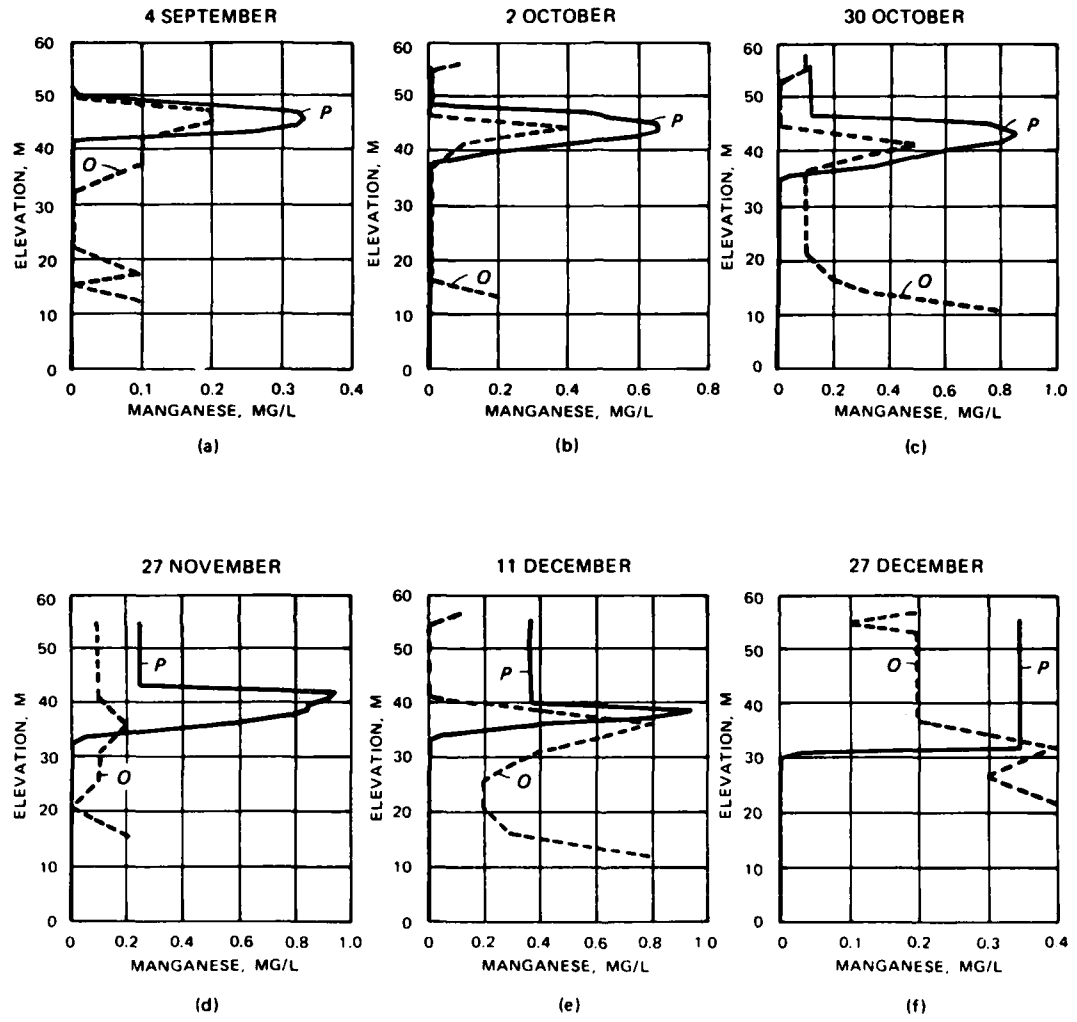


Figure 17. Selected dissolved Mn^{+2} profiles with sediment release rate = $0.20 \text{ g Mn}^{+2} \cdot m^{-2} \cdot d^{-1}$ (P = predicted value; O = observed)

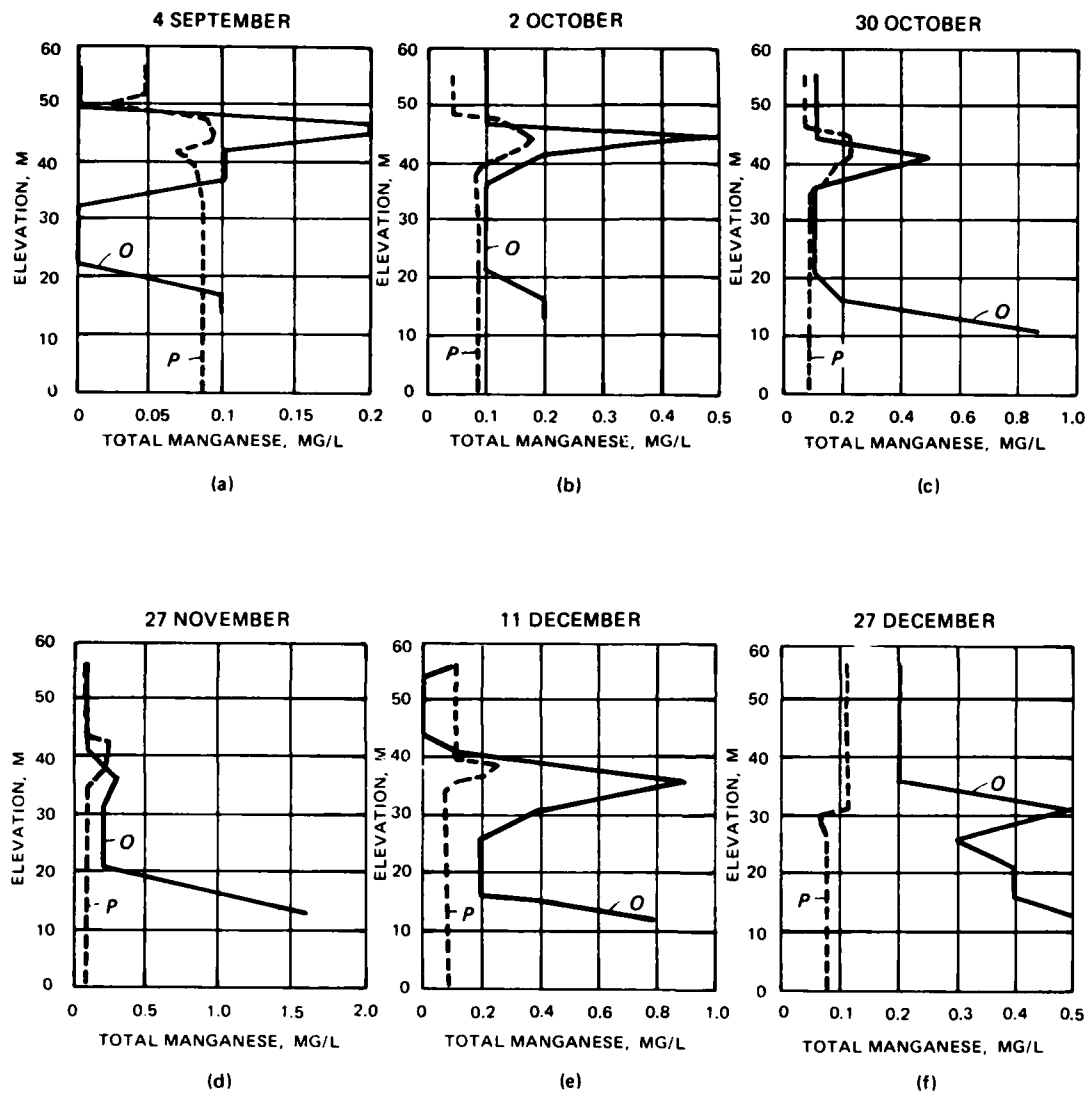


Figure 18. Selected total Mn profiles with sediment release rate = $0.05 \text{ g Mn}^{+2} \cdot \text{m}^{-2} \cdot \text{day}^{-1}$ (P = predicted value; O = observed)

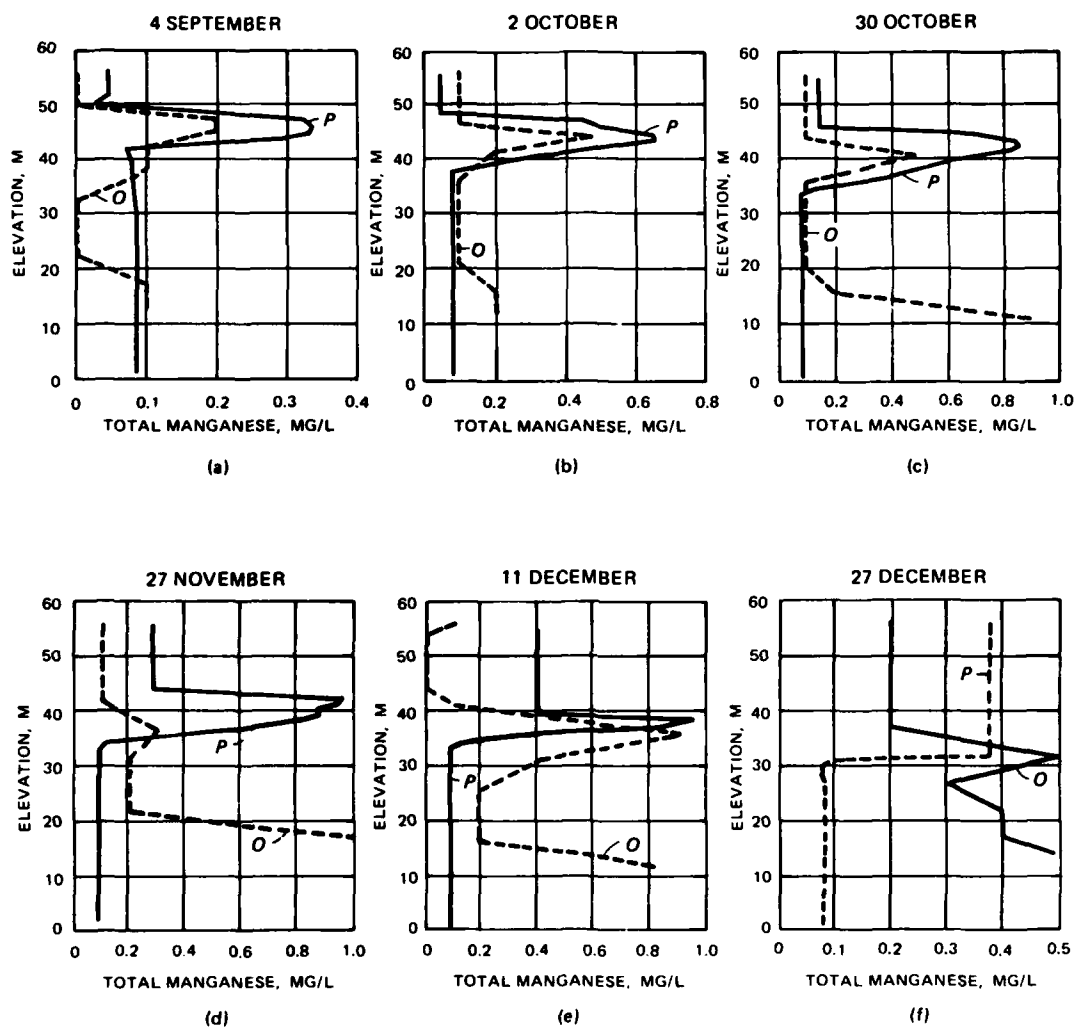


Figure 19. Selected total Mn profiles with sediment release rate = $0.20 \text{ g Mn}^{+2} \cdot \text{m}^{-2} \cdot \text{day}^{-1}$ (P = predicted value; O = observed)

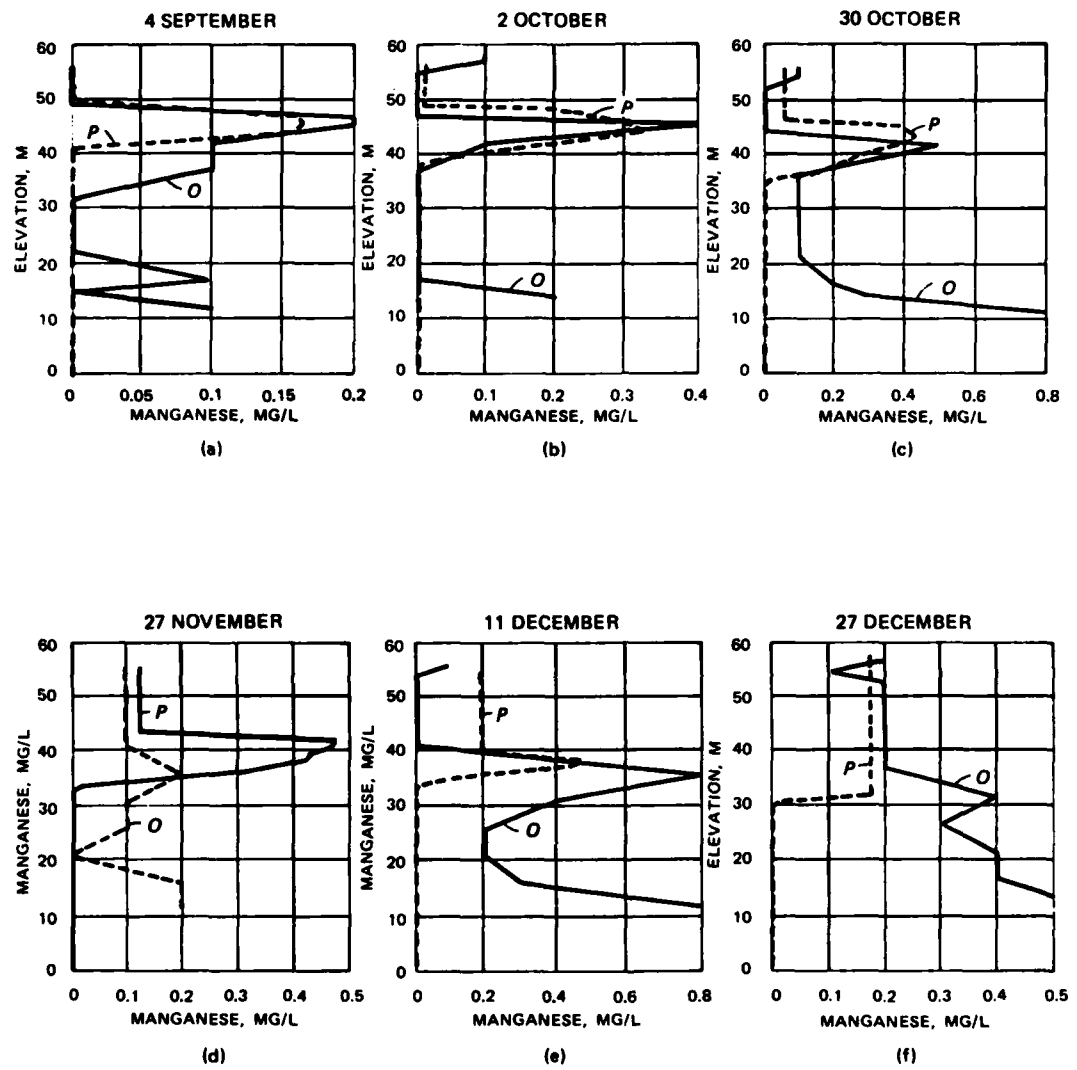


Figure 20. Selected dissolved Mn^{+2} profiles with Mn (IV) reduction rate = 0.00 day^{-1} (P = predicted value; O = observed)

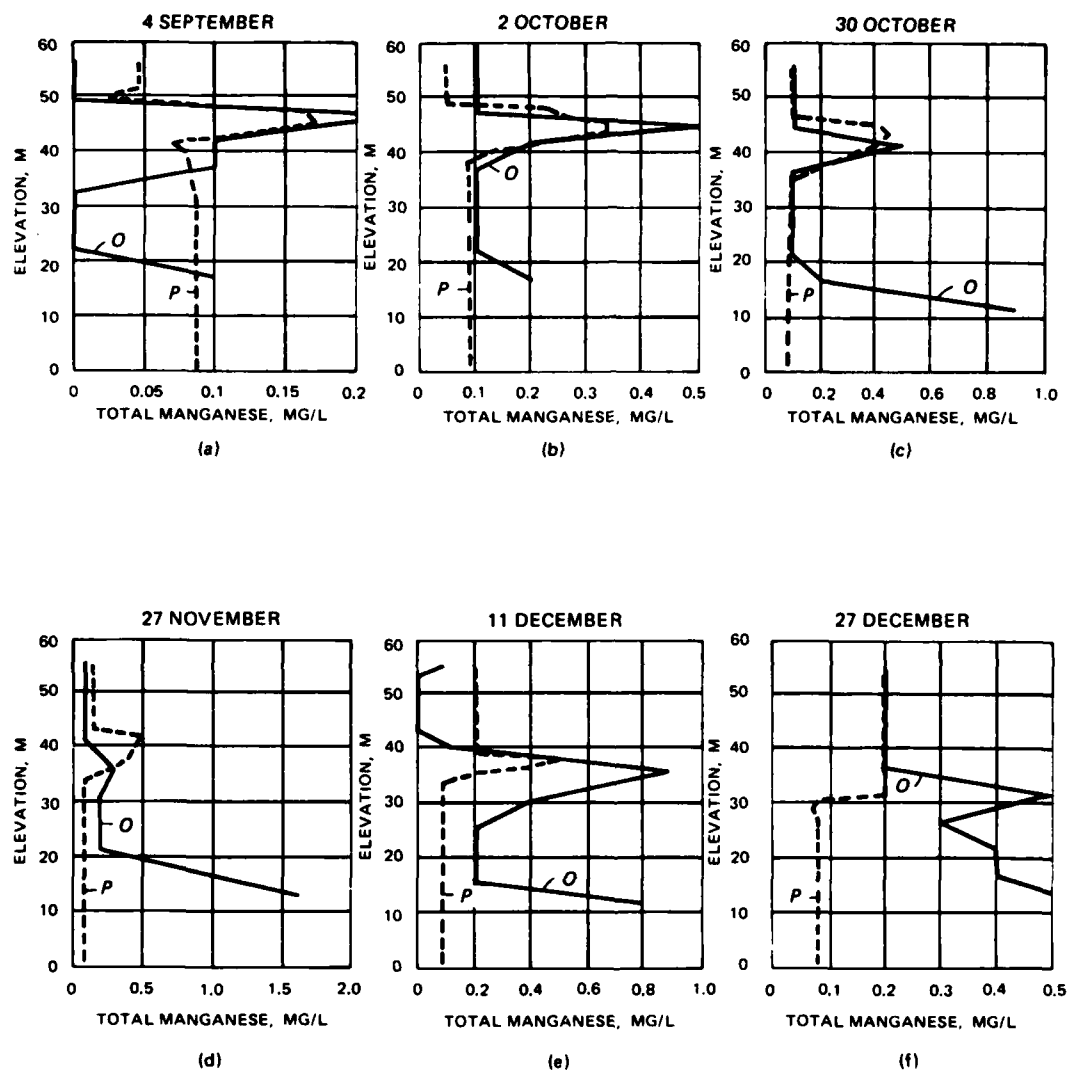


Figure 21. Selected total Mn profiles with Mn (IV) reduction rate = 0.00 day^{-1} (P = predicted value; O = observed)

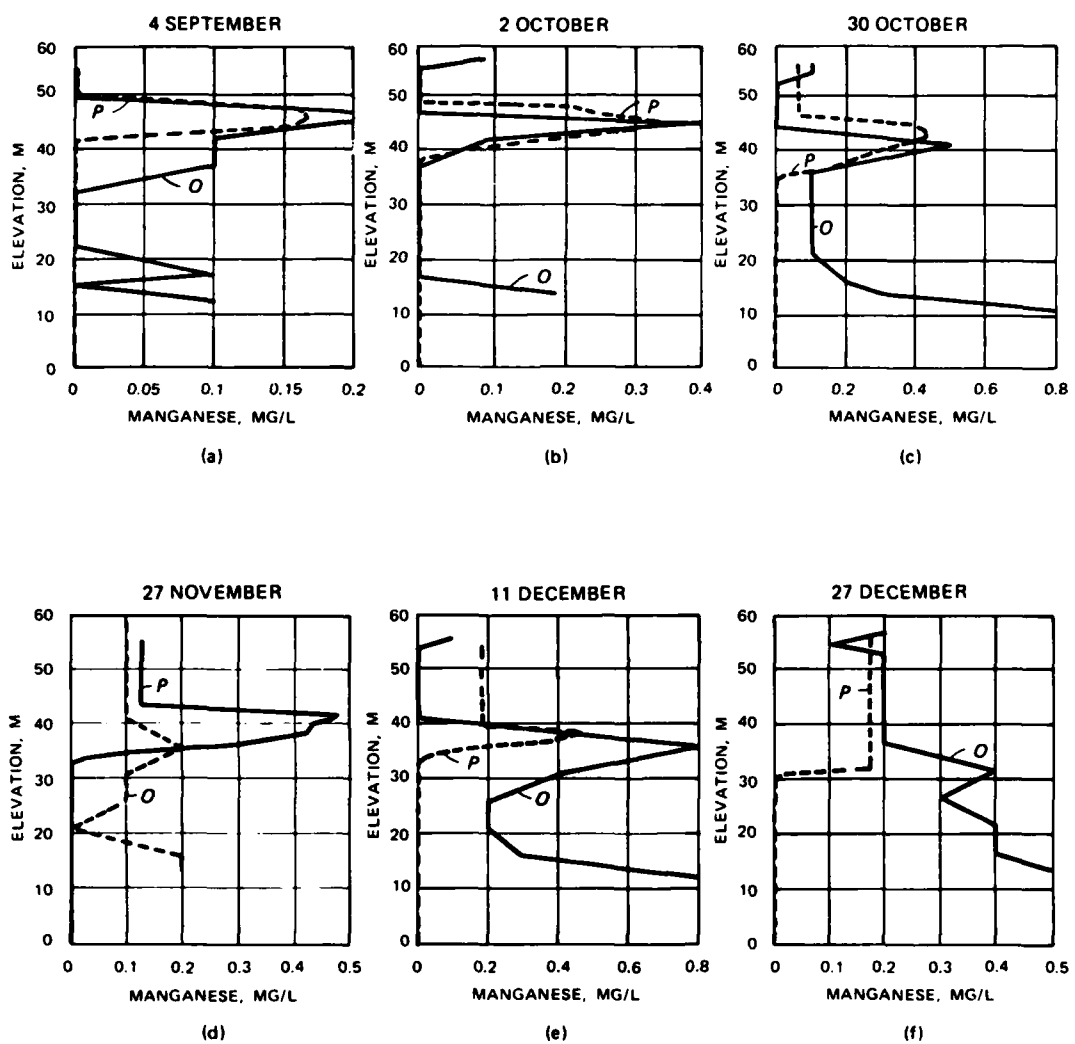


Figure 22. Selected total Mn profiles with Mn (IV) reduction rate = 0.04 day^{-1} (P = predicted value; O = observed)

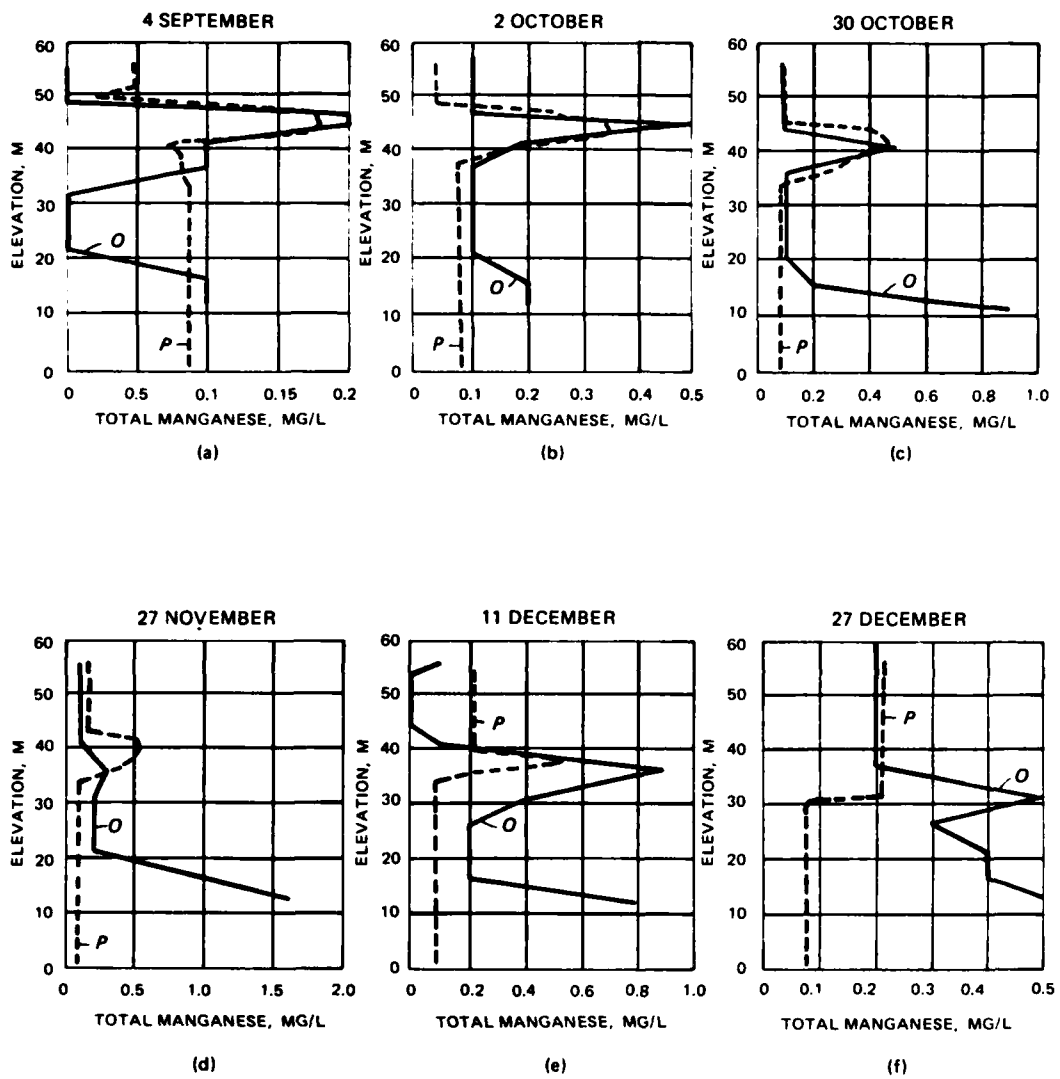


Figure 23. Selected total Mn profiles with Mn (IV) reduction
 $\text{rate} = 0.04 \text{ day}^{-1}$ (P = predicted value; O = observed)

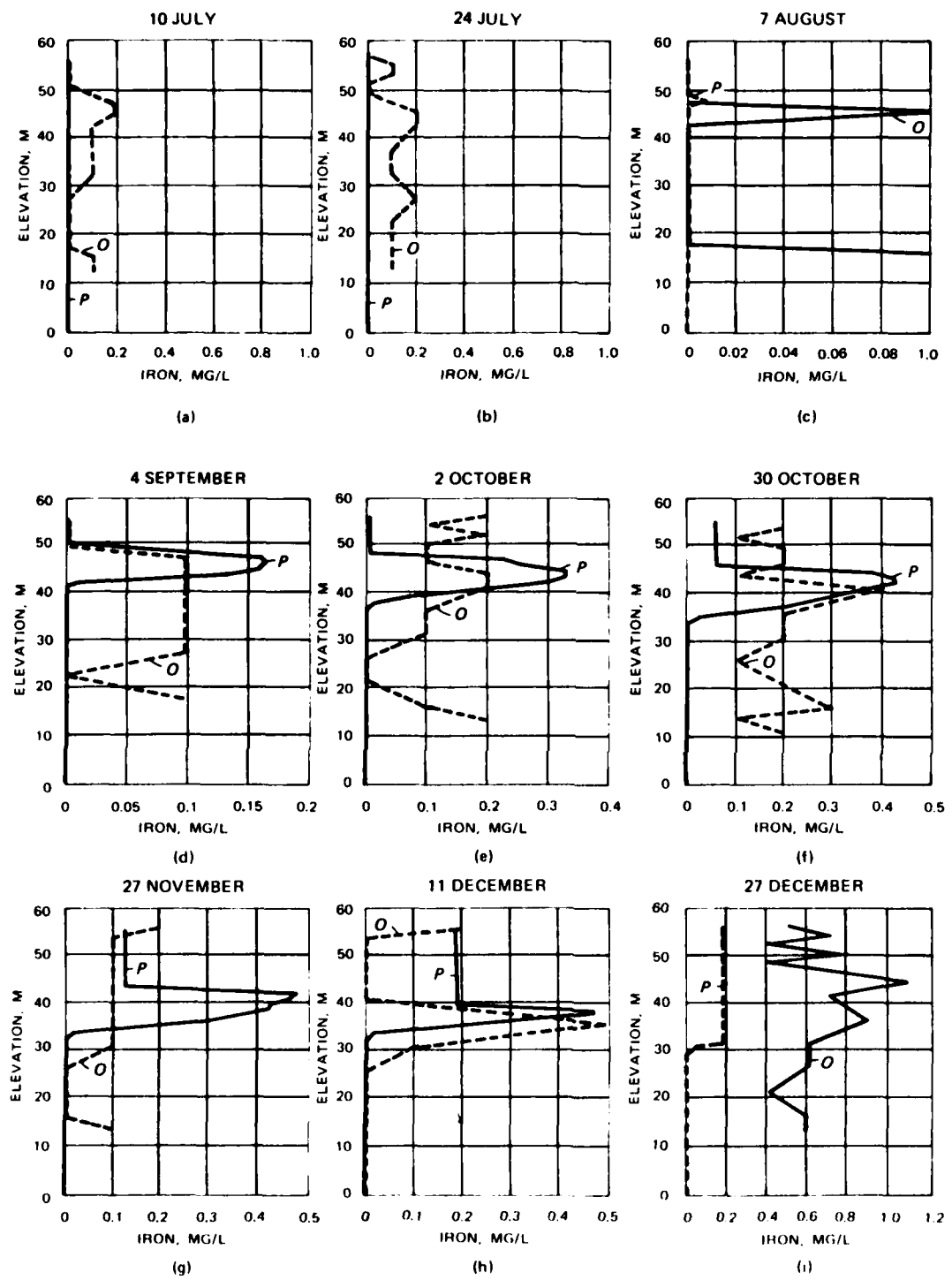


Figure 24. Selected dissolved Fe^{+2} profiles in DeGray Lake in 1979 (P = predicted value; O = observed)

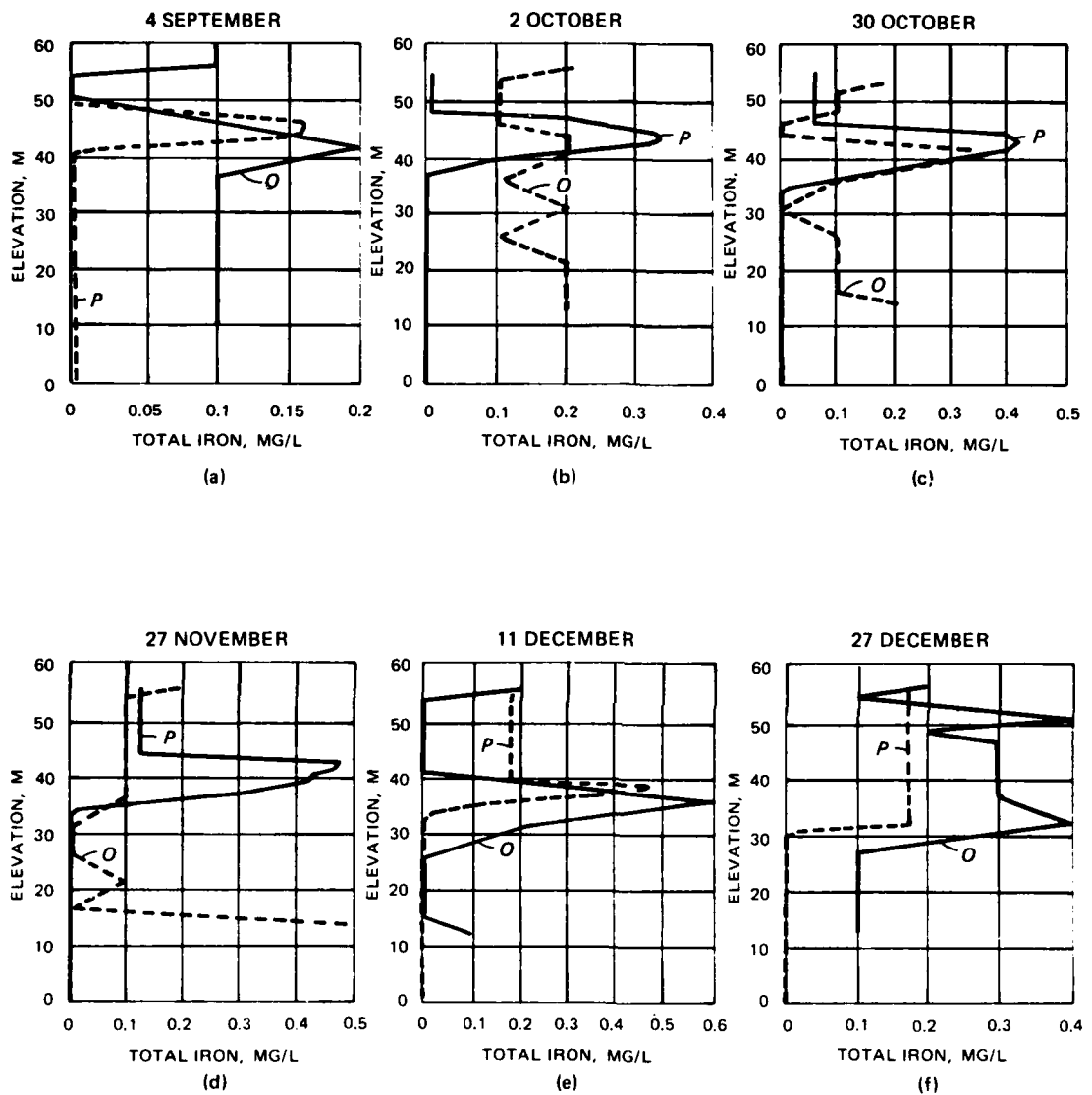


Figure 25. Selected total Fe profiles in DeGray Lake in 1979 (P = predicted value; O = observed)

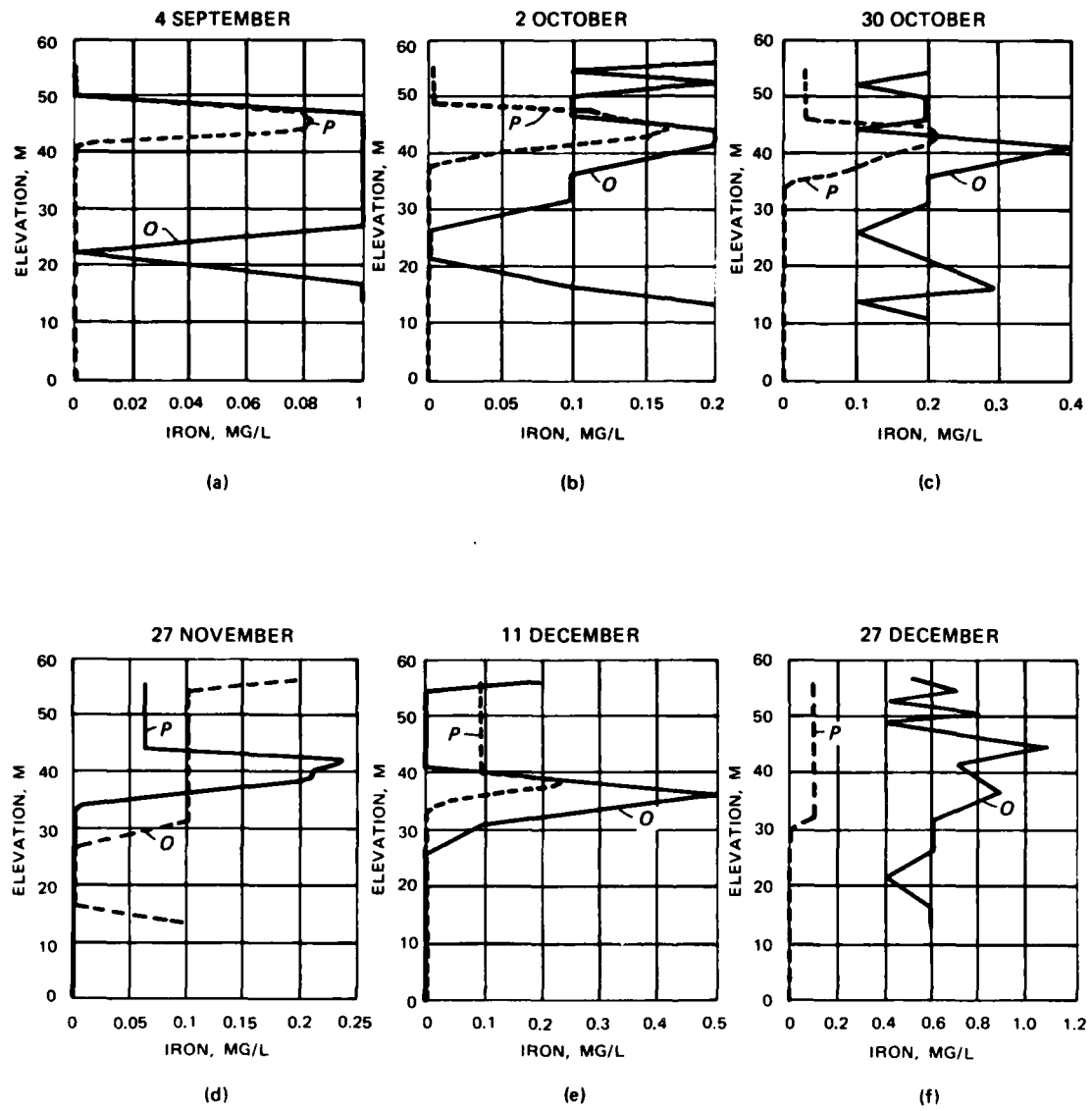


Figure 26. Selected dissolved Fe^{+2} profiles with sediment release rate = $0.05 \text{ g Fe}^{+2} \cdot \text{m}^{-2} \cdot \text{day}^{-1}$ (P = predicted value; O = observed)

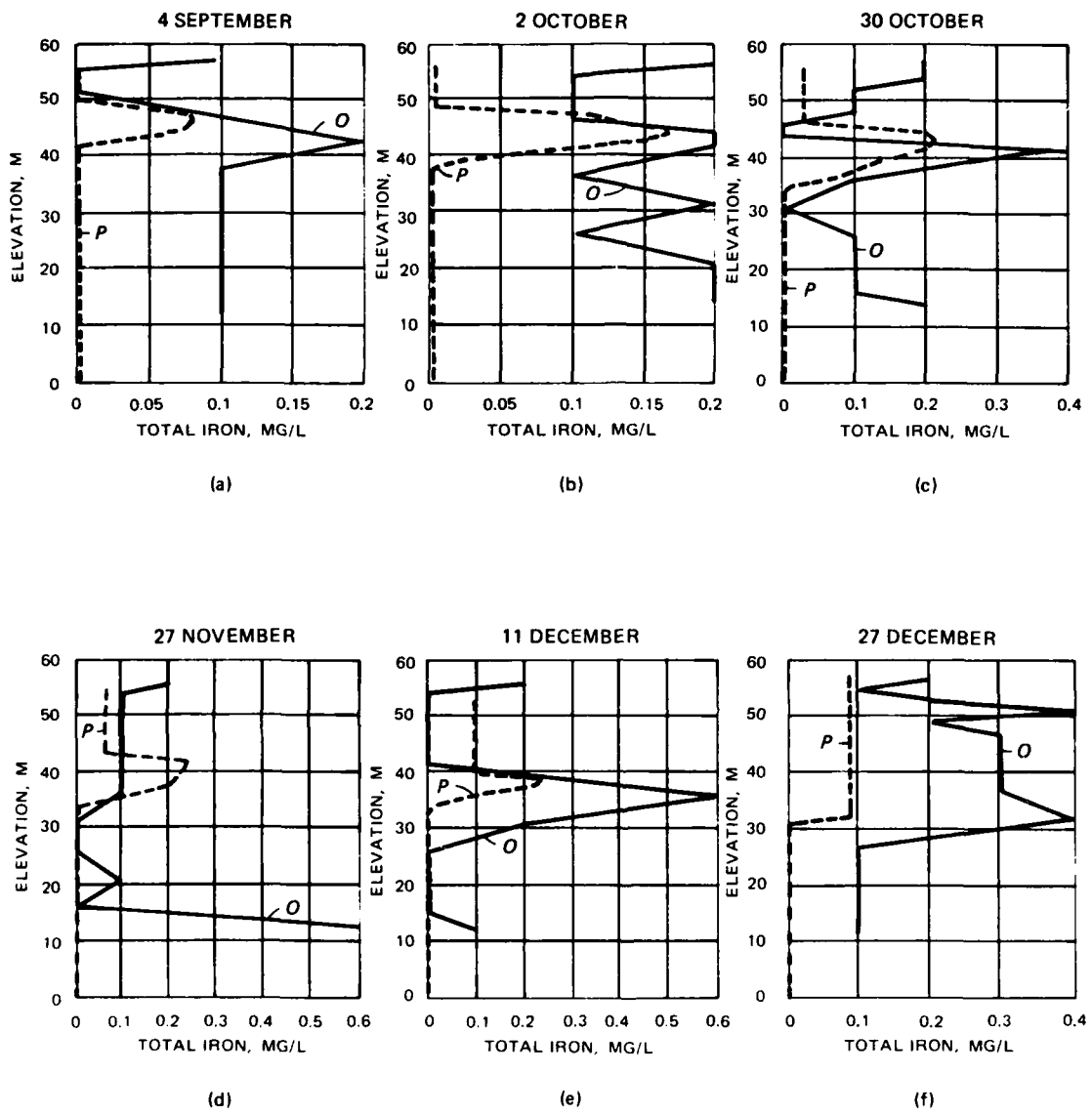


Figure 27. Selected total Fe profiles with sediment release rate
 $= 0.05 \text{ g Fe}^{+2} \cdot \text{m}^{-2} \cdot \text{day}^{-1}$ (P = predicted value; O = observed)

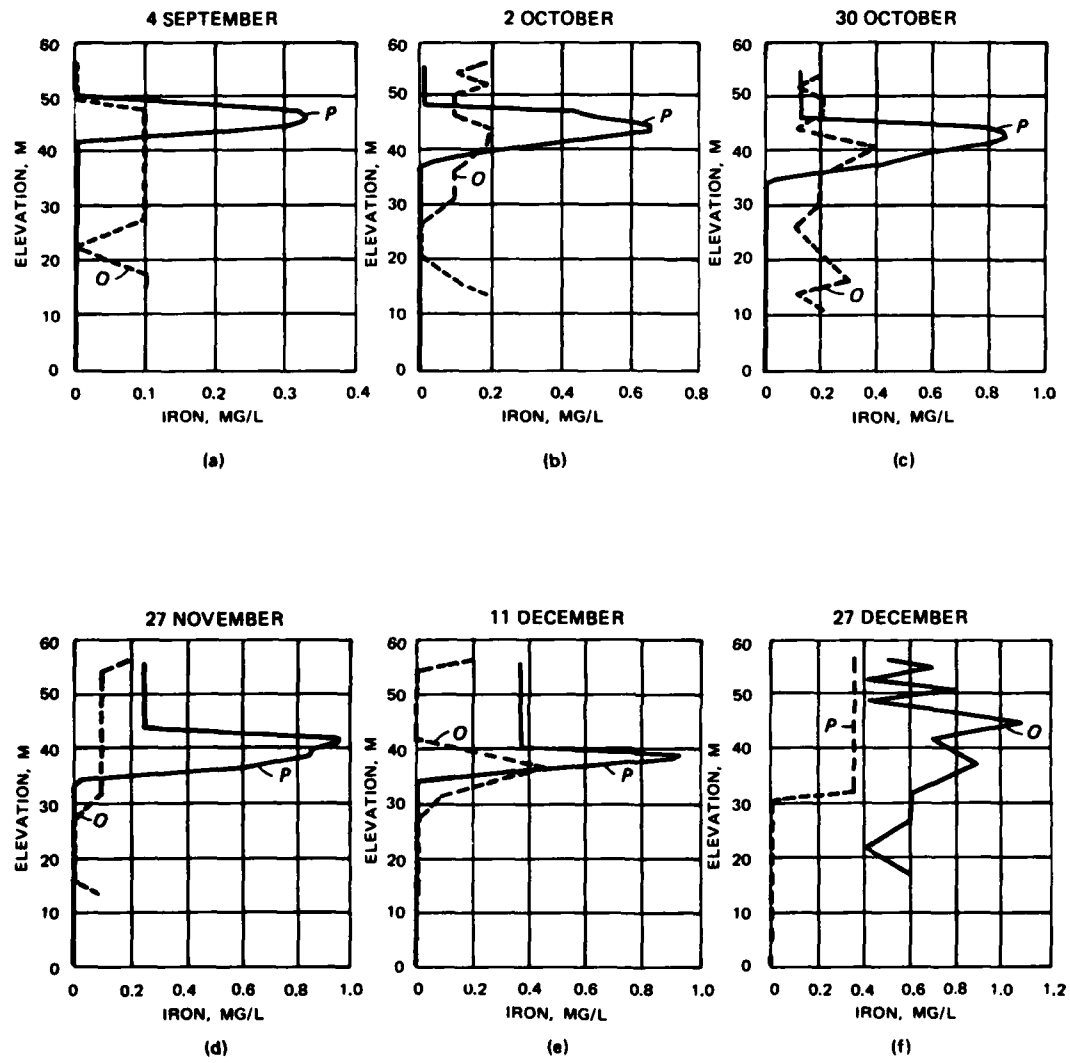


Figure 28. Selected dissolved Fe^{+2} profiles with sediment release rate = $0.20 \text{ g Fe}^{+2} \cdot \text{m}^{-2} \cdot \text{day}^{-1}$ (P = predicted value; O = observed)

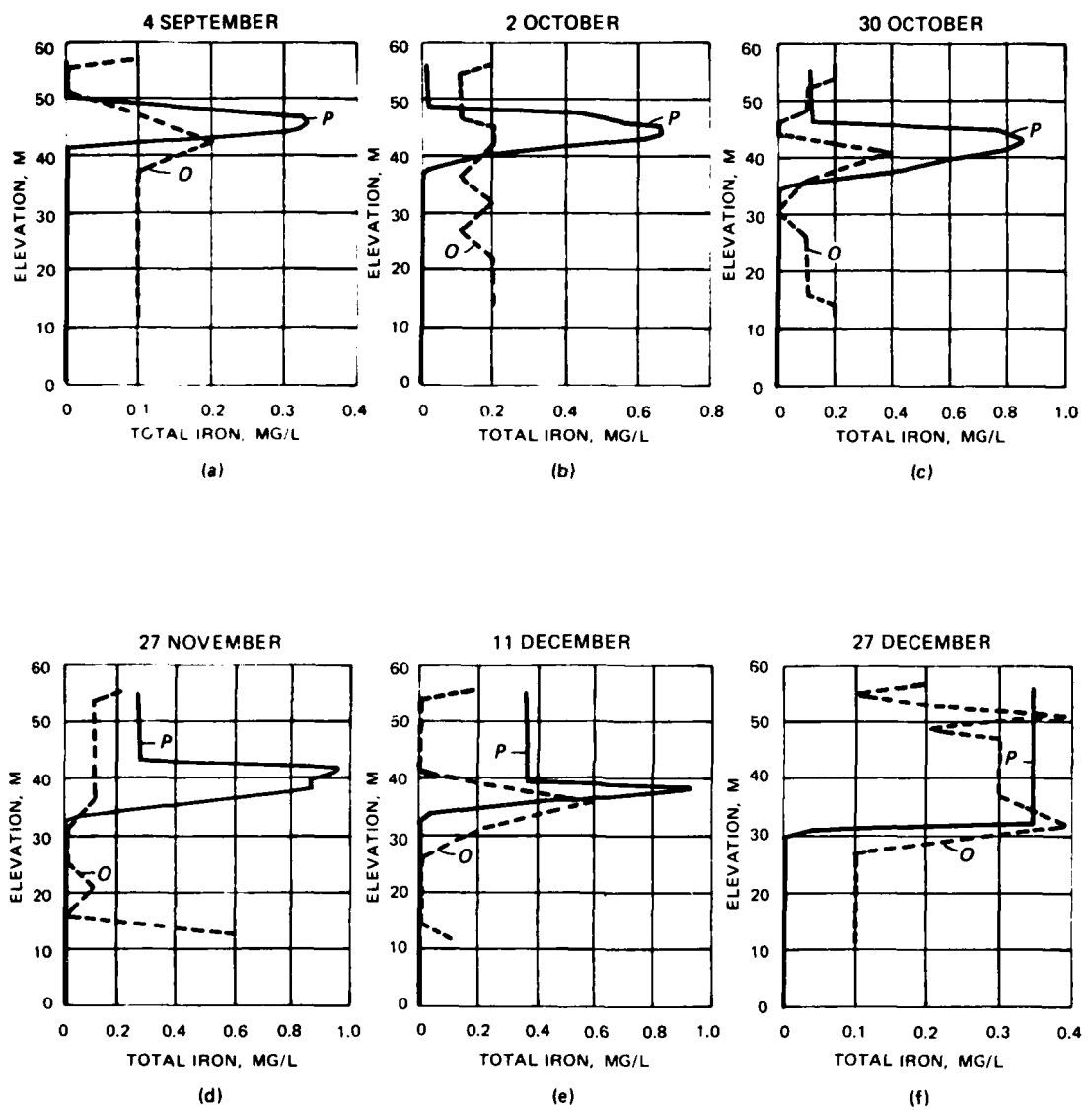


Figure 29. Selected total Fe^{+2} profiles with sediment release rate = $0.20 \text{ g Fe}^{+2} \cdot \text{m}^{-2} \cdot \text{day}^{-1}$ (P = predicted value; O = observed)

There may exist a thin anoxic zone along the sediment-water interface that could not be detected during sampling. Halving or doubling the Fe^{+2} release rate affects dissolved and total iron in direct proportion to the rate change (Figures 26-29).

56. Lowering the iron reduction rate to 0.00 day^{-1} apparently has no effect on dissolved or total iron concentrations (Figures 30 and 31). Doubling the rate to 0.06 day^{-1} also does not alter the iron profiles (Figures 32 and 33).

57. Again, like manganese, iron concentrations appear most significantly affected by release rates from the sediments.

Sulfur

58. Sulfur, in the reduced form of sulfide (S^{-2}), is primarily controlled by its release rate from sediment, reaction with reduced iron to form insoluble iron sulfide, and SO_4^{-2} reduction. Figure 34 depicts sulfide profiles for a release rate of $10^{-5} \text{ g S}^{-2} \cdot \text{m}^{-2} \cdot \text{day}^{-1}$. Considering the wide variability in observed data, the simulations seem quite reasonable. Simulated sulfide levels peak in late November (Figure 34d) and drop to nearly zero by late December (Figure 34f), when the upper water layers have become oxygenated; observed S^{-2} levels drop in November (Figure 34d) and increase again in December. As in the iron and manganese profiles, the model does not account for the presence of some hypolimnetic sulfide.

59. Increasing the sulfide sediment release rate from $10^{-5} \text{ g S}^{-2} \cdot \text{m}^{-2} \cdot \text{day}^{-1}$ to 10^{-4} g has no effect on sulfide profiles, implying that the model is quite insensitive to this parameter (Figure 35).

60. Setting the SO_4^{-2} reduction rate to 0.000 day^{-1} effectively eliminates all sulfide from the water column (Figure 36). Doubling the initial reduction rate from 0.001 to 0.002 day^{-1} doubles the sulfide concentration (Figure 37).

61. Thus, it would seem that SO_4^{-2} reduction dominates sulfide formation dynamics, with sediment release an insignificant factor in the model. However, if the SO_4^{-2} reduction rate is set to 0.000 day^{-1} and the sulfide release rate is set to $0.1 \text{ g S}^{-2} \cdot \text{m}^{-2} \cdot \text{day}^{-1}$, sulfide profiles of significant magnitude can be generated (Figure 38). Sulfate

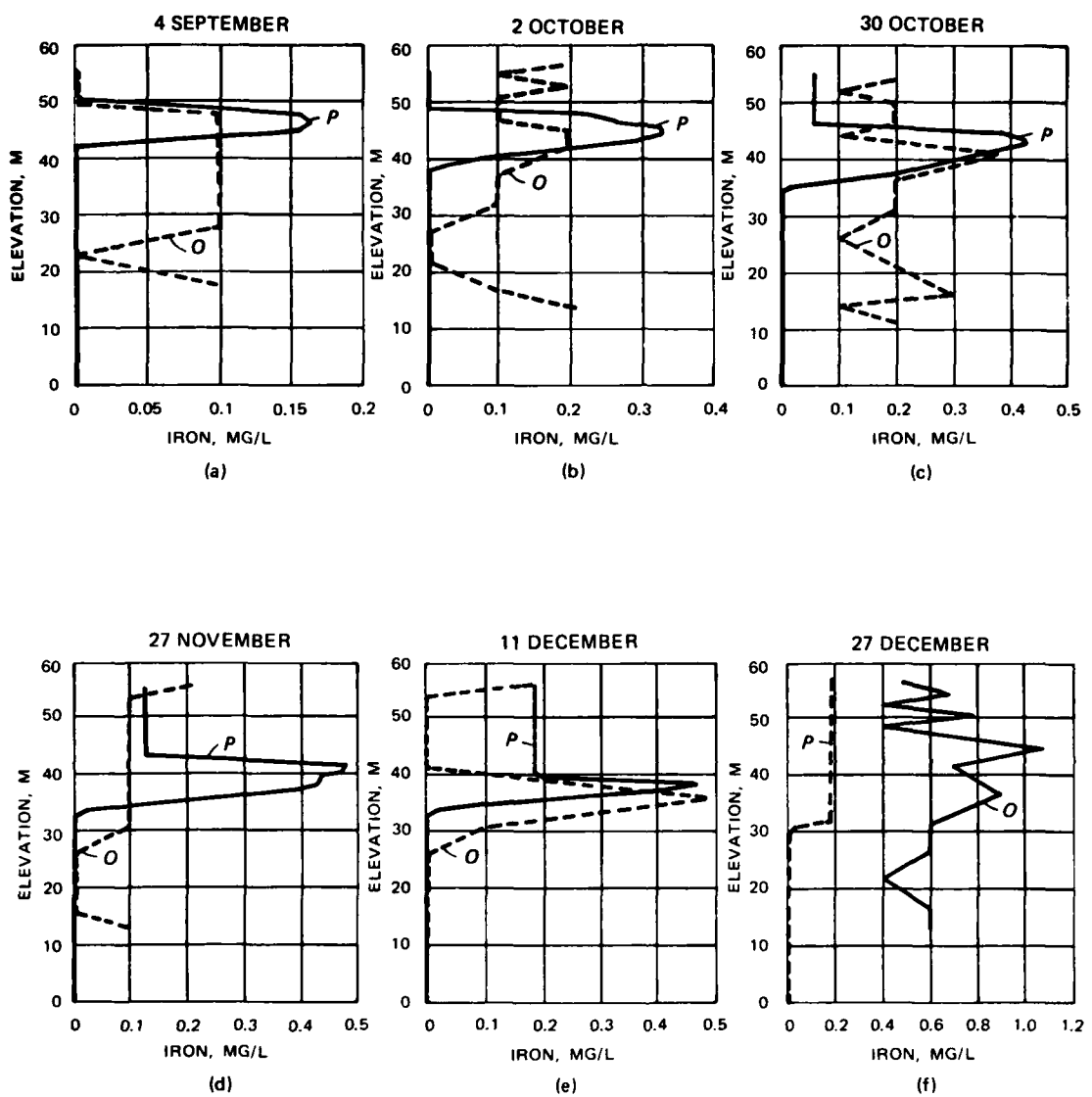


Figure 30. Selected dissolved Fe^{+2} profiles with $\text{Fe}(\text{III})$ reduction rate = 0.00 day^{-1} (P = predicted value; O = observed)

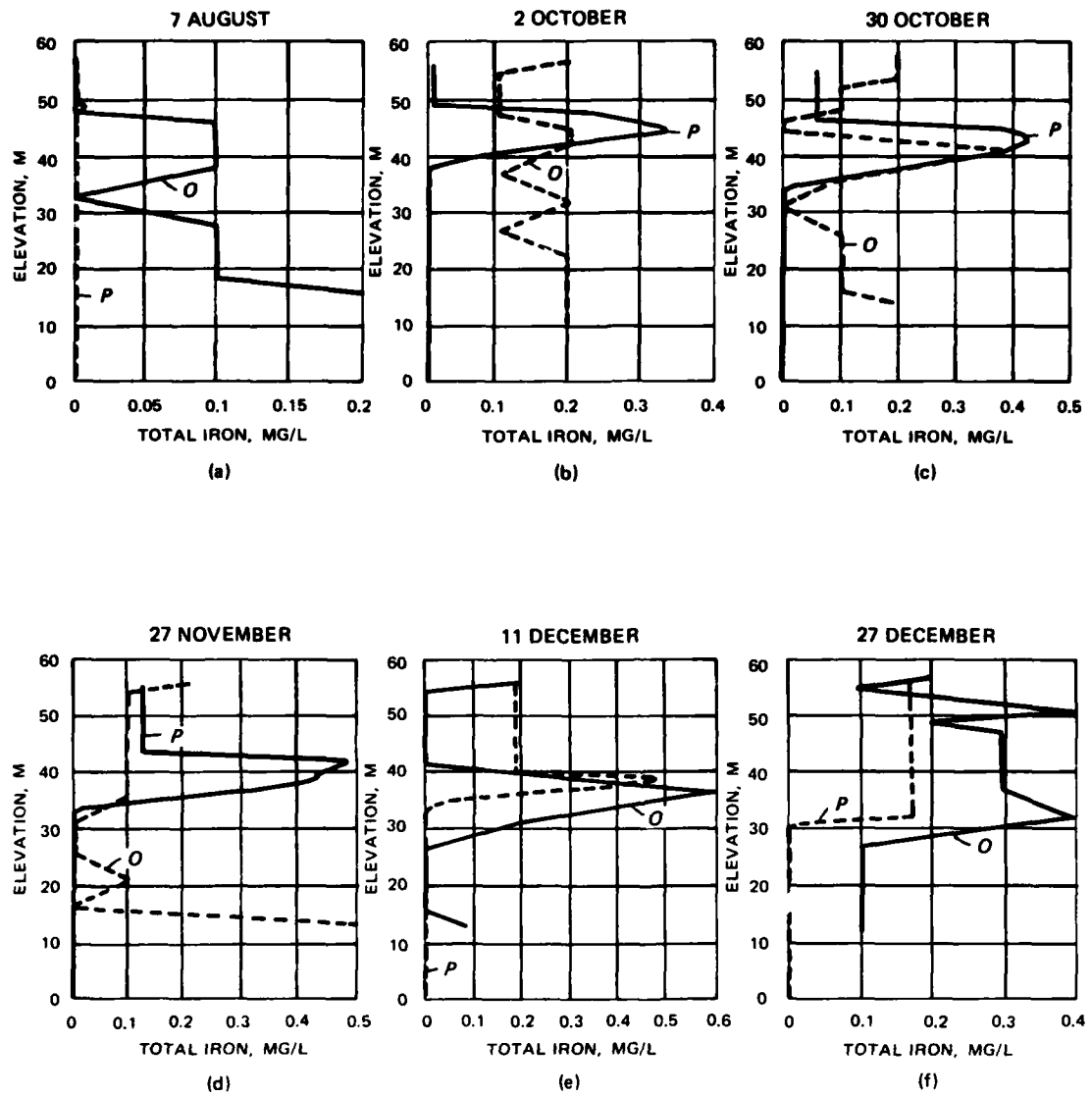


Figure 31. Selected total Fe profiles with Fe(III) reduction
 $\text{rate} = 0.00 \text{ day}^{-1}$ (P = predicted value; O = observed)

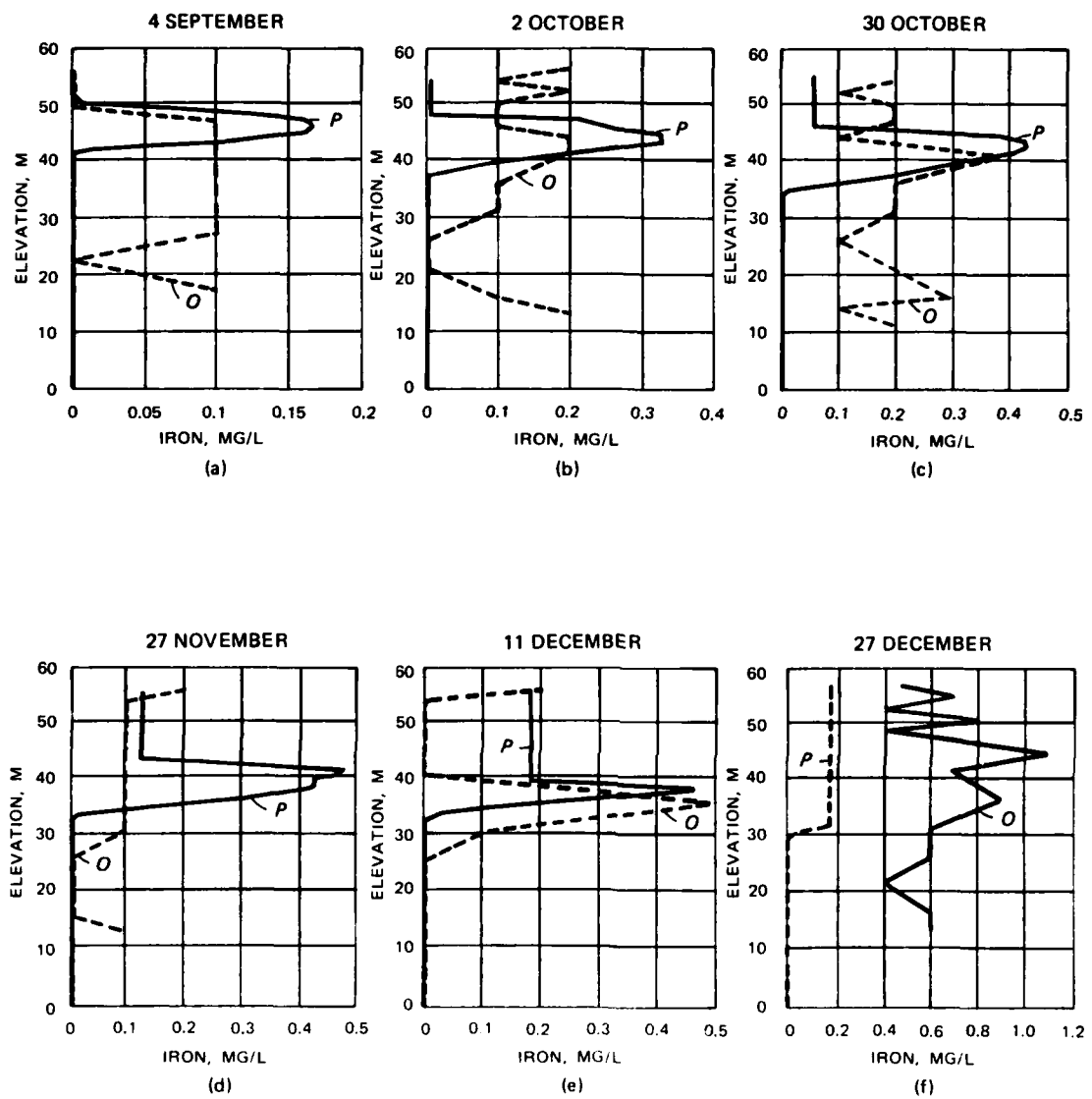


Figure 32. Selected dissolved Fe^{+2} profiles with Fe(III) reduction rate = 0.06 day^{-1} (P = predicted value; O = observed)

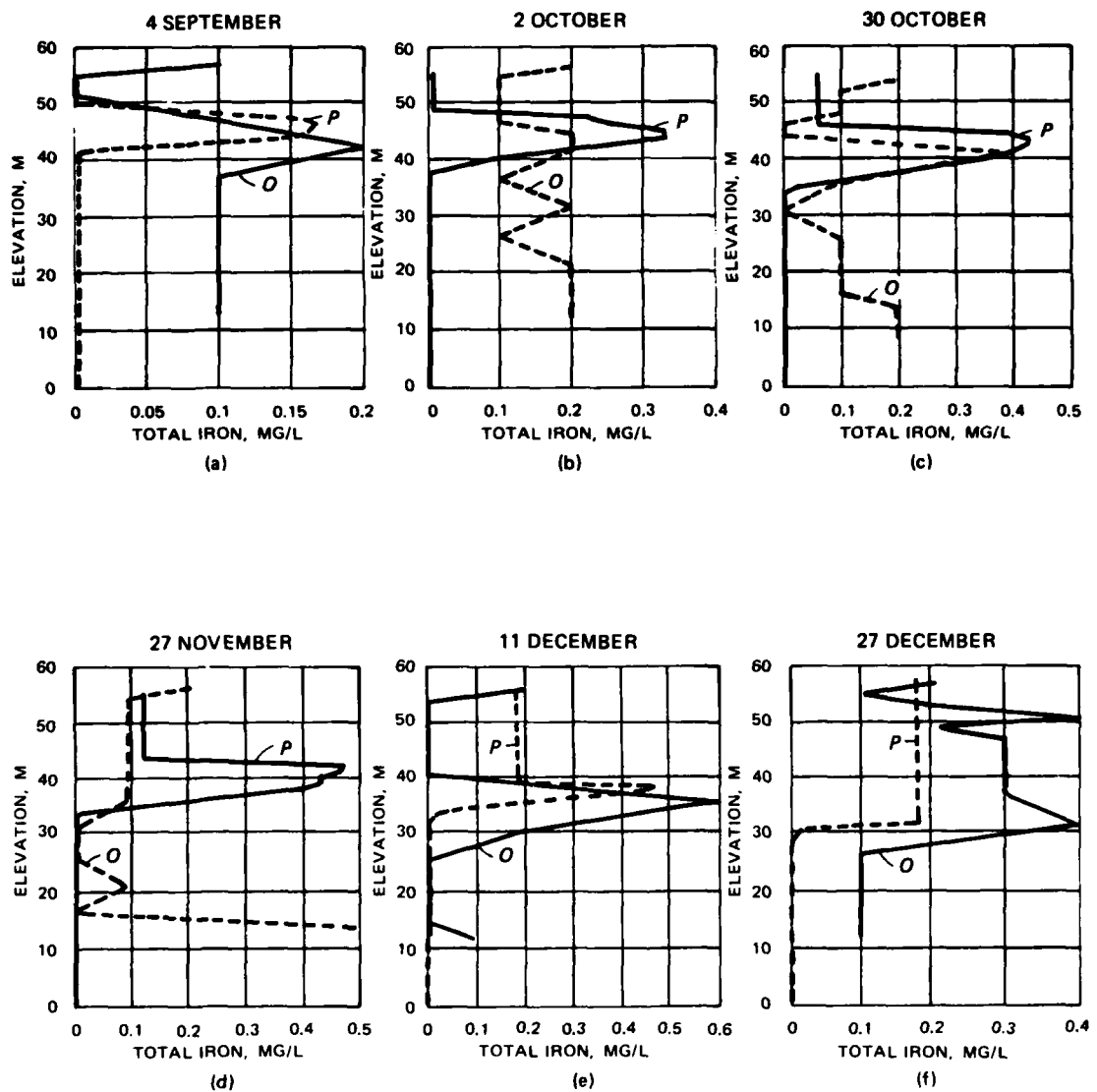


Figure 33. Selected total Fe profiles with Fe(III) reduction
 $\text{rate} = 0.06 \text{ day}^{-1}$ (P = predicted value; O = observed)

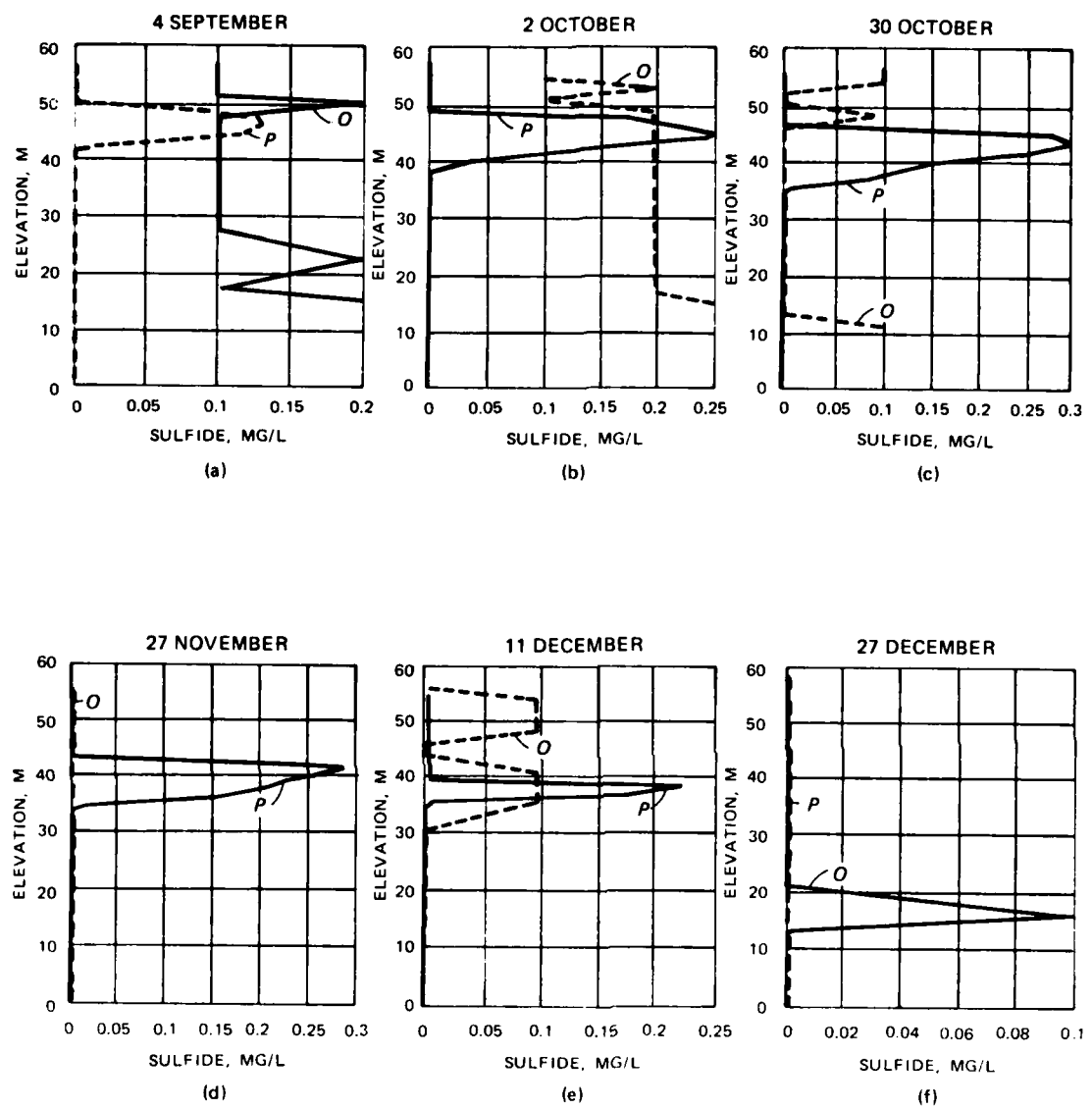


Figure 34. Selected S^{-2} profiles for DeGray Lake in 1979
(P = predicted value; O = observed)

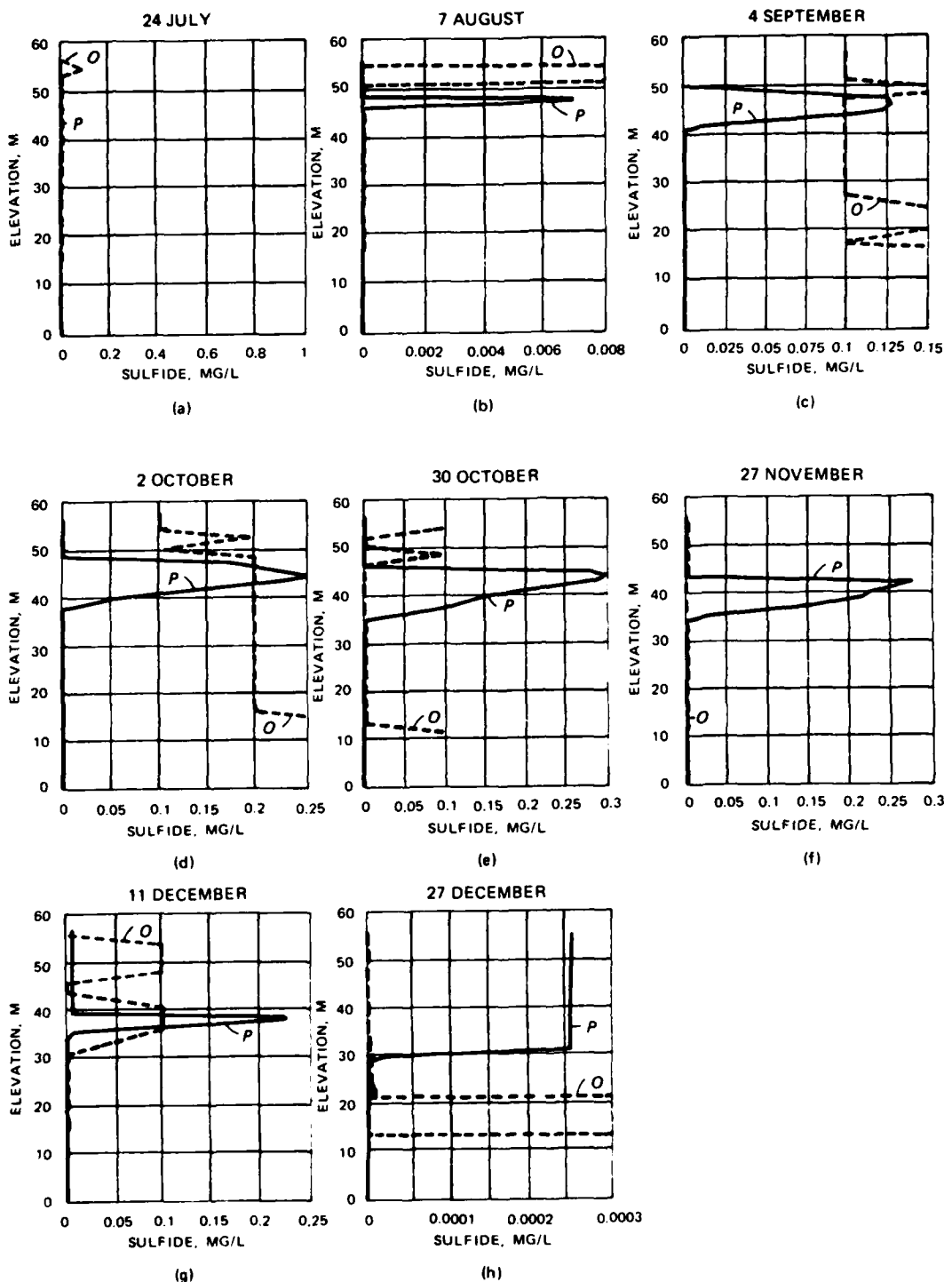


Figure 35. Selected S^{-2} profiles with sediment release rate
 $= 10^{-4} \text{ g } S^{-2} \cdot m^{-2} \cdot \text{day}^{-1}$ (P = predicted value; O = observed)

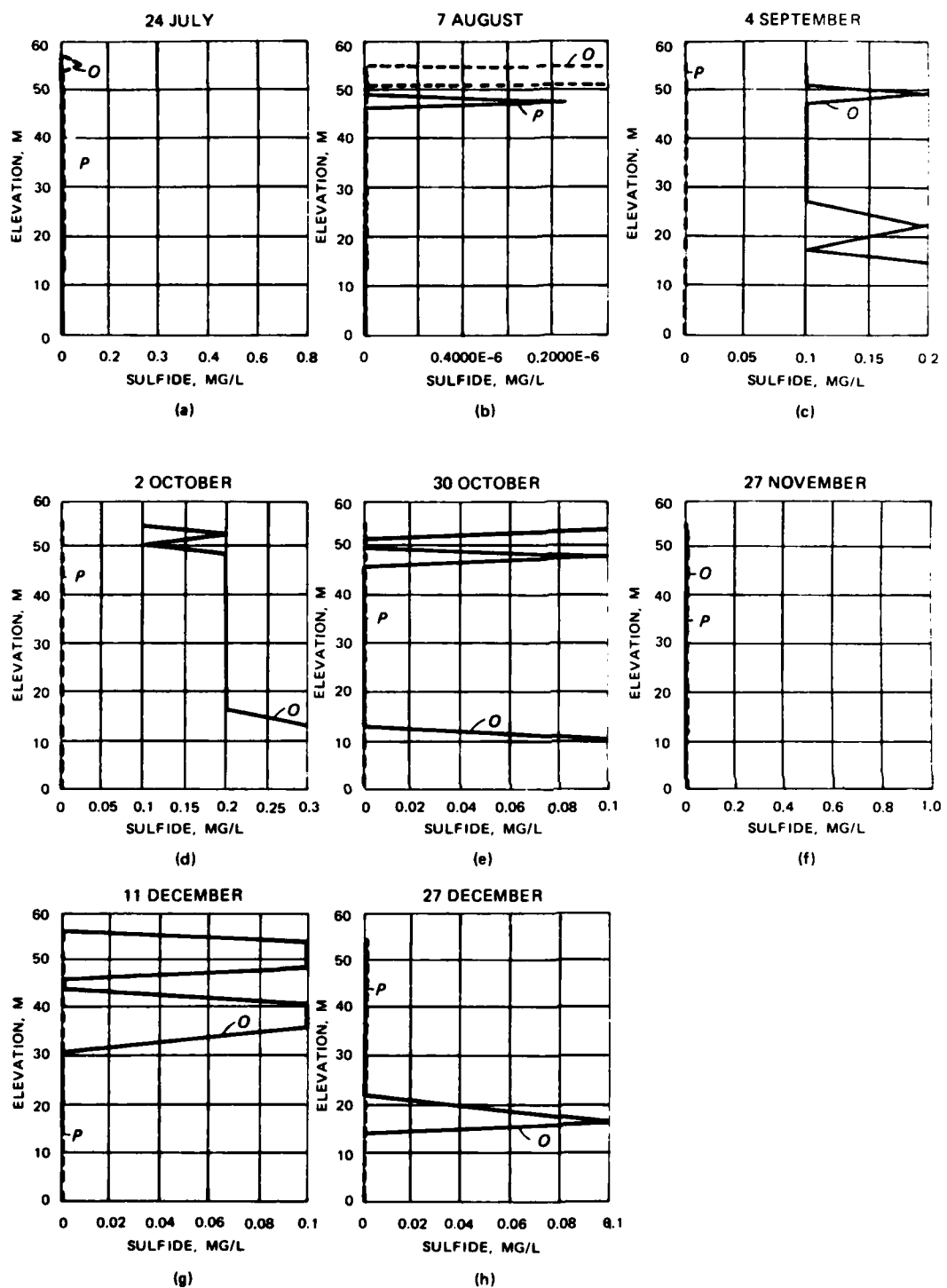


Figure 36. Selected S^{2-} profiles with SO_4^{2-} reduction rate = 0.00 day^{-1} (P = predicted value; O = observed)

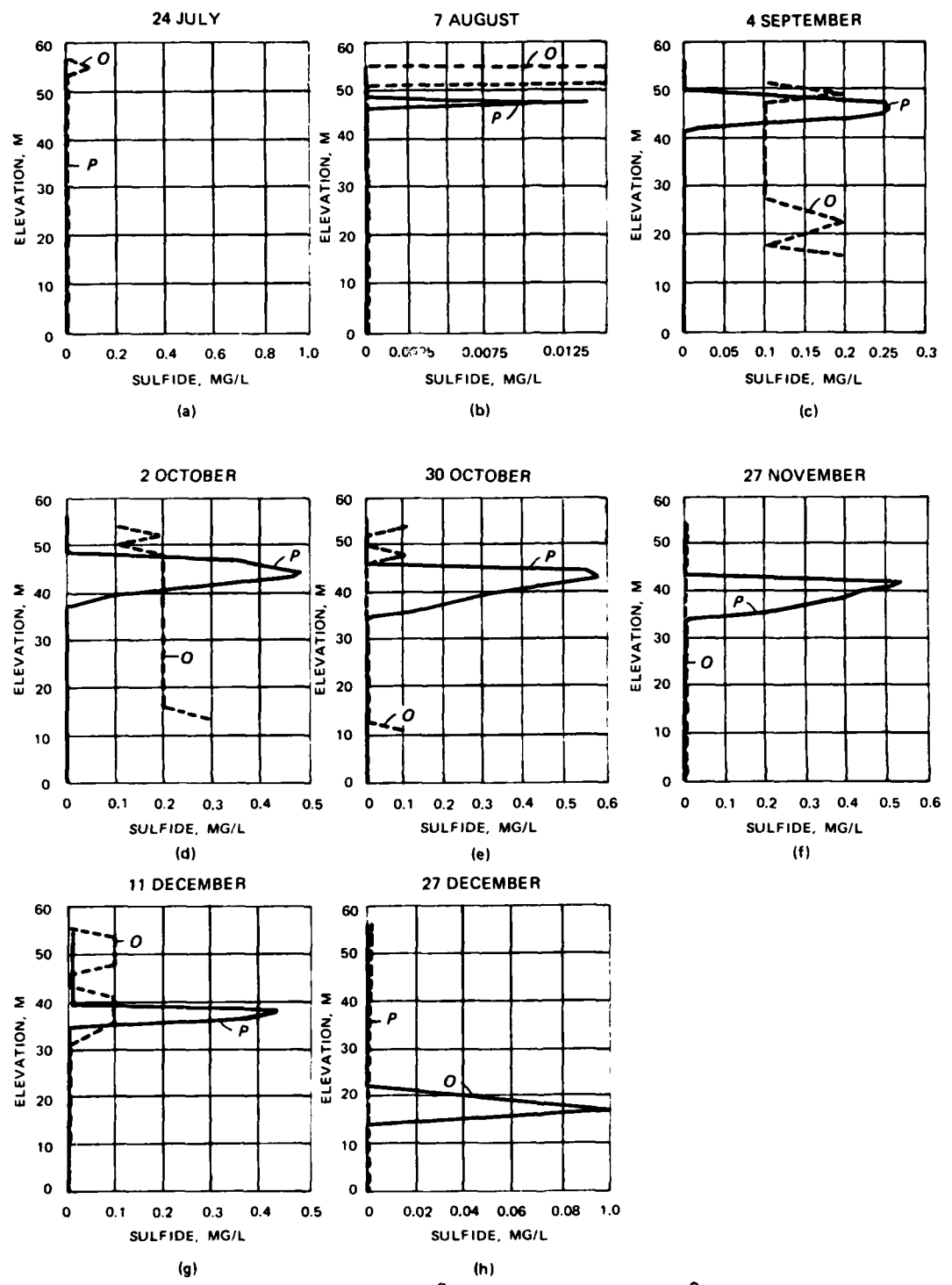


Figure 37. Selected S^{2-} profiles with SO_4^{2-} reduction rate = 0.002 day^{-1} (P = predicted value; O = observed)

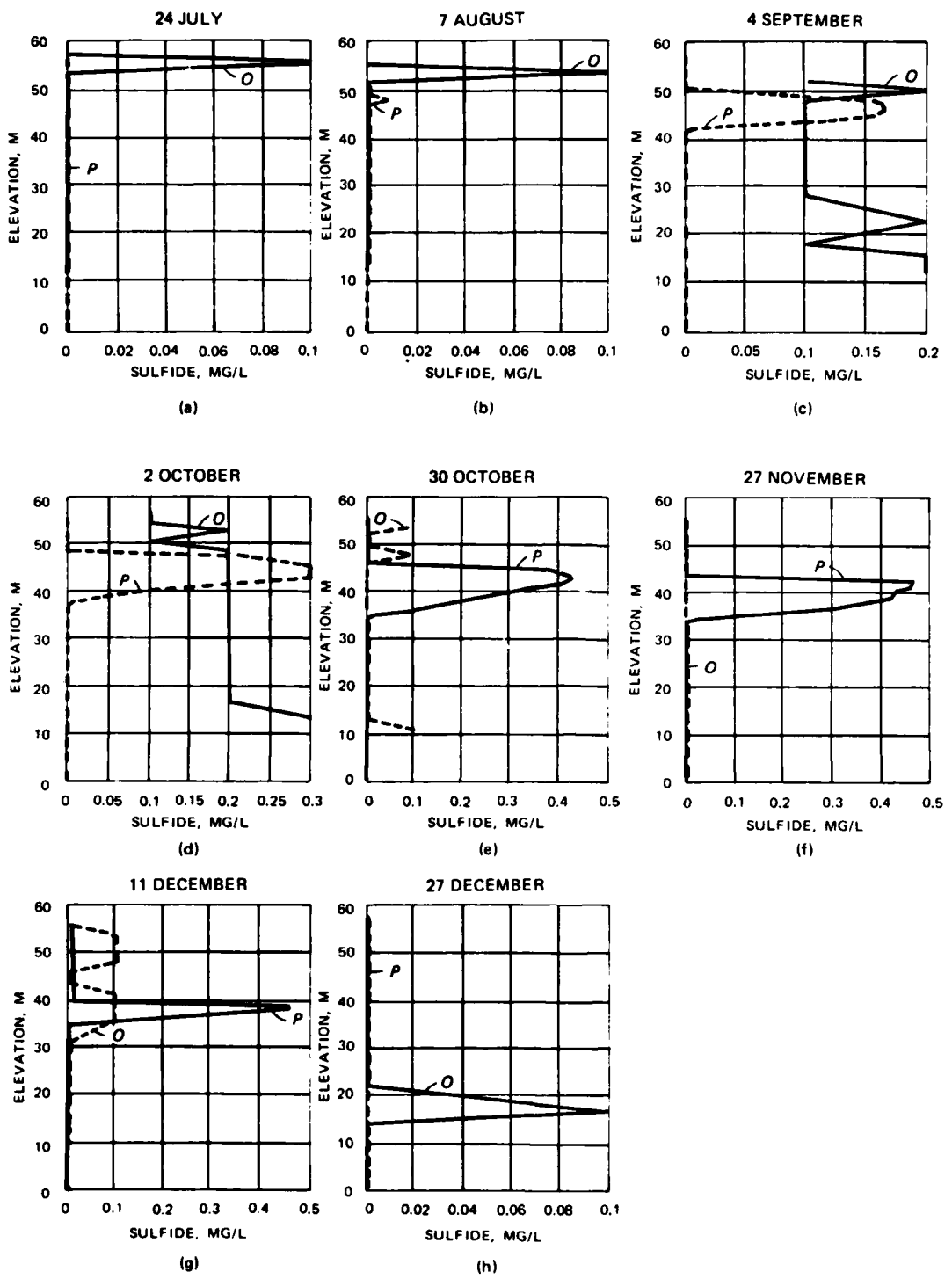


Figure 38. Selected S^{-2} profiles with SO_4^{-2} reduction rate = 0.00
 day^{-1} and S^{-2} sediment release rate = $0.10 g S^{-2} \cdot m^{-2} \cdot day^{-1}$
(P = predicted value; O = observed)

reduction initially predominated, largely because of the relatively high concentration of sulfate in the water column.

Discussion

62. This discussion attempts to examine inadequacies of the anaerobic subroutines, to assign sources of error, to point out the overall reliability of the simulations, and to suggest where future improvements may be made. For the most part, discrepancies between predicted and observed values may be as much due to variability in sampling and analysis and limitations of the one-dimensional approach as to subroutine formulation.

63. Release of NH_4^+ -N and PO_4^{3-} -P from sediments, generally referred to as nutrient regeneration, should constitute an extremely important aspect of a water quality model simulating anaerobic processes. However, too high NH_4^+ -N and PO_4^{3-} -P concentrations under simulated aerobic conditions preclude observation of any anaerobic effects. (Following the completion of this report, research aimed at understanding the mechanisms transporting and recycling nutrients in the DeGray Lake system has resolved these discrepancies.)

64. Another difficulty arises in attempting to simulate hypolimnetic release of anaerobic materials with the $0.5 \text{ mg DO} \cdot \text{L}^{-1}$ cue. Simulated oxygen concentrations in the hypolimnion fail to fall low enough to initiate sediment release in the deeper hypolimnetic layers. Field data, too, would indicate that DO appears too high to allow the presence of dissolved, reduced materials. However, all anaerobic materials show up in spite of accepted chemical constraints. Three possible explanations for the occurrence of dissolved metals in aerobic hypolimnia come to mind. First, the definition of dissolved (= reduced) metal is an operational one based on passage through a filter of specific pore size, not on electrochemical considerations; an oxidized molecule may be able to pass through the filter. Second, the metal may exist in a dissolved state in association with an organic complex or colloid. Third, advection may create localized pockets of reduced materials in zones of

relatively high oxygen concentration. This problem is, indeed, a difficult one, which limnologists have not yet resolved and which may require modification of the model to allow release and slow oxidation of dissolved anaerobic materials in aerobic hypolimnia.

65. Two aspects of the field data contribute to less than ideal calibration results. First, the data are highly variable temporally and spatially; they demonstrate an occasional lack of continuity in trends. An example of this behavior is the drop in concentration of anaerobic materials in late November (27 November sample). Since the decline does not appear associated with any increase in DO, one may conjecture that the anomaly resulted from sample handling. In particular, the sulfide analysis is extremely sensitive to the slightest oxygen contamination. In this particular case, it has been suggested that a hydrological event, missed between samples, affected the trend.*

66. Second, anaerobic materials occur in low concentrations, a factor that may also contribute to their relatively high variability. Concentrations of Mn, Fe, and S are reported in increments of $0.1 \text{ mg} \cdot \text{l}^{-1}$, although analytical techniques should yield higher degrees of resolution. Since many data values fall near zero and are generally less than $0.5 \text{ mg} \cdot \text{l}^{-1}$ for any anaerobic material, variability of $0.1\text{--}0.2 \text{ mg} \cdot \text{l}^{-1}$ in field observations can add a degree of uncertainty to the model evaluation.

67. While the simulations do not precisely mirror field situations, they do match observed data in terms of initiation of release, magnitude of concentrations, and general trends. Agreement between simulated and observed conditions is actually better than originally expected when taking into account potential sources of error and uncertainty, such as simplicity of the model formulation, the one-dimensional assumption, use of estimated parameters and coefficients, variability in environmental sampling conditions, and chemical analyses.

* Personal Communication, 1984, J. Nix, Professor, Ouachita Baptist University, Arkadelphia, Ark.

PART III: 1980 CONFIRMATION SIMULATION

68. The same coefficients and rate constants used for the 1979 calibration study form the basis for a simulation of 1980 reservoir conditions. This procedure, referred to as verification or confirmation, may serve several purposes and its results may be interpreted in different ways. In general, an attempt is made to ascertain the validity of the model examined, or of any of its parts, including coefficients. In the present case, the 1980 simulation is evaluated to determine how well the new anaerobic subroutines model conditions observed in DeGray Lake for a year other than that used in the calibration study.

69. Since DO integrates physical, chemical, and biological effects, this variable's profiles throw light on the adequacy of CE-QUAL-R1 to model the reservoir system. Figure 39 traces the simulated development of anoxic conditions in the reservoir and compares the predictions with observed conditions. As the graphs indicate, CE-QUAL-R1 predicts that metalimnetic anaerobic conditions ($DO \leq 0.5 \text{ mg} \cdot \text{l}^{-1}$) begin in late July (Figure 39g), whereas reservoir DO does not really reach that level until late September (Figure 39k).

70. Other discrepancies in DO profiles exist. Following stable thermal stratification in April, epilimnetic DO predictions match observed conditions quite well until July, when they begin to diverge significantly, a phenomenon which persists and becomes more marked as the year progresses. In addition, simulated hypolimnetic DO never drops as low as field data indicate.

71. Physical and meteorological conditions may combine to affect the accuracy of DO profiles in 1980 simulations. Wind speed, inflowing water volume from tributaries, and thermal structure of the water column differ in 1979 and 1980; these three environmental factors contribute to the calculation of the diffusion coefficient. After the tapering off of high-volume inflows following the first 3-4 months of the year (1979 and 1980), wind speed is the primary influence on the diffusion coefficient; the average wind speed in 1980 is greater than in 1979, possibly resulting in higher diffusion coefficients in 1980. Calibrating the diffusion

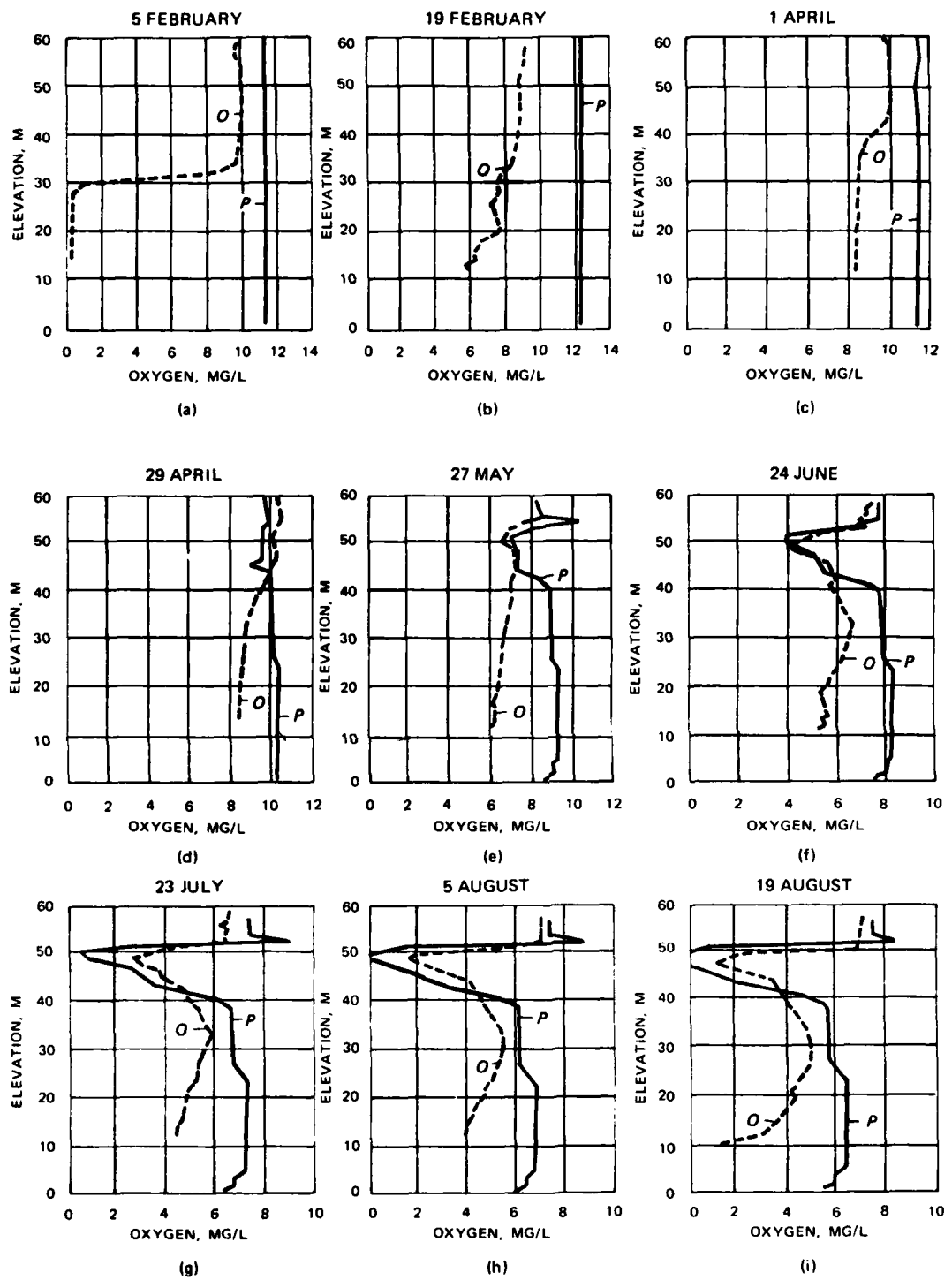


Figure 39. Dissolved oxygen profiles in DeGray Lake in 1980
(P = predicted value; O = observed) (Continued)

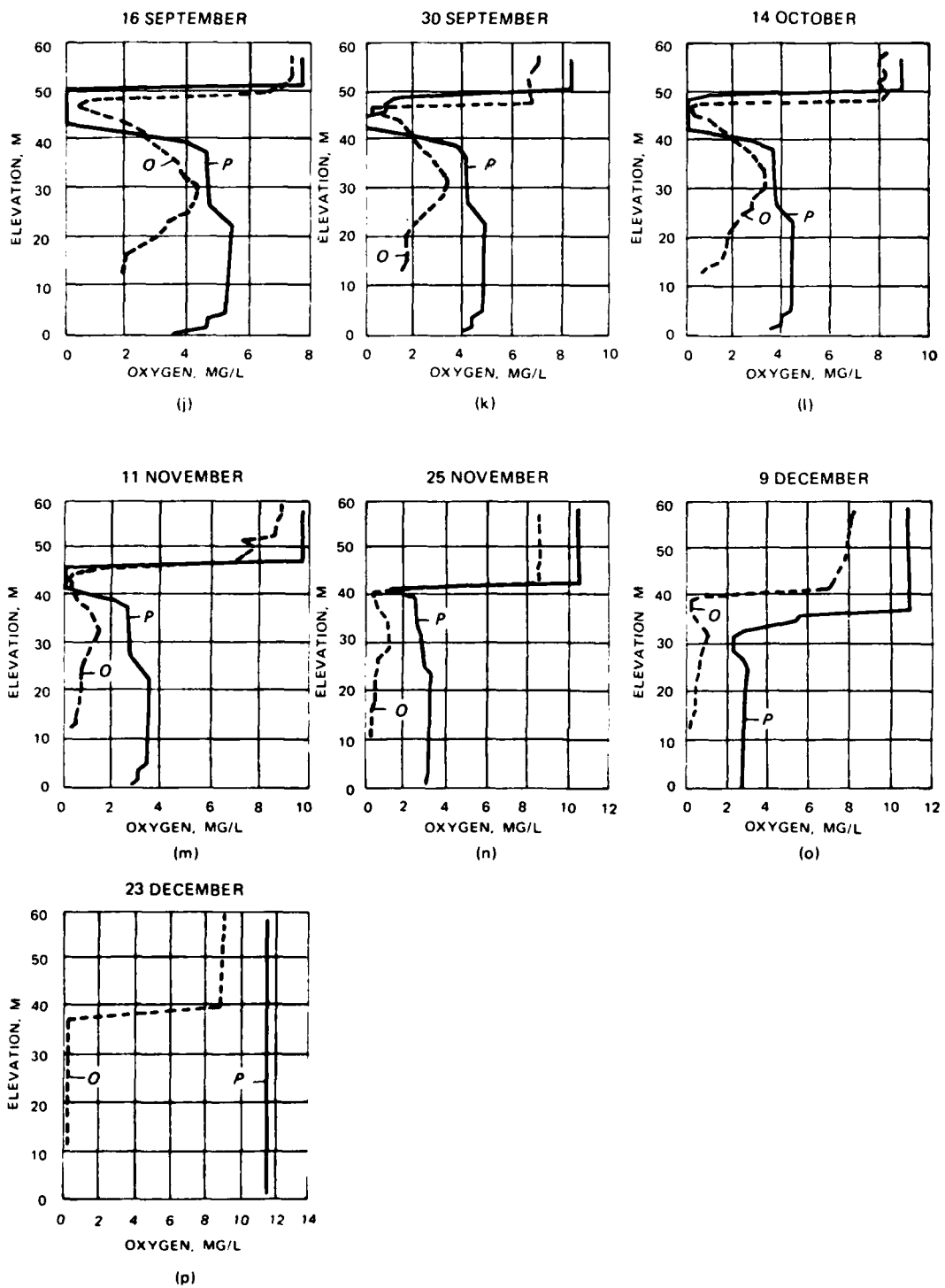


Figure 39. (Concluded)

coefficient functions based on 1979 data may lead to excessive mixing and increased DO throughout the water column in 1980. (If the sheltering coefficient is too high, similar situations may develop.) Another effect of increased mixing is recharging surface waters with nutrients previously depleted by algal production. Algal productivity induced by these nutrient additions can contribute additional O_2 to the surface waters.

72. Since NH_4^+ -N and PO_4^{3-} -P dynamics could not be calibrated properly with the anaerobic subroutines, these materials will not be included in evaluating 1980 model output.

73. Considering that simulated anaerobic conditions start 2 months earlier than they should, and assuming all other factors equal, one would expect the model to generate anaerobic materials in excess of actual concentrations. This expectation is borne out. Concentrations of dissolved Mn^{+2} and Fe^{+2} remain higher than observed values until some time after the anoxia criterion ($DO \leq 0.5 \text{ mg} \cdot \text{L}^{-1}$) is achieved in the reservoir (Figures 40 and 41). In addition, one should note that hypolimnetic concentrations of Mn^{+2} and Fe^{+2} remain high in spite of high DO. This situation results from Mn^{+2} and Fe^{+2} oxidation rates having been set to 0.00 day^{-1} in the 1979 calibration study. In the present simulation, initial concentrations of these anaerobic materials are relatively high, but oxidation does not affect them. In future calibration work on different systems, it may be advisable to maintain at least a low, but positive, default value for oxidation rates. The materials Mn^{+2} and Fe^{+2} experience more dynamic changes in the epilimnion because mixing, dilution, and outflow affect their concentrations.

74. Sulfide, on the other hand, does have a nonzero oxidation rate and so does not appear in hypolimnetic simulations. As in the 1979 calibration comparisons, observed S^{2-} concentrations vary considerably with no discernible trends (Figure 42). To compound the difficulty in studying 1980 simulations, field data for the last 2 months of the year do not include S^{2-} .

75. In spite of the early onset of anaerobic conditions predicted by the model and the 0.00 day^{-1} oxidation rates for Mn^{+2} and Fe^{+2} , the

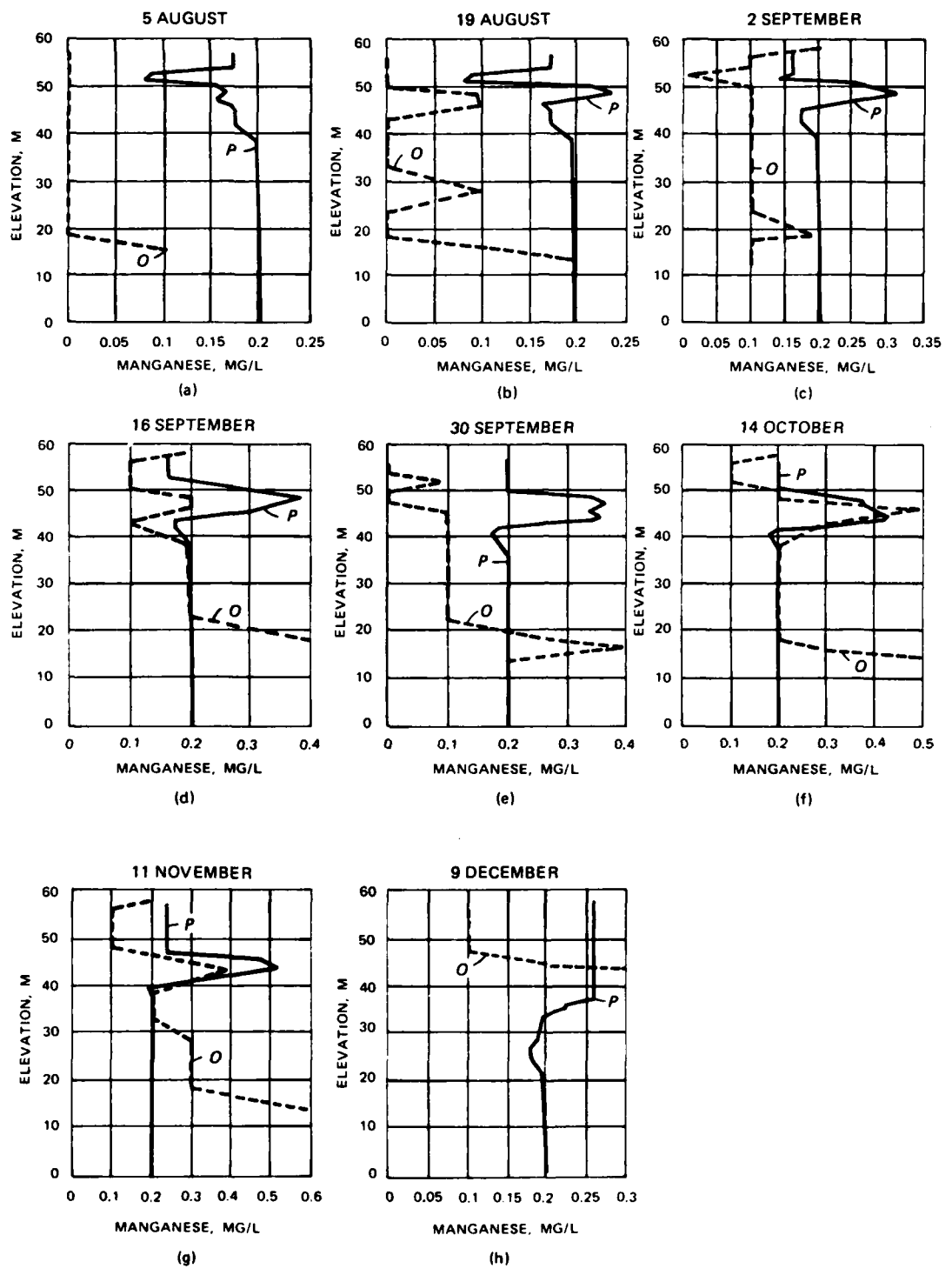


Figure 40. Selected Mn^{+2} profiles in 1980 (P = predicted value; O = observed)

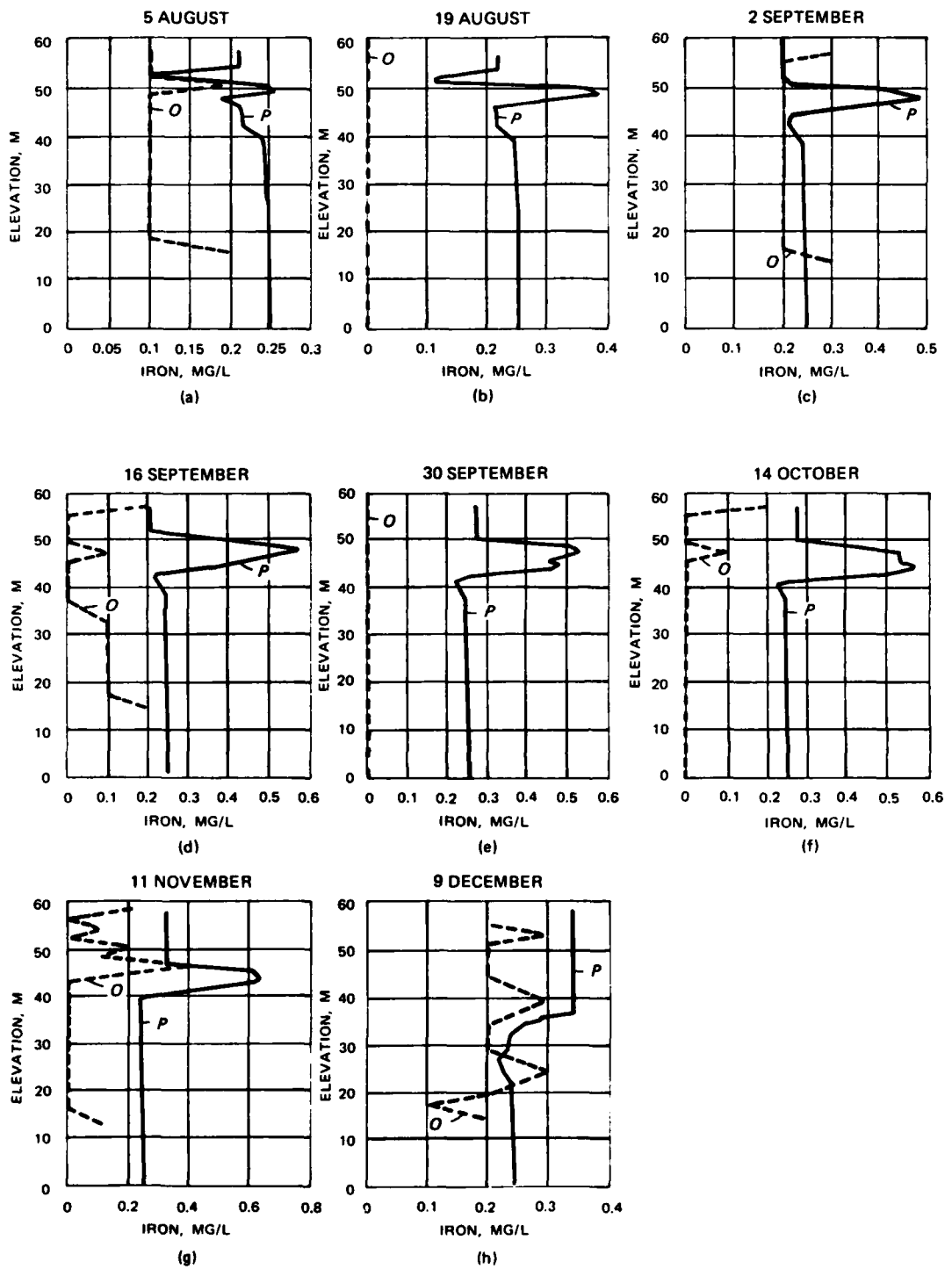


Figure 41. Selected dissolved Fe^{+2} profiles in 1980
(P = predicted value; O = observed)

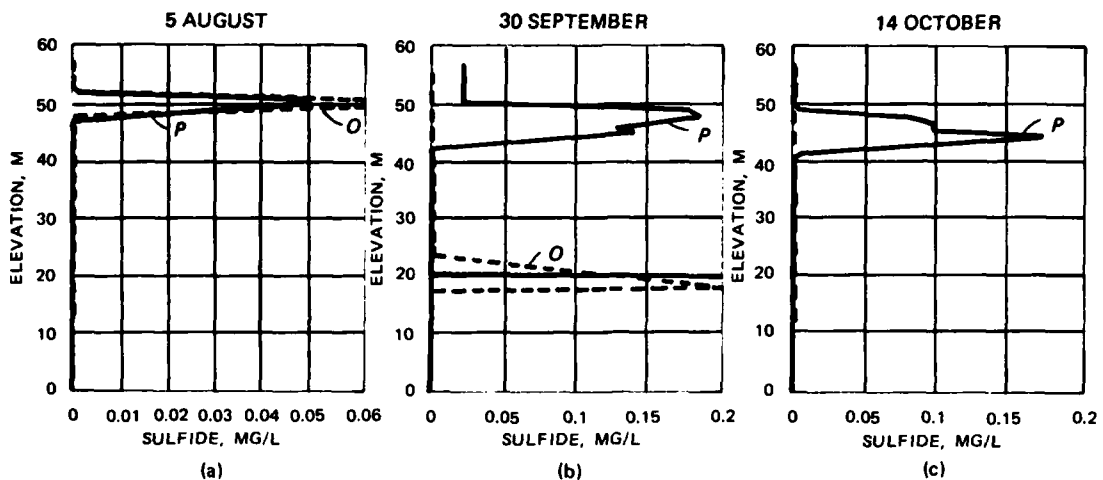


Figure 42. Selected S^{-2} profiles in 1980 (P = predicted value; O = observed)

magnitudes of their concentrations never become unreasonably high; S^{-2} concentrations, likewise, are moderate. Initially, one might assume the model insensitive to the increased duration and extent of anaerobic conditions. More likely, the calibrated rates are extremely low, which is in line with observations that DeGray Lake at the sampling site never experiences serious anoxic water quality problems. Another reason for seemingly low accumulations of anaerobic materials in the metalimnion is that withdrawal of water from the reservoir is largely limited to the metalimnion in 1980, whereas the epilimnion and metalimnion contributed in 1979. Thus, large concentrations of anaerobic materials do not develop in the metalimnion. Furthermore, water budget data for 1974 to 1980 (Ford and Stein 1984) indicate that 1979 was an atypical year. Springtime releases were considerably greater than normal (1980 was a normal year), and annual release volume approximately doubled that for 1980. In spite of the great complexity of the model linking physical, chemical, and biological attributes of reservoirs, the simulations yield results which, in general, reflect actual reservoir conditions and operations.

PART IV: IMPACT OF ANAEROBIC SUBROUTINES ON CE-QUAL-R1

76. One way to assess a new version of a model is to compare its predictions with its predecessor's. Oxygen, the only variable that integrates effects of all anaerobic processes in the model, is the obvious choice as a basis for comparison. Since the earlier version of the model has received many modifications other than the addition of anaerobic subroutines, a direct comparison of oxygen profiles between the two versions would be invalid; any number of changes could have altered oxygen profiles. Therefore, to attempt this comparison, only the most recent version of CE-QUAL-R1 is used, either with or without implementing the anaerobic subroutines. Setting the value of the DO cue to -1.0 effectively bypasses the anaerobic subroutines, allowing comparisons between two otherwise identical algorithms.

77. Figure 43 shows how similar the two sets of oxygen profiles are; for the most part, they are identical. However, starting on 2 October (Figure 43e) and continuing through the year, very minor differences appear in the metalimnion and hypolimnion. As expected, in the simulations which incorporate anaerobic processes, oxygen concentrations are slightly lower than in those which circumvent anaerobic processes, since reduced materials create an extra oxygen demand. Differences are small because concentrations of reduced materials are quite low and may be masked by oxygen demands of organic decay processes. Nevertheless, the results indicate the model is sensitive enough to be affected by the anaerobic-aerobic chemistry even with reduced species present in such low concentrations. Clearly, in a system experiencing severe anoxic conditions, the improved simulations resulting from the inclusion of the anaerobic subroutines would be more apparent. Additionally, the ability to simulate the presence of reduced species may be of prime importance.

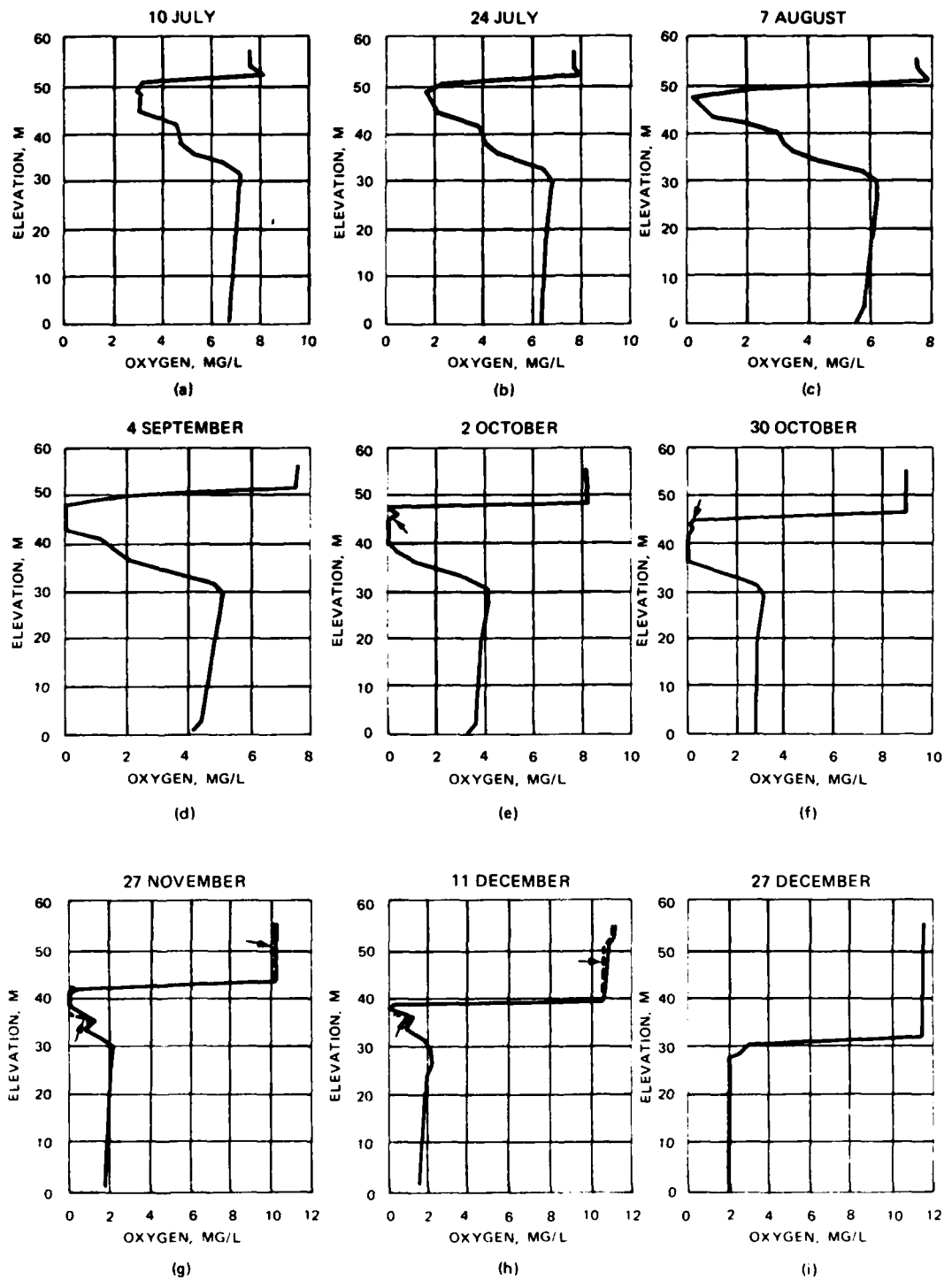


Figure 43. Comparison of oxygen profiles between simulations using the anaerobic subroutines (dashed lines) and simulations bypassing anaerobic subroutines (solid lines). Arrows indicate points of deviation between simulations

PART V: SUMMARY

78. This report documents early testing and development of 13 new algorithms added to CE-QUAL-R1 to simulate anaerobic biogeochemical processes in reservoirs. In light of this initial evaluation, further improvements and modifications have been made in CE-QUAL-R1. Some of these refinements are cited here. However, as the refinements postdate this study, they are not incorporated in it. Thus, this report also serves as an introduction to the algorithms and as a guide to calibrating the model for further studies.

79. Two important simplifying assumptions based on field data and other similar modeling studies facilitate predictions related to water quality under low DO conditions. First, a DO concentration of 0.5 mg/l in the water column is used to initiate these processes. Second, products of anaerobic processes are released simultaneously from sediments using zero-order rate kinetics.

80. In order to develop good predictions of the effects of anaerobic conditions, temperature and DO predictions must first be accurate. Prior to calibration and testing of the portions of the model dealing with anaerobic conditions, thorough examinations of the variables affecting thermal structure and depletion of DO in the water column were undertaken. In this series of calibrations, the DO predictions for the model of DeGray Lake proved very sensitive to changes in DOM decay rate and somewhat less sensitive to detritus and sediment decay rates.

81. Numerous simulations were made to calibrate CE-QUAL-R1 with the new algorithms using 1979 data from DeGray Lake field studies. Overall, concentrations of anaerobic products were most sensitive to changes in sediment release rates. Problems with simulations of ammonia and phosphate concentrations have been resolved by inclusion of adsorption algorithms (Wlosinski and Collins 1985a). Calibrations of metalimnetic oxygen depletion gave realistic results; hypolimnetic profiles deviated more from field observations. Some differences can be reconciled by recognizing that field data for comparison were obtained

from a shallower site, farther up the reservoir. Most of the hypolimnetic deviations can be interpreted as consequences of relatively weak, benthic, anaerobic conditions, typical of DeGray Lake, that create low concentrations of reduced species localized near the bottom which are difficult to resolve with the model. Recent testing of the model on Eau Galle Lake, Wisc., where anaerobic conditions were more severe, produced better comparisons with less calibration (Wlosinski and Collins 1985b). In spite of low concentrations of reduced materials in DeGray Lake, the model reflects their slight impact on DO concentrations.

82. Discrepancies between modeled and observed conditions in the confirmation simulations for 1980 can be ascribed to the same causes as in the calibration work. Differences in conditions early in 1980 also contributed to predicted water quality deviating from actual system behavior. In particular, in early February 1980 the reservoir was isothermal but still chemically stratified. However, the isothermal condition caused the model to induce mixing prior to its occurrence as indicated by field data. This result indicated the need to examine criteria controlling mixing. Adjustments of the relevant coefficients might have improved results for 1980 without compromising 1979 results. Overall, trends and concentration peaks match field data well, particularly in the metalimnion which is more important for the DeGray Lake system; these results can be attributed to calibrating the model for metalimnetic conditions which become anaerobic earlier and more severely.

REFERENCES

Brannon, J. M., Gunnison, D., Butler, P. L., and Smith, I., Jr. 1978. "Mechanisms That Regulate the Intensity of Oxidation-Reduction in An-aerobic Sediments and Natural Water Systems," Technical Report Y-78-11, US Army Engineer Waterways Experiment Station, Vicksburg, Miss.

Environmental Laboratory. 1982. "CE-QUAL-R1: A Numerical One-Dimensional Model of Reservoir Water Quality," Instruction Report E-82-1, US Army Engineer Waterways Experiment Station, Vicksburg, Miss.

Fillos, J., and Molof, A. H. 1972. "Effect of Benthal Deposits on Oxygen and Nutrient Economy of Flowing Water," Journal of the Water Pollution Control Federation, Vol 44, pp 644-662.

Ford, B., and Stein, A. B., III. 1984. "The Hydrometeorology of DeGray Lake," Miscellaneous Paper E-84-3, US Army Engineer Waterways Experiment Station, Vicksburg, Miss.

Golterman, H. L. 1975. Physiological Limnology: An Approach to the Physiology of Lake Ecosystems, Elsevier Scientific Publishing Company, New York.

Gunnison, D., and Brannon, J. M. 1981. "Characterization of Anaerobic Chemical Processes in Reservoirs: Problem Description and Conceptual Model Formulation," Technical Report E-81-6, US Army Engineer Waterways Experiment Station, Vicksburg, Miss.

Hem, J. D. 1981. "Rates of Manganese Oxidation in Aqueous Systems," Geochim. Cosmochim. Acta, Vol 45, pp 1369-1374.

Keeley, J. W., Mahloch, J. L., Barko, J. W., Gunnison, D., and Westhoff, J. D. 1978. "Identification and Assessment of Environmental Quality Problems and Research Program Development," Technical Report E-78-1, US Army Engineer Waterways Experiment Station, Vicksburg, Miss.

Kennedy, R. H., Montgomery, R. H., and James, W. F. 1983. "Phosphorus Dynamics in an Arkansas Reservoir: The Importance of Seasonal Loading and Internal Recycling," Miscellaneous Paper E-83-1, US Army Engineer Waterways Experiment Station, Vicksburg, Miss.

Lum, L. W. K., Armstrong, N. E., and Fruh, E. G. 1981. "Incorporation of Chemical Equilibrium, Physico-Chemical Reactions and the Simulation of Inorganic Qualities in a Reservoir Ecologic Model," Ecological Modelling, Vol 14, pp 95-123.

Stumm, W., and Morgan, J. J. 1981. Aquatic Chemistry, Wiley-Interscience, New York.

Thornton, K. W., and Lessem, A. S. 1978. "A Temperature Algorithm for Modifying Biological Rates," Transactions of the American Fisheries Society, Vol 10, No. 2, pp 284-287.

Thornton, K. W., Kennedy R. H., Magoun, A. D., and Saul, G. E. 1982.
"Reservoir Water Quality Sampling," Water Resources Bulletin, Vol 18,
pp 471-480.

Wang, L. K., Poon, C. P. C., Wang, M. H., and Bergenthal, J. 1978.
"Chemistry of Nitrification-Denitrification Process," Journal of Environmental Science, Vol 21, pp 23-28.

Wlosinski, J. H., and Collins, C. D. 1985a. "Analysis and Revision of a Reservoir Water Quality Model," Technical Report in preparation, US Army Engineer Waterways Experiment Station, Vicksburg, Miss.

_____. 1985b. "Confirmation of the Water Quality Model CE-QUAL-R1 Using Data from Eau Galle Reservoir, Wisconsin," Technical Report in preparation, US Army Engineer Waterways Experiment Station, Vicksburg, Miss.

END

DTIC

6-86